



UNIVERSITÀ  
DEGLI STUDI  
DI PADOVA

Università degli Studi di Padova

Dipartimento dei Beni Culturali: Archeologia,  
Storia dell'Arte, del Cinema e della Musica.

Master's degree in  
ARCHAEOLOGICAL SCIENCES  
Curriculum in  
APPLIED SCIENCES TO CULTURAL HERITAGE MATERIALS AND SITES

Integrating Archaeometry of mortar and stratigraphy, using  
BIM for Dating monuments: a case study based in Oratorio  
di San Michele.

Supervisor:

Alejandra Chavarria Arunau

Co-supervisor:

Prof. Michele Secco

Master Candidate

Kankanige Don Binoli Navodya Nimmadi

Student ID-2072855

ACADEMIC YEAR 2023/2024



*"Archaeology, science, and engineering must work hand in hand to uncover the secrets of the past and address the challenges of the present. By combining our expertise, we can develop innovative approaches and technologies that allow us to better understand ancient civilizations and preserve our cultural heritage for future generations."*

Sarah Parcak (January 2017)

"Satellite Remote Sensing: Tools for Archaeology in the 21st Century."  
Annual Meeting of the Archaeological Institute of America, Boston, MA.

# Contents

List of Figures.....	7
List of Tables.....	11
Acknowledgment.....	12
Abstract.....	14
<b>Chapter I: Introduction.....</b>	<b>19</b>
1.1 Introduction.....	19
1.2 Objectives.....	19
1.2.1 Main Objective.....	19
1.2.2 Specific Objectives.....	20
1.3 Brief introduction to the context.....	20
1.4 Outcomes.....	20
1.5 Dissertation Outline.....	21
<b>Chapter II: Historical Context.....</b>	<b>23</b>
2.1.Christianization of Padua.....	23
2.2. Theories about the age of Oratorio di San Michele.....	24
2.3. Management and Maintaining phase.....	25
2.4. Reconstruction and Expansion Phase.....	27
2.5. Restoration Phase.....	31
<b>Chapter III: Geographical Context.....</b>	<b>34</b>
3.1. Significance in the roman Period.....	34
3.2. Military Importance in the Lombard Period.....	36
3.3. Ecclesiastical Significance and Architectural Evolution.....	37
<b>Chapter IV: Stratigraphic Analysis.....</b>	<b>40</b>
4.1. Architectural Evolution Based on Literature.....	40
4.2. Stratigraphy of the remaining walls.....	49
4.3. Methodology of the Stratigraphic analysis.....	50

4.4. Results of the stratigraphic analysis.....	51
4.5. Discussion of the stratigraphic analysis.....	55
4.6. Conclusion of the stratigraphic analysis.....	56
<b>Chapter V: Historic Building Information Modeling.....</b>	<b>58</b>
5.1. Introduction to BIM.....	58
5.2. Methodology of BIM analysis.....	64
5.3. Results of BIM analysis.....	66
5.4. Discussion of BIM analysis.....	70
5.5. Conclusion of BIM analysis.....	70
<b>Chapter VI: Archaeometry of Mortars.....</b>	<b>72</b>
6.1. Introduction to Mortar.....	72
6.2. Dating Mortars Using <sup>14</sup> C Technique.....	76
<b>Chapter VII: Methodology.....</b>	<b>79</b>
7.1. Action Plan Overview.....	79
7.2. Photographical Records.....	83
7.3. Colorimetry.....	86
7.4. (XRPD): X-ray Powder Diffraction.....	87
7.5. (OM): Optical Microscopy.....	89
7.6. (SEM & EDS): Scanning Electron Microscopy & Energy Dispersive Spectroscopy.....	90
<b>Chapter VIII : Results .....</b>	<b>93</b>
8.1. Colorimetry Results.....	93
8.2. X-Ray Powder Diffraction (XRPD) Results.....	94
8.2.1. Composition Analysis.....	94
8.2.2. Reaction Phases.....	94
8.2.3. Construction Technology.....	95
8.2.4. Sample Clustering.....	95
8.3. Optical Microscopy (OM) Results.....	96

8.3.1. Sample 01 - optical microscopy Scans.....	97
8.3.2. Sample 02 optical microscopy Scans.....	98
8.3.3. Sample 03 optical microscopy Scans.....	99
8.3.4. Sample 04 optical microscopy Scans.....	99
8.3.5. Sample 05 optical microscopy Scans.....	100
8.3.6. Sample 06 optical microscopy Scans.....	101
8.4. Scanning Electron Microscopy with Energy-Dispersive Spectroscopy (SEM-EDS) Results.....	102
8.4.1. SEM Scans of Sample 01.....	102
8.4.2. SEM Scans of Sample 02 & 03.....	102
8.4.4. SEM Scans of Sample 04 & Sample 05.....	103
8.4.6. SEM Scans of Sample 06.....	104
<b>Chapter IX: Discussion.....</b>	<b>106</b>
9.1 Interpretation of colorimetry data.....	106
9.2 Interpretation of X-ray Powder Diffraction data.....	107
9.3. Interpretation of Optical Microscopy data.....	109
9.4. Interpretation of SEM-EDS data.....	110
<b>Chapter X: Conclusion.....</b>	<b>113</b>
<b>Chapter XI: References.....</b>	<b>118</b>

# List of Figures

Figure 1: Reused materials visible on the North wall of S. Michele. ....	15
Figure 2: The workflow from stratigraphy of walls, BIM model to calculate area and volume, Sample locations and archaeometry of mortars to pick the best candidate for C14 dating. ....	16
Figure 3:1117 .01. 03, Verona Earthquake with a magnitude of 6.9 with MMI IX Violent intensity Wikipedia – 1117 Verona Earthquake. ....	27
Figure 4:Frescos by Jacopo da Verona in Oratorio di San Michele.....	27
Figure 5:Detail of I miracoli di Cristo. Fina Buzzaccarini alongside her husband Francesco I da Carrara and Italian poet Francesco Petrarca, Wikipedia- Francesco I da Carrara. ....	28
Figure 6:Chapel Bovi, South Wall, Inscription panel ,1398 (Tobias, 2013).....	29
Figure 7: A.G.C.P. Gennaro Borsella, Photographic inspection, June 1990 (Talami, 2024).32	
Figure 8: A request to restore oratorio di san michele, Padova from Biblioteca civica Padova. ....	32
Figure 9: An old map of Padua’s urban grid, from A. Portenari 1623.....	34
Figure 10:An old map of the position of the Oratorio di San Michele (Beltrame G. Anno XXV Feb). ....	35
Figure 11:Area of S.Michele and Capella Bovi in the map by Giovanni Valle, 1784 (Gasparotto, 1969). ....	38
Figure 12: Reconstruction of the church in the 7th Century. ....	40
Figure 13:Reconstruction of 14th Century appearance (Talami, 2024).....	41
Figure 14:Reference plan supported the reconstruction models (Talami, 2024). ....	42
Figure 15: Reference plan supported the reconstruction models (Talami, 2024). ....	43
Figure 16: Plan of the San Michele Arcangelo Complex with Cappella Bovi on Riviera Tiso da Camposampiero(1816-1876) (Maiolo,2001). ....	44
Figure 17:San Michele Arcangelo with Cappella Bovi, Padua: Floor plan showing various viewer locations and lines of sight based on the historical spatial experience (reconstruction by Tobias Ertel, 2010).....	44
Figure 18:Visible proof of whitewashing.....	45
Figure 19:Reconstruction of 1815 appearance (Talami, 2024).....	46
Figure 20:Reconstruction of 1864 appearance (Talami, 2024).....	46
Figure 21:Reconstruction of 1874-77 apperence (Talami, 2024). ....	46
Figure 22:Digital Reconstruction of 1880 appearance (Talami, 2024).....	47

Figure 23:Digital Reconstruction of the current appearance of oratorio di San Michele (Talami, 2024).....	48
Figure 24:Recording the walls through photographs. ....	50
Figure 25:A basic recording form, for stratigraphy of the Oratorio di San Michele. ....	50
Figure 26:Identification of Stratigraphic units in the North wall.....	51
Figure 27:Orthophoto of North wall. ....	52
Figure 28:Material study of North wall, all measurements are in cm.....	52
Figure 29:Stratigraphy sequence of North wall. ....	52
Figure 30:Stratigraphic analysis of North wall. ....	52
Figure 31:Stratigraphy Analysis of West wall. ....	53
Figure 32:Orthophoto and the position of the West wall. ....	53
Figure 33:Stratigraphy Sequence of West wall.....	53
Figure 34:Position of the Northern excavation wall. ....	54
Figure 35:Orthophoto of the Northern excavation wall.....	54
Figure 36:Stratigraphy sequence of Northern excavation wall.....	54
Figure 37:Stratigraphy analysis of Northern excavation wall.....	54
Figure 38:Reconstruction of Oratorio di San Michele in Sketchup 3D warehouse.....	56
Figure 39:Father of BIM, Charles M.Eastman (Farias, 2020).....	58
Figure 40:Software used for HBIM.....	58
Figure 41: Diagram of a Building Information Modeling (BIM) work process (Rocha, Luis Mateus, Fernandez, & Ferreira, 2020). ....	59
Figure 42:Diagram of a HBIM work process.....	59
Figure 43:Diagram of a HBIM work process.....	59
Figure 44:LIDAR Model of a part of the oratorio di San Michele using 3d Sanner app.....	61
Figure 45:Phasing Tool for Dating and Remodeling Early Phases, AutoCAD Revit.....	61
Figure 46:Structural Analysis Tool for Structural Vulnerability, Auto CAD - Revit.....	62
Figure 47:Ability integrate mechanical, thermal and physical properties to the 3D model, Auto CAD - Revit. ....	63
Figure 48:3D scanner app in iOS used for LIDAR of Oratorio di San Michele.....	64
Figure 49:Autocad drawing of the measurements of the West wall, measured by Mileseeey Laser scanner with a 2mm +/- precision. All measurements are in Meters. ....	64
Figure 50: Data tracing from LIDAR models. ....	66
Figure 51:Creating the model based on the floor plan. ....	66
Figure 52: Using the Phasing feature to visually observe different stratigraphy of all the walls together.....	66



Figure 53:Using unique colors to symbolize different stratas from the oldest to most recent as 1001 to 1005.....	67
Figure 54:Creating the oldest to most recent construction phases as different stratigraphies. ....	67
Figure 55: Using parametric modeling and wall scheduling feature to calculate the volume and the area of each stratigraphy of Oratorio di San Michele. ....	67
Figure 56: The final Stratigraphy sequence covering all the remaining walls.....	68
Figure 57:Final BIM model of oratorio di San Michele with architectural elements and stratigraphical relationships referred to the Harris Matrix diagram of the stratigraphy sequence.....	69
Figure 58:Exporting area and volume data from Revit to Microsoft EXCEL.....	69
Figure 59:Binders based on carbonates, their nature and reaction processes. (Artioli, Secco, & Addis, 2019).....	72
Figure 60: The steps of Cryo2sonic version 2.0 (v.2.0) ( Addis, et al., 2019).....	76
Figure 61:Flow chart of the identification of datable materials within the mortars and their possible contaminations. ....	77
Figure 62: Flow chart of the most common mortar contaminants. ....	77
Figure 63:Strata 1001 of remaining walls at Oratorio di San Michele. ....	80
Figure 64:Plan view of the sample locations. ....	81
Figure 65:3D view of the sampling locations. ....	81
Figure 66:2D Views of the sampling Locations.....	82
Figure 67:Sampling process of SM_01.....	83
Figure 68:Sampling Process of SM_02.....	84
Figure 69:Sampling process of SM_03.....	84
Figure 70:Sampling process of SM_04.....	85
Figure 71:SAmping Process of SM_05.....	85
Figure 72:Sampling Process of SM_06.....	86
Figure 73:Grinding tools and the Grinded samples. ....	87
Figure 74:RD Mill Mc Crone.....	87
Figure 75: Fine grinded sample with ethanol on watch glasses for drying.....	87
Figure 76: Analytical Balance and the Tools used for mixing and backloading the samples. ....	88
Figure 77: The Instruments used to create the thin sections for Optical Microscopy.....	89
Figure 78: Quorum Q150R Rotary pump Coater used for gold coating.....	91
Figure 79: COXEM EM-30AX + SEM. ....	91

Figure 80: Brightfield image, plane polars transmission image and crossed polars transmission image of SM_01.....	97
Figure 81: Brightfield image, plane polars transmission image and crossed polars transmission image of SM_02.....	98
Figure 82: Brightfield image, plane polars transmission image and crossed polars transmission image of SM_03.....	99
Figure 83: Brightfield image, plane polars transmission image and crossed polars transmission image of SM_04.....	99
Figure 84: Brightfield image, plane polars transmission image and crossed polars transmission image of SM_05.....	100
Figure 85: Brightfield image, plane polars transmission image and crossed polars transmission image of SM_06.....	101
Figure 86: SEM at x500 and WD-12.7 of SM_01. ....	102
Figure 87: SEM-EDS analysis demonstrating the M-S-H phases and para pozzolanic reactions of SM_01.....	102
Figure 88: SEM -EDS Analysis of SM_02 demonstrating the presence of an association of anthropogenic carbonates and M-(A)-S-H phases. ....	103
Figure 89: SEM-EDS analysis of SM_03 demonstrating M-S-H phase with shoe shaped plagioclase particle.....	103
Figure 90: SEM -EDS of SM_04 demonstrating the preservation of dolomite. ....	103
Figure 91: SEM -EDS of SM_05 demonstrating the lime-based nature of the binder and the absence of para-pozzolanic reactions.....	104
Figure 92: SEM-EDS of SM_05 highlighting Calcic Composition, indicating an Aerial Reaction with No Evidence of M-S-H or Para-Pozzolanic Reactions.....	104
Figure 93: PCA of Colorimetry data for powdered form of mortar samples. ....	106
Figure 94: Clustering of the mortar samples based on the colorimetry data.....	107
Figure 95: PCA of X-R-P-D Data. ....	107

# List of Tables

Table 1:Overview of Methodology .....	79
Table 2:Sample population of the study.....	82
Table 3: Colorimetry results on the powder form of the mortar samples. ....	93
Table 4:XRPD results on Powder form of mortar samples.....	94
Table 5:Clustering of mortar samples based on XRPD Data.....	96
Table 6:Summery of Best sample candidate for C14 from each technique followed.....	114

# Acknowledgment

“I owe a huge thank you to my supervisors, Prof. Alejandra Chavarria Arnau and Prof. Michele Secco. Your guidance has been nothing short of inspirational. My heartfelt gratitude to Engineer Luca Sbrogiò and Professor Maria Rosa Valluzzi for their informative insights into Building Information Modeling. Thank you to my dear colleagues, Ngosa Bwalya, Kasara Shahrokhinejad, and Alya Rekhi, Ishara Ranasighe and Elisa Talami for transforming research into a true team effort.

Sincere appreciation goes to my family and my mentor, Prof. Sudharshan Seneviratne from Sri Lanka. Deep gratitude to my boyfriend, Andrea Stoppa and his family. Your unwavering love, encouragement, and understanding have been my anchor during the most challenging times. Your support has been truly invaluable.

Finally, I thank the Ministry of External Affairs and Cooperation of Italy for funding my education. I am forever grateful for all the people I met, everything I learned, and the piece of the world I discovered. I truly hope I can contribute to our collective future.”



# Abstract

† The case study on the Oratorio di San Michele integrates historical records and scientific data using information modeling to date the monument accurately. Historical records confirm the building's age is unknown, but materials in the remaining walls reveal hidden construction phases. Stratigraphic analysis identified optimal sample locations, and these layers were integrated into a Building Information Model (BIM) using Revit, facilitating future structural and seismic assessments. Analytical techniques such as colorimetry, SEM, XRD, and polarizing microscopy determined mortar composition and construction techniques. PCA revealed that samples 04 and 05 were suitable for C14 dating, with 04 selected as the best candidate. This study demonstrates the potential of combining historical data with scientific analysis and BIM for understanding and preserving historical structures.

---

## I. INTRODUCTION

The Church of S. Michele, situated near the Riviera Tiso da Camposampiero in Padua, holds a significant place in the region's historical and architectural heritage. The age of the Oratorio di San Michele remains uncertain due to the lack of definitive information about its origin. The primary pieces of evidence include the association of the name "Santi Arcangeli" with the site, a name commonly linked to the Lombards, its strategic location, the presence of Roman materials in the surviving walls, inaccessible archaeological excavation reports, and the earliest written record, which dates to 970, when Bishop Gauslino mentioned Holy Archangels (Santi Arcangeli) in a generous donation confirming its title and existence (Colecchia, 2017). However, these elements are insufficient to conclusively date the Oratorio or identify its original commissioner. Scholars have proposed various time periods for its construction, with some suggesting the Byzantine period between 569 and 602, during which the area housed a well-equipped Byzantine garrison (Beltrame D. G., 2000). The construction style and materials suggest it may date back to at least the Lombard period (Bellinati & Puppi, Padova Basiliche e Chiese – Parte Prima, 1975). The alternation between the titles "Holy Archangels" and "Saint Michele" reflects the early medieval devotion to St. Michael, particularly during the Lombard period, when St. Michael was revered as the patron of the Kingdom of Italy following the Lombard victory over the Byzantines in 663 (Gasparotto, 1969). Despite the architectural diversity and the scarcity of written sources related to the church's construction, the exact age of the Oratorio di San Michele remains uncertain.

## II. METHODOLOGY

The surviving architectural features of S. Michele represent a collage of different phases, with its original phase remaining unknown. It could potentially be one of the oldest churches in Padua.

Notable for its rough masonry work and the reuse of Roman stone materials, the church incorporates elements such as tombstones and architectural fragments, particularly evident in the lower parts of the Western main wall. This resourceful yet disorderly construction technique reflects its early



Figure 1: Reused materials visible on the North wall of S. Michele.

medieval origins. To ensure accurate dating and a comprehensive understanding of the Oratorio di San Michele's construction, a multi-faceted analytical approach was employed.

a) Stratigraphy Analysis- involved visual assessment of the remaining walls, focusing on shape, color, size, and mortar joint patterns, guiding the selection of sample locations.

b) Archaeometry Analysis of mortar using:

- ∴ Colorimetry- assess color variations within the mortar samples, indicating differences in raw materials, manufacturing processes, and weathering effects.
  - ∴ X-ray Diffraction (XRD)- determines the mineralogical composition of the mortar samples, identifying crystalline phases present in the binder and aggregate materials.
  - ∴ Scanning Electron Microscopy with Energy Dispersive Spectroscopy (SEM-EDS) provided high-resolution images and detailed elemental composition data, identifying specific elements and their distribution.
  - ∴ Optical Microscopy- Thin sections of mortar were examined under polarized light to observe optical properties and birefringence, offering insights into the mortar microstructure and material properties.
  - ∴ Principal Component Analysis (PCA) to determine the underlying patterns and relationships in the dataset, helping to simplify and interpret XRD and Colorimetry data.
- c) Building Information Modeling (BIM) using Revit software reflects the stratigraphy confirmed by scientific results, providing a comprehensive digital representation of the building's evolution.

### III. RESULTS

Based on the stratigraphy of remaining walls six samples were taken for the archaeometry analysis of the mortar to filter out the best sample for the C14 analysis. The results are as follows.

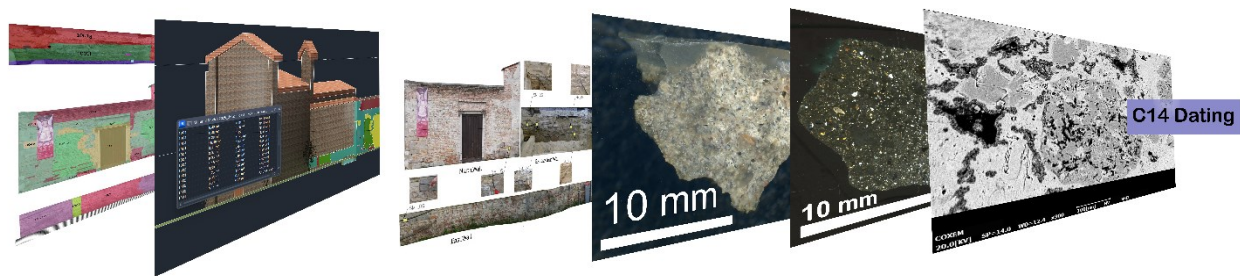


Figure 2: The workflow from stratigraphy of walls, BIM model to calculate area and volume, Sample locations and archaeometry of mortars to pick the best candidate for C14 dating.

SEM-EDS analysis shows that Sample 01 has a complex matrix with para pozzolanic reactions involving the formation of M-S-H and anthropogenic Calcium Carbonates with dolostones releasing Mg to form M-S-H; Sample 02 displays strong pozzolanic reactions in multiple areas; Sample 03 has the presence of the M-A-S-H phase and distinct plagioclase particles; and Samples 04, 05, and 06 show no strong precipitation or para pozzolanic reactions, with better-preserved dolomite indicating minimal reactivity.

Colorimetry data explains Sample 06 as the lightest and most neutral color profile, Sample 01 is the darkest with a grayish tint, Samples 02 and 03 have an average lightness, and Samples 04 and 05 have the strongest red and yellow tints with an average lightness of 85.0 and RGB values of 223.5, 210.5, 194.5.

Optical microscopy shows that Sample 01 has a fat white binder phase with fine aggregates, indicating sand from the Bacchiglione River and a dark binder matrix suggesting para pozzolanic reactions; Samples 02 and 03 are high in silicates, have fine binder fractions, and noticeable pozzolanic reactions with similar aggregate dimensions to Sample 01; Samples 04 and 05 have coarser aggregates with fat binder phases, significant lime lumps, and higher calcite and carbonate aggregates; and Sample 06, being newer, has many aggregates, a different preparation method, and distinct binder characteristics.

Polarized light microscopy reveals that Sample 01 exhibits a well-reacted binder with para pozzolanic reactions, with fine aggregates and lime lumps visible; Samples 02 and 03 have fine binder fractions, high silicate content, and clear pozzolanic reactions with aggregate dimensions similar to Sample 01; Samples 04 and 05 have coarser aggregates, significant lime lumps, and higher calcite content, reflecting traditional lime mortar with carbonate aggregates; and Sample 06, being newer, has distinct aggregate and binder characteristics, indicating different sources or preparation methods.

XRD analysis shows that Sample 01 is predominantly composed of calcite (38.20%) and amorphous materials (22.97%), with the presence of hydrocalumite indicating high pozzolanic activity; Samples 02 and 03 have lower calcite content (28.35% and 24.62%) but are rich in quartz and silicate sands, with hydrocalumite and hydrotalcite suggesting strong pozzolanic reactions;




Samples 04 and 05 are rich in calcite (44.88% and 37.90%) and dolomite (13.62% and 16.99%), with moderate pozzolanic reactions indicating traditional lime mortar; and Sample 06 has high calcite (34.19%) and dolomite (14.94%), with no evident pozzolanic reactions, indicating a distinct binder matrix dominated by carbonate aggregates.

#### **IV. DISCUSSION**

The comprehensive analysis of six mortar samples (SM\_01 to SM\_06) reveals significant insights into their composition and suitability for C14 dating. Colorimetry results show variations in lightness and color, with Samples 04 and 05 are the most vibrant. SEM-EDS analysis indicates that Samples 04, 05, and 06 have minimal pozzolanic reactions, suggesting more stable binder phases, whereas Sample 01 exhibits significant pozzolanic reactions. Optical and polarized light microscopy further confirm these findings, with Sample 01 showing a well-reacted binder and fine aggregates, while Samples 04 and 05 display coarser aggregates and higher calcite content, indicative of traditional lime mortar. XRD analysis supports these observations, highlighting the mineralogical composition and reactivity differences among the samples. Based on this multi-faceted analysis, Samples 04 and 05 are identified as the best candidates for C14 dating due to their minimal geological carbon content and stable mineral composition, ensuring accurate dating results and reliable historical insights.

#### **V. CONCLUSION**

The archaeometry assessment of the Oratorio di San Michele's mortars has yielded significant insights into the construction techniques, materials, and knowledge employed during its development. The integration of stratigraphic analysis with advanced analytical methods such as polarized microscopy, X-ray diffraction, colorimetry, and SEM-EDS facilitated a thorough examination of the mortar samples. This comprehensive analysis identified Samples 04 and 05 as the optimal candidates for C14 dating, owing to their minimal geological carbon content and stable mineral composition, thereby ensuring accurate historical insights. Furthermore, the integration of a Building Information Modeling (BIM) model substantially enhanced the study, providing valuable insights into the building's historical evolution and structural integrity. The findings underscore the importance of interdisciplinary collaboration in the field of heritage conservation and management. By combining historical research, scientific analysis, and digital modeling, this study has deepened our understanding of the Oratorio di San Michele's construction history and established a robust framework for its preservation.



**HELP ME!!!**  
**RECALL MY PAST.**  
**THEY SAY I'M AMONG**  
**THE OLDEST IN PADUA!**

**HOW OLD**  
**ARE YOU ?**

**CRACK!**

**ARRGH!**

# Chapter I: Introduction

## 1.1 INTRODUCTION

The Oratorio di San Michele, widely regarded as the first sacred building in Vanzo, that was dedicated to the holy archangels Michael, Raphael, Gabriel, and Uriel, reflecting Byzantine traditions. This oratory was spared by the Lombards, who promoted the cult of Saint Michael following their victory over the Saracens in 663, leading to widespread devotion and the dedication of many churches to him. However, the exact dating of the building remains unconfirmed and relies solely on historical references to its old name, the Church of the Holy Archangels.

This study aims to determine the precise age of the Oratorio di San Michele using scientific dating methods based on the archaeometry of binders, while also examining the construction techniques, materials, and knowledge employed in its development. A critical aspect of this material study involved selecting appropriate sample locations, which was achieved through stratigraphic analysis based on the shape, color, size, and mortar joint patterns of the remaining walls.

The samples were analyzed using optical microscopy, X-ray diffraction, colorimetry, and scanning electron microscopy with energy-dispersive spectroscopy (EDS). A Building Information Modeling (BIM) model was created to reflect the confirmed stratigraphy derived from the scientific results, elucidating the building's evolution and identifying the most suitable sample for carbon dating. The BIM model not only provides insights into the historical development of the Oratorio di San Michele but also serves as a tool for identifying the most vulnerable parts of the structure, facilitating future reinforcement efforts. The results provide valuable insights into the construction history of the Oratorio di San Michele and underscore the importance of interdisciplinary collaboration in heritage conservation and management.

## 1.2 OBJECTIVES

### 1.2.1 MAIN OBJECTIVE

The primary objective of this academic dissertation is to integrate archaeometry of mortar and stratigraphic analysis of remaining walls, using Building Information Modeling (BIM) to date the Oratorio di San Michele, Padua. This includes selecting the most suitable samples for C14 dating, understanding the composition of the materials, and creating a BIM model that integrates historical data with scientific analysis as visual documentation.

The aim is to provide a comprehensive understanding of the construction methods, materials, and historical context of this significant structure.

### 1.2.2 SPECIFIC OBJECTIVES

To achieve the main objective, the study will pursue the following specific objectives:

- ∴ Reconstruct the historical and geographical context of the Church of S. Michele through bibliographic research, emphasizing its architectural and strategic significance.
- ∴ Analyze the general composition of the mortars using various analytical techniques to determine the interaction between the binder and aggregate fractions.
- ∴ Identify the chemical and mineralogical compositions of the binder fractions of the mortar samples while exploring current methodologies in mortar characterization.
- ∴ Explore variations in manufacturing processes over time by correlating analytical data with historical context.
- ∴ Creating a BIM model that integrates historical data, visual documentation, and scientific analysis, and developing a website with all the results. This website will be accessible via a QR code, which can be distributed with the entrance ticket.

## 1.3 BRIEF INTRODUCTION TO THE CONTEXT

The archaeometry analysis of mortars is a relatively recent but growing field, offering valuable insights into ancient construction techniques, materials, and preservation methods. In this dissertation, mortar samples from the Church of S. Michele in Vanzo will be thoroughly analyzed using established laboratory techniques. This study aims to characterize the physical, chemical, and mineralogical properties of the mortars, both as integral units and as isolated binder fractions. The findings will enhance our understanding of the historical construction practices in Padua and provide a detailed narrative of the church's architectural evolution.

## 1.4 OUTCOMES

The dissertation aims to identify the mortar recipes and manufacturing techniques used in the construction of the Church of S. Michele. Key outcomes include:

- ∴ Detailed characterization of the physical and chemical properties of the mortar samples.
- ∴ Identification of mineralogical and chemical profiles of the binder fractions.
- ∴ Insights into the manufacturing techniques and recipes used in the early medieval period.
- ∴ Correlation of analytical results with historical context to reveal variations in construction methods over time.
- ∴ Creation of a comprehensive Building Information Modeling (BIM) model reflecting the church's historical evolution and structural integrity.

## **1.5 DISSERTATION OUTLINE**

- ∴ Chapter 1: Introduction to the study, including objectives, research context, and expected outcomes.
- ∴ Chapter 2: Overview of mortars, including definitions, types, properties, historical evolution, and current analytical approaches.
- ∴ Chapter 3: Detailed historical context of the Church of S. Michele, including its architectural significance and strategic location.
- ∴ Chapter 4: Geological context of Padua, focusing on potential sources of raw materials used in mortar production.
- ∴ Chapter 5: Methodology, including descriptions of analytical techniques and procedural details.
- ∴ Chapter 6: Presentation of raw data obtained from the analyses.
- ∴ Chapter 7: Discussion and analysis of results, including statistical analysis and contextual correlation.
- ∴ Chapter 8: Summary of findings, conclusions, and evaluation of the research process.
- ∴ Chapters 9-10: Relevant bibliography and appendices/annexes.



SANTI ARCHANGELI, VANZO 

# Chapter II: Historical Context

The key factors that remain for determining the age of the Oratorio di San Michele are:

1. The name "Santi Arcangeli" is associated with the site.
2. The strategic location of the Oratorio di San Michele.
3. The presence of Roman materials in the remaining walls.
4. The archaeological excavation report that is not accessible.
5. The earliest written record dates to 970.

None of these resources are sufficient to definitively date the Oratorio di San Michele or to identify the person who commissioned its construction. Therefore, this thesis aims to establish a more accurate date using C14 (radiocarbon) dating. However, it is crucial to analyze the historical context of ancient Padua to connect the dots and provide a more precise interpretation. The Oratorio di San Michele could have been erected during the Byzantine period, late antiquity, or perhaps after the Romans conquered the city. This chapter explores the Christianization of Padua during these periods and examines the various theories proposed by scholars and authors regarding the origin of this building.

## 2.1. CHRISTIANIZATION OF PADUA

Before the Christian era, Padua was a quintessentially Roman city, replete with robust fortifications, a bustling port, an extensive road network, a sewage system, a central forum, and various public buildings. The fragmentary nature of archaeological data from this period makes it challenging to fully reconstruct the city's pre-Christian landscape. Culturally and religiously, Padua was steeped in Roman traditions, characterized by a well-established urban infrastructure and a polytheistic religious culture that dominated every facet of life—setting the stage for the transformative introduction of Christianity.

From the late 3rd to the 5th centuries, Christianity began to establish its roots in the region. Early ecclesiastical structures started to appear, as evidenced by archaeological excavations dating back to the 4th century. The transition towards Christianity was not merely a religious shift but also intertwined with significant political changes across the broader region. The decline of the Roman Empire and subsequent administrative reorganizations during the Carolingian period played pivotal roles in shaping the Christian landscape of Padua. This era witnessed the emergence and consolidation of Christian communities, profoundly influenced by the existing Roman infrastructure and later by the sweeping socio-political changes. Archaeological findings highlight an active ecclesiastical presence and elaborate on the development of religious structures that catered to the

growing Christian population, underscoring a period of significant religious and cultural transformation in Padua (Chavarría Arnau, 2017).

The Oratorio di San Michele in Vanzo, initially dedicated to the Holy Archangels, first appears in written records from 970, as noted in a document during the episcopate of Bishop Gauslino. This document lists it among the assets of the monastery of Santa Giustina, describing it as "the church of the Holy Archangels, located outside the city of Padua in a place known as Vantio, along with its boundaries." There are earlier, contested references to a church of St. Michael from as far back as 828, though these are believed to pertain to St. Michael of Torre rather than the one in Vanzo (Colecchia, 2017).

The suburban basilica of Santa Giustina in Padua, established in the city's southern cemetery near a key route to Adria and 300 meters from the Roman walls, was instrumental in the political and military restructuring of Northern Italy under King Theodoric in the early 6th century. Its strategic location, along with similar sites, was vital for maintaining control over the region, connecting Padua to essential trade and military routes, and reinforcing Christian influence. Santa Giustina, along with other churches in Monselice and Este, likely formed part of a broader network of Gothic fortifications and religious centers, possibly with Arian associations, designed to strengthen Theodoric's authority (Brogiolo, 2017).

The establishment and significance of the Oratorio di San Michele in Padua, particularly its connection to Santa Giustina, highlights the intricate process of Christianization in Northern Italy, suggesting that sites like the Oratorio di San Michele may have been established or gained prominence as part of this broader reorganization effort.

## **2.2. THEORIES ABOUT THE AGE OF ORATORIO DI SAN MICHELE**

A document from 970 specifically mentions the church of S. Michele, initially referred to as "Ss. Arcangeli": "ecclesiam sanctorum Archangelorum, quae constructa est foris civitate Patavii, in loco, qui dicitur Vantio." This suggests that the church was located outside the city of Padua in a place called Vantio, near a canal that faced the Torlonga castle. The church's construction style and materials indicate its origin dates back at least to the Lombard period. The church is mentioned as being under the jurisdiction of the monastery of S. Giustina (1014). It is listed in all records of parish churches and appears as a "capella" (chapel) in documents from the late 14th century (Bellinati & Puppi, Padova Basiliche e Chiese – Parte Prima, 1975).



Between 563 and 602, Padua, like much of Northern Italy, was under the influence or control of the Byzantine Empire. This period followed the Gothic Wars (535-554), where the Byzantine Empire, under Emperor Justinian I, sought to reconquer Italy from the Ostrogoths and reestablish Roman rule over the Italian Peninsula. During this time, the Byzantines implemented administrative and military strategies to consolidate their control, including promoting Christian institutions that aligned with their religious and cultural policies. The establishment of churches dedicated to saints, particularly archangels like Michael, Gabriel, and Raphael, was common in Byzantine territories. These saints were revered in the Eastern Orthodox tradition, and their veneration was encouraged as part of the Byzantine strategy to integrate conquered territories into their cultural and religious sphere. The Oratorio di San Michele, originally known as "Ss. Arcangeli" (Holy Archangels), suggests that it may have been established during or shortly after this Byzantine period, when the influence of Byzantine Christianity was strong in the region. The dedication to the archangels, especially Archangel Michael, who was seen as a protector and warrior, aligns with Byzantine practices, making it a fitting dedication during a time of military and political turmoil. The Hungarian invasion of 899 led to widespread destruction, including the burning of the Cathedral and its archives, resulting in a significant loss of records that likely included earlier documents about the Oratorio di San Michele, thus obscuring much of its early history. The restructuring of Padua's ecclesiastical structure during the Carolingian period significantly impacted the Oratorio di San Michele. The synod of Cividale in 791, led by Patriarch Paulinus of Aquileia, reinforced the Nicene-Constantinopolitan creed, promoting unity with Rome and Catholic orthodoxy, which helped in establishing and strengthening local places of worship like the Oratorio di San Michele. Bishop Rodrigo's efforts in the mid-9th century to secure privileges from Emperor Louis II, echoing those from Charlemagne and Lothair, further solidified the oratory's status by confirming the bishop's ownership of baptismal churches and oratories (Bellinati & Puppi, Padova Basiliche e Chiese-Parte Seconda, 1975).

### **2.3. MANAGEMENT AND MAINTAINING PHASE**

- ∴ *12<sup>th</sup> century*: The oratory existed without a priest, congregation, or its own land. It was one of several small churches where private Masses and divine offices were held. "Fossam cum flumine quae est a capella sancti Michaelis usque and portum de ponte de Festumbas," indicating the area surrounding the Chapel of St. Michael, particularly the waters and lands from the chapel to the Festumbas bridge, was placed under strict control. No one could build mills, operate locks, establish fishponds, or erect structures without the bishop's permission. These restrictions and the bishop's authority over the area were officially confirmed and expanded on June 26, 1090, in favor of Bishop Milone. From around the year 1000 to 1808,

significant changes and the evolution of parishes, including the rise of chapels, influenced the Oratorio di San Michele.

- ∴ As Padua expanded beyond its ancient walls, oratories originally managed as "tituli" without the right to liturgical functions evolved into "chapels" with their own territories, congregations, and assets. By 1079, the church in Vanzo, initially known as the "church of the Holy Archangels," began to be identified as St. Michael, marking a shift in its identity and patronage. Throughout the 11th and 12th centuries, confirmations of the church's status and donations, such as those by Bishops Burcardo and Olderico, supported the oratory's role in the community.
- ∴ On March 15, 1123, Pope Callistus II placed the Monastery of St. Justina under apostolic protection at the request of Abbot Benzoni, confirming all its legitimate properties and jurisdictions. Notably, the Church of St. Michael the Archangel was not mentioned in this decree. Instead, other churches named St. Michael, along with St. Giuliana and St. Matteo, were listed as new donations. This raises the question of whether the title of "chapel" given to St. Michael in the imperial diploma of 1079 implied that the church already had some limited pastoral duties. Considering its suburban location in Vanzo and the tendency for older chapels to be situated far from the main church (the "Matrix"), it is likely that St. Michael did indeed have a pastoral role. Further documents trace the evolution of St. Michael's status. In February 1014, Bishop Orso of Padua reconfirmed the Monastery of St. Justina's properties. By the mid-11th century, the Cathedral of Padua had become the central parish, with St. Michael continuing as a chapel. Documents from 1034, 1064, and later reconfirm the donations and properties associated with St. Michael, highlighting its ongoing importance. St. Michael's chapel is first mentioned by name in the imperial diploma of July 23, 1079, when King Henry IV confirmed the church's assets and granted additional rights. By 1681, the rights and responsibilities of the church were managed by prominent Venetian families, who appointed priests to the parish, a practice that continued until 1822 (Beltrame G. , Anno XXV Feb).

## 2.4. RECONSTRUCTION AND EXPANSION PHASE



Figure 3:1117.01.03, Verona Earthquake with a magnitude of 6.9 with MMI IX Violent intensity Wikipedia – 1117 Verona Earthquake.

- ∴ **12th Century:** The Oratorio di San Michele was significantly impacted by the earthquake of 1117 and the fire of 1174, which caused extensive damage to Padua's religious structures. These events led to the reconstruction of the cathedral and other important churches, incorporating new architectural styles and reinforcing structures to prevent future damage. The Oratorio di San Michele was part of this broader effort to rebuild and enhance the city's religious infrastructure, solidifying its role in the community's spiritual life. In 1155 and 1170, documents mention the first known priest, Chaplain Arnaldo, serving St. Michael. By 1178, the chapel's boundaries were delineated, showing its suburban nature. The Oratorio di San Michele transitioned from a simple chapel to a significant part of the emerging parish system, serving not only as a place of worship but also as an integral part of the community's spiritual and administrative life.
- ∴ **13th Century:** By 1202, St. Michael was part of the Duomo district, and in 1221, it was listed among 16 sites in the "cartula dathie episcopatus" of Padua. This inclusion highlights the oratory's importance within the ecclesiastical structure of the city. The Oratorio di San Michele played a crucial role in the religious and social life of Padua, ensuring the bishop's influence extended throughout the city.



Figure 4:Frescos by Jacopo da Verona in Oratorio di San Michele.

- ∴ **14th Century:** The Oratorio di San Michele continued to be an important religious site. The Capel of Santa Maria was constructed in 1397 and adorned with frescoes by Jacopo da Verona, adding considerable artistic and cultural value to the church. This period marked an important phase in the development of oratory, with significant contributions from wealthy patrons, religious orders, and the community.
- ∴ The church was a site for significant burials and memorials, including those of prominent families such as the Carraras. Fina Buzzaccarini, the wife of Francesco I da Carrara, mentioned in her will date September 22, 1378, that masses for her soul should be held at San Michele, indicating her significant connection to the church. This function added to its religious significance, making it a place where the faithful could seek spiritual solace and eternal remembrance. The Carrara family, also known as the Carraresi, was a prominent noble family that played a significant role in the history of Padua, Italy, during the late Middle Ages and the Renaissance. Their influence spanned several centuries, particularly from the 13th to the 15th centuries, during which they were central to the political, cultural, and social life of the region. The Carrara family ruled Padua intermittently from the early 14th century until the late 14th century.
- ∴ Their governance was marked by attempts to maintain autonomy against the encroaching powers of neighboring states such as Venice and Milan. Their legacy includes contributions to the University of Padua, which became one of Europe's leading universities. The Carraras' ambition to maintain and expand their power inevitably led to conflicts with the Republic of Venice, a dominant regional power. The protracted struggle culminated in the fall of Padua to Venice in 1405. The capture of Francesco II da Carrara marked the end of the family's rule. The Venetians imprisoned and executed him, effectively dismantling the Carrara dynasty's control over Padua.



*Figure 5:Detail of I miracoli di Cristo. Fina Buzzaccarini alongside her husband Francesco I da Carrara and Italian poet Francesco Petrarca, Wikipedia- Francesco I da Carrara.*

- ∴ The inscription on a stone slab next to the fresco at San Michele Arcangelo likely outlines the church's historical and architectural significance, including its dedication to St. Michael, its architectural evolution, and notable restorations, especially those following Padua's recapture from the Visconti. Additionally, it likely mentions the church's role in local religious practices and its association with the Carrara family, who contributed to its artistic and cultural heritage through various commissions and donations.



*Figure 6: Chapel Bovi, South Wall, Inscription panel, 1398 (Tobias, 2013)*

- ∴ **15th Century:** In 1479, Pope Pius IV transferred St. Michael to the Canons Regular of the Holy Spirit of Venice, a significant religious order that established a convent adjacent to the church, which caused complaints from the previous monks. This connection to the Congregation marked a new chapter in the church's history, as it became part of a larger network of religious institutions. However, in 1556, the Church, along with its properties, was put up for auction by the Republic of Venice. This sale led to a series of ownership changes, starting with Don Domenico Mistura, who was the first to purchase the church. It then passed through several prominent Venetian families, including the Dolfin, Mocenigo, Soranzo, Pisani, and Rizzini families, each of whom contributed to its upkeep and management.
- ∴ **16th and 17th Centuries:** The Holy Spirit Congregation governed the parish until 1656 when Pope Alexander VII sold its assets. During this period, the oratory continued to serve the community, although it faced challenges due to changes in ownership and administration. Furthermore, in 1650, another Roman monument was found in the garden of St. Michael, reinforcing the site's long-standing historical importance. These discoveries highlight the deep historical roots of the church, connecting it to the ancient Roman past and underscoring its significance as a cultural and historical landmark in Padua. (Barzon, 1955)
- ∴ In the **18th century**, the Oratorio di San Michele experienced significant changes. In 1792, an unfortunate decision was made to repaint the oratory from top to bottom,

resulting in the loss of much of its original decoration. Despite this, Tomaso Soranzo managed to save the atrium and the Chapel of the Virgin, preserving some of the oratory's historical and cultural heritage.

- ∴ In the early **19th century**, significant changes affected the Oratorio di San Michele. In 1808, it ceased to be a parish due to safety concerns, leading to the relocation of the parish headquarters to the Sanctuary of the Madonna Addolorata del Torresino. Although the church continued to retain its bell tower and organ until 1810, it eventually faced severe deterioration. The church was officially closed on July 31, 1812, and partially demolished in May 1815, with only the Chapel of Pietro de' Bovi surviving, adorned with a small Gothic façade and the motto of St. Michael: "Quis ut Deus?" This marked the end of the Oratorio di San Michele as an active religious site, though its legacy persisted through the preserved chapel and its historical significance.
- ∴ The Church of St. Michael sits on a site rich with historical significance, evidenced by several archaeological discoveries. In 1888, G. A. Ferretto uncovered a Roman tombstone beneath a layer of plaster on the church's northwest wall. This stone, measuring one meter in length and inscribed with Roman characters and numerals, suggests the ancient origins of the site. (Barzon, 1955)
- ∴ The church, located near the Castel dei Carraresi, was demolished in 1880, and what remained of the site fell into disuse. During World War II, the remaining structures were occupied by a displaced person who repurposed the space as a carpenter's shop. This led to significant damage, including nails being driven into the walls and wood being piled up, which further deteriorated the remaining frescoes and the building itself. Today, the site was in a state of disrepair, with what is now a wood warehouse potentially hiding valuable frescoes by Jacopo da Verona. Visible remnants of these artworks include images of Madonnas, strong figures of saints, and an expressive face of a praying figure, particularly a moving depiction of the Virgin Mary nursing the Baby Jesus.
- ∴ Despite the closure, the Oratorio di San Michele continued to experience changes throughout the 19th century. Minor restoration efforts were made to prevent further deterioration, yet comprehensive preservation plans were not established. The once grand structure was reduced to the central part up to the height of the main door, with only the Chapel of Pietro de' Bovi remaining intact. These efforts, though limited, helped in maintaining a part of the oratory's historical and cultural heritage amidst the challenges of the time.

## 2.5. RESTORATION PHASE

In the early *20th century*, the Oratorio di San Michele continued to suffer from neglect and environmental damage, despite various attempts to raise awareness and secure funds for restoration. It wasn't until the 1960s and 1970s that local historians and scholars, including C. Gasparotto, began to systematically study the church's historical and artistic value. Gasparotto's research suggested that the church dated back to at least the second half of the 7th century, underscoring the importance of a thorough examination of the foundations and subsoil of S. Michele.

- ∴ Professor Claudio Bellinati played a crucial role in bringing renewed attention to the church during this period. In 1968-69, he conducted extensive research and published works highlighting the significance of the Church of S. Michele and its frescoes. His advocacy led to increased calls for serious restoration efforts, emphasizing the need for comprehensive preservation and restoration. This movement gained momentum, with scholars, local authorities, and art historians advocating for the church's preservation from the late 20th century to the present.
- ∴ Efforts have included thorough documentation and research of the frescoes and architectural elements, public awareness campaigns, and various funding initiatives. These initiatives have sought local government funds, private donations, and European cultural heritage grants. Proposed restoration plans have involved relocating the frescoes to a museum for protection and public accessibility, stabilizing existing walls, repairing the roof, and preserving remaining original architectural elements. Conservation efforts for the frescoes remaining in situ have focused on cleaning, stabilizing paint layers, and protecting them from further environmental damage.
- ∴ The Torresino community has actively participated in preservation efforts, holding meetings, discussing plans, and addressing the church's urgent needs. Ongoing and future projects aim to fully restore the church and its frescoes, ensuring their accessibility and preservation for future generations. Potential plans include establishing a dedicated museum space or a cultural heritage site for the church, restoring it to its former glory. (Bellinati, *San Michele da salvare*, 1971).
- ∴ A temple of art has been desecrated. The Superintendence of Monuments, Galleries, and Arts must intervene to restore the Oratory of San Michele to its former glory. 18-01-1947. (Catalogo collettivo fino al 1968)

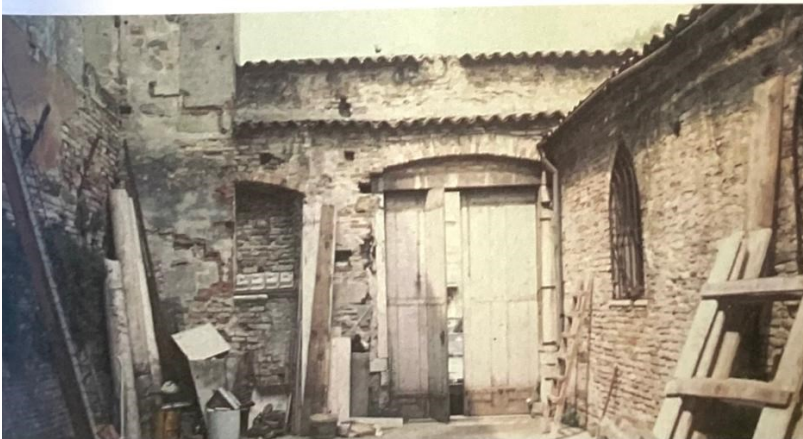
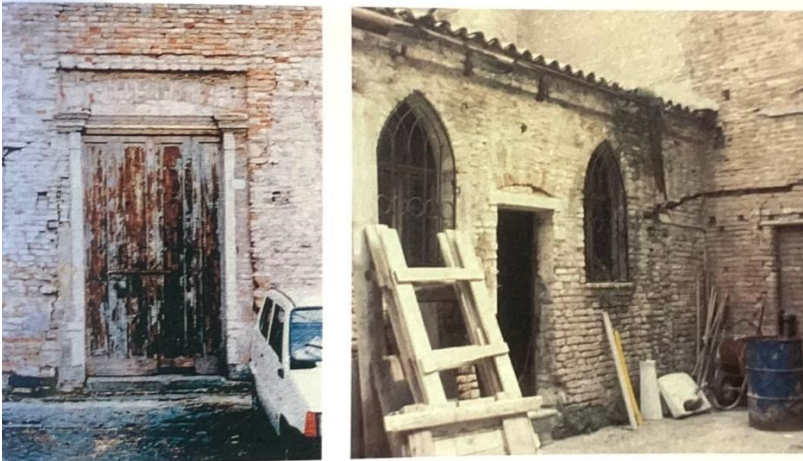


Figure 7: A.G.C.P. Gennaro Borsella, Photographic inspection, June 1990 (Talami, 2024).

B.C. BP. 1004 ~ 0,

Padova, Oratorio di S. Michele.

Un tempio dell'arte profanato.  
 Occorre che la Soprintendenza ai Monumenti  
 di Galliera e alle Opere d'Arte... intervengano  
 per rimettere in efficienza l'Oratorio di S. Michele...  
 In: «La Voce» dei campi, dei mercati... 18/vi/1947.

Figure 8: A request to restore oratorio di san michele, Padova from Biblioteca civica Padova.





Paleocapa bridge

Oratorio di San Michele

# Chapter III: Geographical Context

The Oratory of San Michele in Padua is located at latitude 45.4015° N, longitude 11.8697° E, on Riviera Tiso di Camposampiero, southwest of the city. Its topography is characterized by its position near the canal and the Torlonga castle, providing a strategic defensive location. The area was historically significant as it was once a Roman necropolis, indicated by the discovery of a trachyte funerary stone suggesting family tombs. The nearby Roman wall circuit, developed along the Meduacus Maior, played a crucial role in urban defense and flood containment, underscoring the strategic importance of this location.

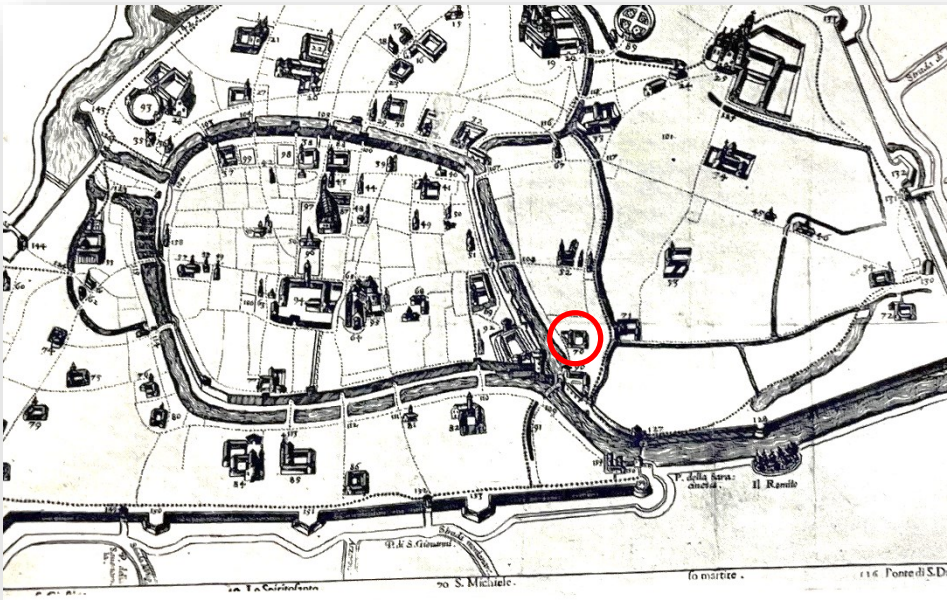


Figure 9: An old map of Padua's urban grid, from A. Portenari 1623.

## 3.1. SIGNIFICANCE IN THE ROMAN PERIOD

- ∴ Strategic Location and Urban Defense: The Oratory of San Michele's location was crucial during the Roman period due to its proximity to the Meduacus Maior (Bacchiglione River), the essential Paleocapa bridge, and the Roman wall circuit. This positioning served a dual purpose in urban defense and flood control. Firstly, the Roman wall circuit played a critical role in protecting the city from invasions. The walls were strategically designed to shield the urban center and its inhabitants, leveraging the natural defense provided by the river. By positioning these defenses near the waterway, the Romans maximized the natural barrier effect, making it more difficult for potential invaders to breach the city's defenses. This setup underscores the importance of the Oratory's location in the broader context of urban defense strategies employed by the Romans. Secondly, the site contributed significantly to managing

water flow and preventing flooding in the urban area. Situated near the canal, the location played a vital role in flood control, ensuring the city's infrastructure and population were safeguarded from the periodic flooding that could devastate urban settlements. The dual function of urban defense and flood control highlights the strategic foresight of Roman urban planners in selecting and utilizing this location.

- ∴ Roman Burial Practices: The use of the site as a necropolis underscores its importance in Roman burial customs. One notable artifact is the trachyte funerary stone, likely used to mark family tombs, reflecting the Roman practice of commemorating the deceased with durable and prestigious materials. This practice indicates the high social status of those buried at the site and their desire for lasting memorials. Roman burial customs often involved elaborate rituals and monuments, and the presence of such a necropolis highlights the reverence for the dead and the belief in an afterlife. The funerary practices provide valuable insights into Roman cultural and religious beliefs, particularly their views on death and the afterlife. The necropolis's elaborate nature and the use of high-quality materials for funerary markers signify the importance placed on honoring and remembering the deceased. Furthermore, the archaeological insights gained from the funerary artifacts at the site shed light on Roman funerary architecture and practices, offering a glimpse into the social and familial structures of the time. These artifacts not only reveal the technical skills and aesthetic preferences of the Romans but also their societal values and the importance of family lineage.



*Figure 10: An old map of the position of the Oratorio di San Michele (Beltrame G. Anno XXV Feb).*

- ∴ **Transition to Early Ecclesiastical Use:** The historical significance of the necropolis influenced its selection for early Christian religious purposes, demonstrating a continuity of sacred use. The transition from a pagan burial ground to a Christian religious site illustrates how early Christians often repurposed existing sacred spaces for their worship. This practice reflects the adaptability of early Christian communities and their strategic use of historically significant sites to establish their presence. The existing reverence for the site as a place of the dead made it a fitting location for constructing the Oratory. This reuse of sacred ground underscores the seamless transition from Roman to Christian religious practices, highlighting the continuity and transformation of sacred spaces across different religious and cultural contexts. The foundation of the Oratory on this historically significant site signifies the early Christian community's respect for the past while establishing their new religious traditions.

### **3.2. MILITARY IMPORTANCE IN THE LOMBARD PERIOD**

- ∴ **Lombard Utilization of Roman Infrastructure:** The Lombards, who ruled parts of Italy from the 6th to the 8th centuries, strategically adapted and reinforced existing Roman defenses. They recognized the value of the Roman infrastructure, such as the wall circuit and canal, for their own military strategies. By reinforcing these pre-existing defenses, the Lombards effectively utilized robust Roman engineering to bolster their own defensive capabilities. Proximity to the Torlonga Castle, a key defensive structure, further highlights the strategic importance of the Oratory's location. The castle's placement near the Oratory signifies its role in the broader network of defensive structures that protected the region. The Lombards' adaptation of these defenses reflects their strategic acumen in leveraging the existing infrastructure to enhance their control and defense of the area.
- ∴ **Military and Logistical Role:** The Oratory's location was crucial for military and logistical operations during the Lombard period. Positioned near the Paleocapa bridge over the Bacchiglione River, the Oratory was integral to the network of defensive structures ensuring the protection of key access points to the city. The bridge and the road system connected major routes, facilitating the movement of troops and supplies, which was vital for the region's defense and control. This connectivity ensured that the Oratory played a significant role in regional defense and logistics. The ability to move troops and resources efficiently across the river and along key routes was essential for maintaining control and responding to threats. The strategic location of the Oratory within this network underscores its importance in the broader military and logistical strategies of the Lombards.
- ∴ **Saint Michael's Dedication:** The dedication of the Oratory to Saint Michael, a revered protector and military figure, underscores its strategic and military significance during the

Lombard period. Saint Michael was often invoked as a guardian and warrior, symbolizing protection and strength. The dedication reflects the intertwining of religious reverence and military strategy, emphasizing the Oratory's dual role as a place of worship and a defensive stronghold. The choice of Saint Michael as the patron further signifies the Oratory's importance in the Lombard's military and religious landscape. By dedicating the Oratory to a powerful protector, the Lombards reinforced its role as a site of both spiritual and physical defense, aligning with their broader strategic objectives.

### **3.3. ECCLESIASTICAL SIGNIFICANCE AND ARCHITECTURAL EVOLUTION**

- ∴ Early Ecclesiastical Authority: The Oratory's early ecclesiastical significance is evidenced by its affiliation with the influential monastery of Santa Giustina. By 970, the Oratory was recognized as belonging to this prominent monastery, highlighting its importance within Padua's religious landscape. The monastery's management of numerous properties, including the Oratory, reflects its significant role in the region's ecclesiastical and economic affairs. Historical documents from 997 and 1190 reference the Oratory, indicating its established role in the ecclesiastical hierarchy. These references underscore the Oratory's enduring significance and its integration into the broader network of religious sites managed by Santa Giustina. The early ecclesiastical authority of the Oratory set the foundation for its continued importance in the region.
- ∴ Impact of Regional Conflicts: The 1390 fire, resulting from a battle between Francesco Novello and the Scaligeri, significantly impacted the Oratory. This event underscores the Oratory's proximity to conflict zones and its strategic importance during regional conflicts. The fire necessitated extensive architectural renovations, reflecting the need to restore and enhance the Oratory's structure following the destruction. The subsequent renovations, completed in 1397, transformed the Oratory's architectural style, incorporating new elements that reflected contemporary Gothic influences. These changes marked a significant evolution in the Oratory's architectural heritage, demonstrating its ability to adapt and evolve in response to external challenges. The impact of regional conflicts and the resulting architectural developments highlight the Oratory's resilience and significance in the region's turbulent history.
- ∴ Artistic and Architectural Developments: The post-fire renovations marked a notable evolution in the Oratory's architectural and artistic heritage. The addition of the northern chapel, frescoed by Jacopo da Verona, exemplifies the Gothic architectural style of the time. These artistic enhancements reflect the broader architectural trends and preferences of the medieval period, showcasing the Oratory's dynamic and evolving heritage. The incorporation

of Gothic elements during the renovations underscores the Oratory's commitment to maintaining its relevance and aesthetic appeal in the changing architectural landscape. The artistic developments, including the frescoes and structural enhancements, highlight the Oratory's role as a significant cultural and religious site. These changes illustrate the Oratory's continuous evolution and its ability to integrate contemporary styles and artistic expressions.

- ∴ Conclusion: The historical evolution of Contrà Vanzo and the Oratory of San Michele illustrates the area's enduring strategic and ecclesiastical importance. From its early recognition as a significant ecclesiastical site under the monastery of Santa Giustina to its strategic role in regional defense and connectivity, Contrà Vanzo has played a crucial role throughout various historical periods. The architectural and artistic developments, particularly the renovations following the 1390 fire, further highlight the region's dynamic heritage. Today, the Oratory of San Michele stands as a testament to the rich historical and cultural legacy of Contrà Vanzo, offering valuable insights into the region's past (Colecchia, 2017).



*Figure 11: Area of S. Michele and Capella Bovi in the map by Giovanni Valle, 1784 (Gasparotto, 1969).*



# Chapter IV: Stratigraphic Analysis

## 4.1. ARCHITECTURAL EVOLUTION BASED ON LITERATURE

### † Initial Phase of the Building

- ∴ The oldest written source from 970 explicitly mentions: "the church of the holy Archangels, which was built outside the city of Padua, in a place called Vantio." This indicates that the church was located outside the city walls, near the canal overlooked by the Torlonga castle, and had been established for some time.
- ∴ According to Gasparotto, S. Michele was a typical basilica church, of modest proportions (18.14 m x 9 m), with a classic east-west orientation (Gasparotto, 1969). The church of S.

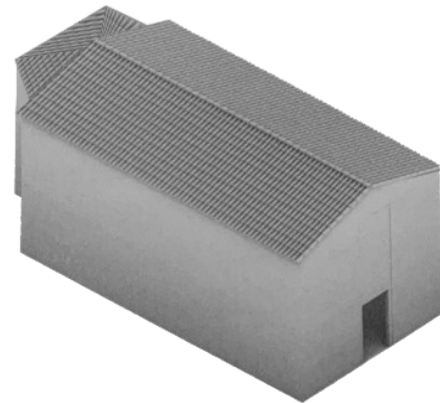


Figure 12: Reconstruction of the church in the 7th Century.

- Michele is distinguished by its extensive use of *Roman stone materials*, a practice that was quite common during the early medieval period. This reuse includes a variety of lapidary elements, decorative stones, and architectural fragments, which were incorporated into the church's construction. This practice was common during the early medieval period to utilize available resources. The rough opus murarium of S. Michele prominently features these repurposed Roman materials, showcasing not only practical building resources but also a continuity with the region's Roman past, reflecting the availability and significance of Roman artifacts in the architectural heritage of the area (Beltrame D. G., 2000).
- ∴ By 1014, the church was under the control of S. Giustina and was included among the chapels listed in parish records ( Bellinati & Puppi, Padova Basciliche e Chiese – Parte Prima, 1975), possibly integrating into many more *changes under the new patronage*.



## † 14<sup>th</sup> Century

∴ In the 14th century, thanks to the Carrara family, Padua became an important artistic-cultural center. In 1390, during the fight between Carraresi and Visconti, *the roof of the Church of San Michele was set on fire*. Francesco Novello da Carrara immediately financed the *reconstruction, housing altars made of Costozza stone and marble inserts, including the main altar dedicated to the Blessed Virgin*, and side altars with statues of Saint Francis of Paola and Saint Christopher.

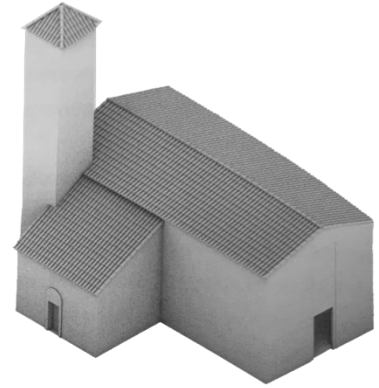


Figure 13: Reconstruction of 14th Century appearance (Talami, 2024).

- ∴ In 1397, Pietro de' Bovi commissioned the renovation of the Church, and the construction of *a chapel dedicated to the Blessed Virgin Mary*. There is limited contemporary documentation on Pietro de' Bovi, but he is identified in the frescoes and was likely closely tied to the Carrara court. The proximity of San Michele to the Carrara Mint has led to speculation about Pietro's occupation, but this remains unproven. The frescoes themselves, with depictions of contemporary figures and heraldic symbols, offer clues about the commissioner's identity and status (DUÒ, 2011).
- ∴ The chapel of the Madonna/Mary was built against the northern side of S. Michele with a passage arch from the main nave and *an adjacent bell tower*, standing 17.30 meters high, had three arches in the bell cell and a tiled roof. The new chapel was later known as the Bovi chapel/ Saint Mary Chapel.
- ∴ The chapel is dedicated to the Blessed Virgin Mary and contains *the fresco cycle of the Stories of the Virgin*. Francesco Jacopo da Verona decorated the walls of the Chapel and part of the nave, which is Jacopo's only signed work, including the fresco "Death of Mary" painted in 1398. Jacopo's style includes detailed everyday scenes that humanize the sacred narratives, drawing inspiration from prominent 14th-century masters like Giotto. The fresco cycle starts from the arch of access between the chapel and the nave, with the Annunciation, and continues counterclockwise around the chapel. The inclusion of portraits of contemporary figures, like the Lords of Padua and possibly the commissioner Pietro de' Bovi, showcases Jacopo's ability as a portraitist. Additionally, isolated votive images, such as Saint Michael weighing souls and Saint Louis of Toulouse, are part of the decoration. Despite damage and overlays, these frescoes remain vital for understanding the transition of the holy archangels to the church with Bovi Chapel. It is suggested that the fresco cycle originally included more episodes, possibly

located in a now-destroyed fore-chapel. This area might have contained scenes like the Crucifixion or the Baptism of Christ. The current arrangement and the survival of certain frescoes indicate significant changes from the original layout (DUÒ, 2011).

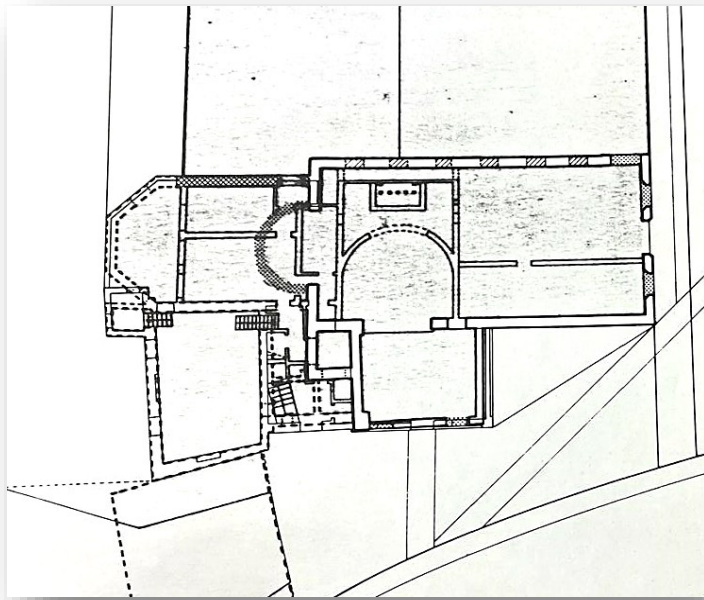


Figure 14: Reference plan supported the reconstruction models (Talami, 2024).

∴ S. Michele's *architectural design* adhered to a rectangular layout, a common feature in early Christian and medieval basilica architecture. Oriented along the east-west axis, the main entrance was typically located at the western end, with the altar at the eastern end, symbolizing the journey from the temporal world to the divine.

- Interestingly, historical records do not mention a bell tower, suggesting it was either not a prominent feature of the original construction or deemed insignificant by contemporary chroniclers and restorers (Bellinati, Padova Da Salvare, 1969).
- ∴ The *internal layout* featured a central nave extending from the entrance to the apse, serving as the primary gathering space. This central nave was flanked by narrower aisles separated by rows of columns or arches. The eastern end housed the apse, a semicircular recess for the altar, serving as a visual and spiritual anchor for the congregation. While not explicitly described, the roofing structure likely followed the typical two-section design of basilica churches, with a higher roof over the central nave creating a clerestory for additional windows. This higher roof facilitated natural light and structural stability, creating a luminous interior. The aisles had lower, sloping roofs that improved ventilation and light penetration into the nave, enhancing the interior environment.
  - ∴ The *structural and decorative elements* were integral to S. Michele's architectural identity. Columns or piers connected by arches separated the nave and aisles, supporting the roof and contributing to the aesthetic rhythm and harmony of the interior space. Notably, the church extensively reused Roman stone materials, including lapidary elements and architectural fragments, reflecting a desire to connect new Christian architecture with the region's Roman

past. This practice added historical depth and continuity to the church's architectural narrative, enriching its cultural and artistic heritage.

## † 15<sup>th</sup> Century

- ∴ In 1479, the church came under the control of the Venetian Holy Spirit Congregation. When this congregation ended in 1656, the Republic of Venice sold its assets, leading to the church's decline ( Bellinati & Puppi, Padova Basiliche e Chiese – Parte Prima, 1975) .

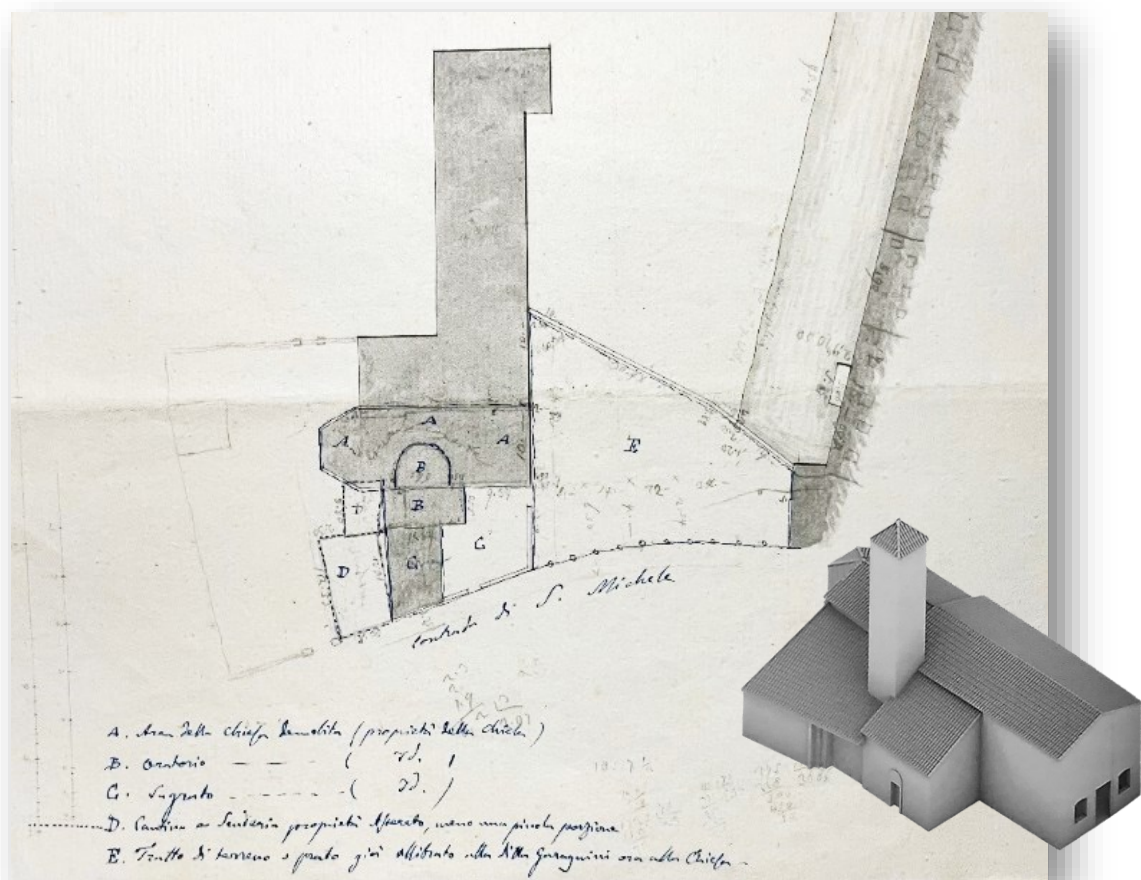


Figure 15: Reference plan supported the reconstruction models (Talami, 2024).

- ∴ A *significant transformation* occurred for the Church of San Michele when Pope Sixtus IV decreed the transfer of its ownership from the Carceri Monastery to the Monastery of the Canons Regular of the Holy Spirit of Venice. This change in stewardship was accompanied by a considerable expansion of the church's architecture, marking an important period in its historical development.
- ∴ One of the primary additions during this expansion was the construction of a *new presbytery*. Elevated by two steps above the nave, the presbytery measured 10.90 meters in length and 6.60 meters in width. It featured a decorated tabernacle, which added to the aesthetic and spiritual significance of space. To ensure proper illumination for the choir, windows were

strategically placed within the presbytery walls. This elevation and enhancement of the presbytery highlighted the importance of the liturgical functions within the church.

- ∴ Adjacent to the presbytery was the anti-temple, or *vestibule*, which housed a baptismal font. This font was located on the left side as one entered, surrounded by a balustrade, signifying its importance in the church's rites and ceremonies. The sacristy, also adjacent to the presbytery, was another critical addition. Measuring 8.28 meters in length and 6 meters in width, the sacristy was accessed through a door in the longitudinal left wall of the presbytery. Its ceiling was decorated with a shell motif based on a stucco frame, adding to the ornate interior design of the church and providing a space for the clergy to prepare for services.
- ∴ The *church's bell tower* was another significant architectural feature added during this period. Standing 2.06 meters square at the base and rising to 17.30 meters high, the bell tower featured a decorative frame at the level of the bell cell, which contained three arches. Above this frame was a tiled roof, giving the tower a distinctive and elegant appearance.
- ∴ Surrounding the church was a *churchyard* that covered approximately 265.42 square meters. This area was enclosed by a masonry parapet covered with Costozza stone, and it had two entrance openings, one facing north and the other west, both decorated with stone pillars. This design provided a defined and protected space for the congregation and visitors.
- ∴ The floor plan with *viewer locations and lines of sight* offers insight into the intended interactions and perceptions of the church's space, enhancing our understanding of its historical and cultural significance. The floor plan of San Michele Arcangelo with Cappella Bovi, reconstructed by Tobias Ertel in 2010, provides a visual representation of various viewer locations and lines of sight based on the historical spatial experience of the church. Spatial Experience refers to how individuals interact with and perceive the physical space within the church.

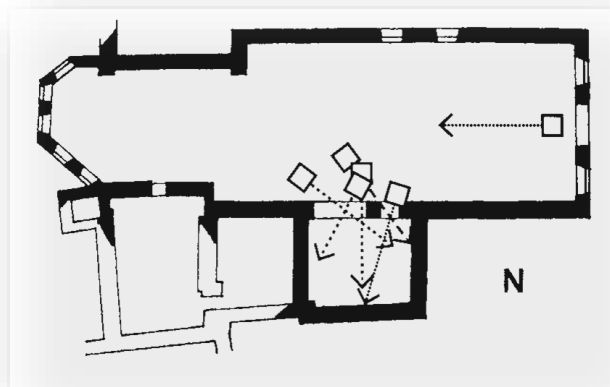


Figure 17: San Michele Arcangelo with Cappella Bovi, Padua: Floor plan showing various viewer locations and lines of sight based on the historical spatial experience (reconstruction by Tobias Ertel, 2010).

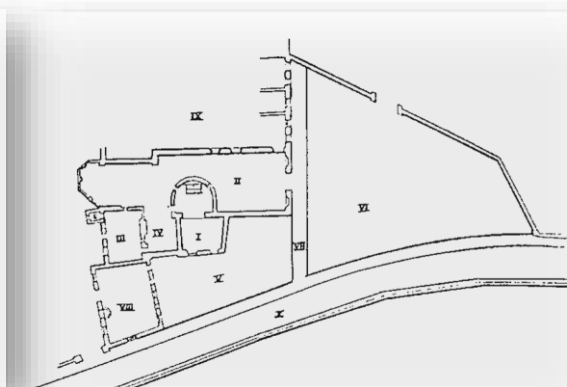


Figure 16: Plan of the San Michele Arcangelo Complex with Cappella Bovi on Riviera Tiso da Camposampiero (1816-1876) (Maiolo, 2001).

- ∴ This involves understanding how different areas of the church were designed to guide movement, focus attention, and create specific experiences for viewers. Key aspects include *Viewer Locations* where individuals typically stood or moved within the church, such as during services, processions, or while viewing artworks. *Lines of Sight*, that illustrates the visual pathways, showing what viewers could see from different locations within the church.
- ∴ This includes the views of altars, frescoes, and architectural elements. Understanding the historical spatial experience helps in appreciating how the church's design influenced religious practices and the congregation's experience. It highlights the intentional placement of artworks and architectural features to enhance the spiritual and aesthetic experience of visitors providing an accurate depiction of how the church was originally intended to be experienced, contributing to historical and cultural studies of the site.

## † 18<sup>th</sup> Century

- ∴ 1774, Gaetano Andreis, who became parish priest in 1774, ordered that the Church of San Michele be *completely whitewashed*, erasing much of its artwork. Tommaso Soranzo, after becoming obscenely aware of this order, ordered that this measure be blocked. When communication of this decision was received, a large part of the Church had already been repainted, but the Chapel of the Virgin was saved. By 1792, the church was whitewashed, and in 1808, it ceased functioning as a fortress. A few years later, it was



*Figure 18: Visible proof of whitewashing.*

- demolished. However, the chapel dedicated to Mary, created by the Fa de' Bovi family, was preserved. It was given a modest Gothic façade and contains a well-known cycle of frescoes, despite being in precarious condition ( Bellinati & Puppi, Padova Basciliche e Chiese – Parte Prima, 1975).
- ∴ Among the *notable figures buried* there was *Abbot Domenico Cerato*. He was a significant figure buried at the Church of S. Michael in Padua. Cerato, an influential architect and

professor at the University of Padua, was involved in various architectural projects in the city, including the transformation of the Specola tower into an astronomical observatory completed in 1777. This work was part of his broader contributions to the architectural landscape of Padua during the 18th century. Domenico Cerato was an influential religious figure, possibly holding a high ecclesiastical position such as abbot. His burial in the Church of S. Michael signifies his importance in the religious community of Padua. The exact date of his burial is not readily available from the sources consulted, but his death occurred in 1792, which suggests his burial at the Church of S. Michael would have happened around that time (Toffanin, 1988).

## † 19<sup>th</sup> Century

- ∴ 1815, The Church of San Michele was closed in 1812 and left to fall into ruin. In May 1815, the demolition and *renovation work on the Chapel of the Virgin Mary* began. The roof of the nave and the presbytery were demolished. The main façade and the left wall of the nave were halved in height and the two windows on the west wall were blocked. A cylindrical wall was also built characterized by a covering of beams arranged in a radial pattern.
- ∴ 1864, In 1854 the first requests to reopen the Oratory were made, but they were not granted by the court. In October 1863 the Municipal Congregation urged the Fabbriceria to have the Oratory of San Michele *restored to worship*. In June 1864 a positive outcome was achieved, but in order to reopen this abandoned place, work was carried out so that the Oratory communicated with a house, so as to allow a caretaker to closely monitor the property.
- ∴ 1874-77: In a letter addressed by the Fabbriceria to the Conservation Commission, the state of deterioration of the complex was reported and the need to provide light and ventilation for the

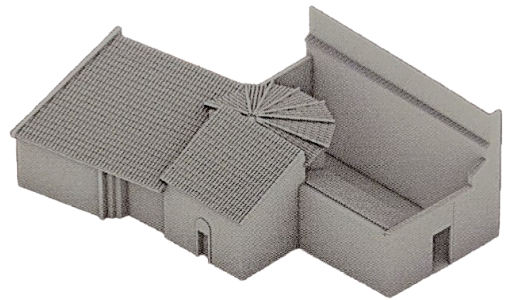


Figure 19: Reconstruction of 1815 appearance (Talami, 2024).



Figure 20: Reconstruction of 1864 appearance (Talami, 2024).

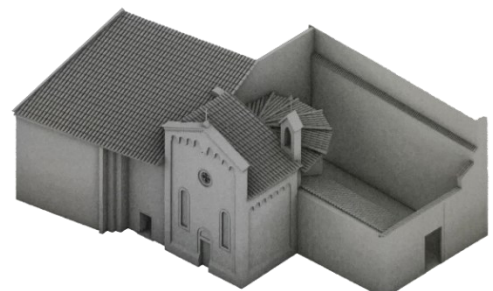


Figure 21: Reconstruction of 1874-77 appearance (Talami, 2024).

frescoes was highlighted, so that they did not suffer rapid deterioration. It was therefore proposed to *raise the existing side walls and build a new façade*.

- ∴ The house communicating with the Oratory, whose construction had been started with the aim of hosting the custodian of the Oratory of San Michele, was almost finished in 1877 but it was proposed to shift the intended *use towards a public purpose*, namely the creation of a work school for poor girls. In May 1880 the patronage of girls and with was inaugurated in the sacristy. In the same year an extension was built to make the Oratory healthier and more suitable for

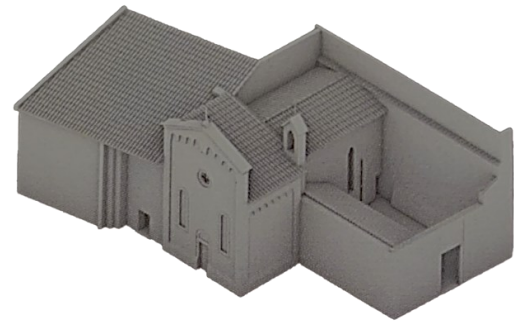


Figure 22: Digital Reconstruction of 1880 appearance (Talami, 2024).

- worship, opening an arch on the semicircular apse and building a wall that delineated a new perimeter. Furthermore, a fake marble floor was laid, and a Gothic Hall was built. The church and the Bovi Chapel underwent significant structural alterations between the late 1700s and early 1800s, which affected the original structure and the preservation of the frescoes. Restoration efforts in 1871, prompted by the Commission for the Conservation of Public Monuments of Padua, helped reopen the church for worship. However, the frescoes have suffered from environmental damage and the use of dry pigments, leading to a loss of the original color (DUÒ, 2011).
- ∴ Over centuries, the church and its frescoes have suffered from neglect and environmental damage. The frescoes have faded, and the structural integrity of the church has weakened. The Superintendence reported the *occupation of the Oratory by a carpenter*. At that time nails had been nailed and wood piled up on the walls. Only in 1949, thanks to the intervention of the Superintendence itself, was it possible to free the place from the carpentry shop (Bellinati, Padova Da Salvare, 1969).

## ∴ 20<sup>th</sup> Century.

- ∴ There have been appeals from local authorities, art historians, and scholars to restore the chapel and protect the frescoes. These calls highlight the church's importance and the urgent need for conservation efforts. One proposed solution is to relocate the frescoes to a museum where they can be preserved and protected from further damage. This would also make them more accessible to the public and researchers. Various campaigns have aimed to raise awareness about the church's condition and gather support for its restoration. Maria Atzori's

thesis at the Academy of Fine Arts in Venice provides a comprehensive study of the frescoes by Jacopo da Verona, emphasizing their artistic value and historical context. Luigi Montobbio's work underscores the importance of the church and its artworks, advocating for immediate preservation actions. These scholarly contributions include unpublished photographs, historical documents, and detailed descriptions of the frescoes and the church's architecture (Bellinati, Padova Da Salvare, 1969).

- ∴ In 2021, UNESCO recognized the frescoes of the Oratory of San Michele as a world heritage site, part of the Padova Urbs Picta site ("Painted City"). The main building has a rectangular plan along the North-South axis, with an adjoining room that serves as a ticket office and courtyard, originally the nave of the Church. The roof of the nineteenth-century chapel, hidden by a wooden false ceiling, is made up of two pitches supported by trusses and beams arranged in a radial pattern (Talami, 2024).

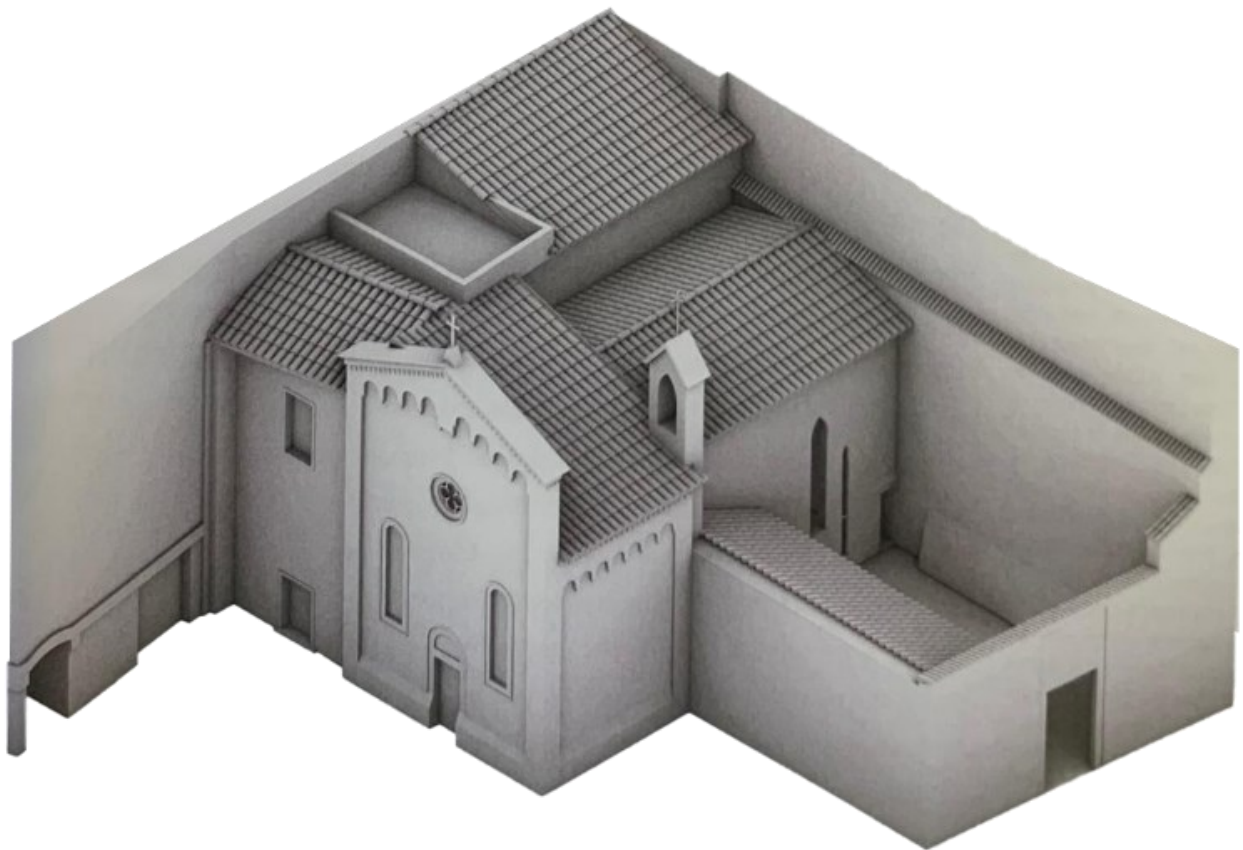


*Figure 23: Digital Reconstruction of the current appearance of oratorio di San Michele (Talami, 2024).*



## 4.2. STRATIGRAPHY OF THE REMAINING WALLS

The integration of BIM with stratigraphy and archaeometry analysis was proposed by Professor Alexandra, who also oversaw the project, to analyze the Oratorio di San Michele. This interdisciplinary approach aimed to provide a comprehensive understanding of the Oratory by combining advanced Building Information Modeling (BIM) techniques with detailed archaeological and material analysis through Archaeometry. This method allows for a more accurate reconstruction and interpretation of the historical and architectural development of the Oratory, offering valuable insights into its preservation and study.

Stratigraphy is the study of rock layers (strata) and layering (stratification), primarily used in geology to understand the natural accumulation of materials over time. There are three primary methods to study buildings: typological analysis, material analysis, and stratigraphical analysis. Stratigraphy in the context of buildings involves examining the different construction layers and phases to reconstruct the history of a structure. Central to the practice of stratigraphy is the Law of Superposition, which suggests that in an undisturbed stratigraphic sequence, the oldest layers are at the bottom, with progressively younger layers above them. Unlike geological stratigraphy, the stratigraphy of buildings often cannot be observed in its complete three-dimensional form unless parts of the building are ruined or removed. Additionally, in architectural stratigraphy, it is not always the case that lower layers are older. Nonlinear sequences can occur due to renovations, additions, and repairs, which might involve the removal or covering of earlier layers. The stratigraphy of buildings reveals information about construction sequences, construction sites, and post-depositional activities. The accuracy of a stratigraphic analysis largely depends on the experience of the operator, the sampling strategy, and the clarity of the stratigraphy.

- **Stratigraphic Unit (SU):** The Stratigraphic Unit is the material result of a single, homogeneous constructive action. It is the most detailed element into which a stratification can be divided. Each unit represents a distinct construction event or activity and is identified by variations in material, construction techniques, or function.
- **Interface:** The interface is the boundary line between one stratigraphic unit and another, marking transitions between construction phases, offering crucial insights into the chronological development of the building.

Buildings can generally be analyzed in three different states: standing buildings, ruined buildings, and buried buildings. Understanding the sequence of a building is essential not only for comprehending its construction process and history but also for Sampling materials like mortars for absolute dating / archeometric analysis.

### 4.3. METHODOLOGY OF THE STRATIGRAPHIC ANALYSIS

The first step in stratigraphical analysis involves creating detailed photographic records of the building. These records should capture all visible layers and features, ensuring that every aspect of the structure is documented for further analysis. In some cases, this can also include a georeferenced Ortho mosaic generated using Meta shape technology, providing a comprehensive visual overview of the building.



Figure 24: Recording the walls through photographs.

**Scheda Architettura Storica**

**Oratorio di San Michele, Padova**

Edificio

ID EDIFICIO     CATASTO MODERNO     CATASTO STORICO

INDIRIZZO  
Piazzetta San Michele 1, Riviera Tiso Camposampiero 38, Padua, 35122

UBICAZIONE	N° PIANI	MATERIALE COSTRUTTIVO		
Nucleato <input checked="" type="checkbox"/>	<input type="text" value="01"/>	Pietra <input type="checkbox"/>	Laterizio <input type="checkbox"/>	Misto <input checked="" type="checkbox"/>
Isolato <input type="checkbox"/>				

DESCRIZIONE

The building located at number 38, Via Riviera Tiso Camposampiero, consists of two main structures: a newer church and two remaining walls from an older church on the north and east sides. The underground foundation of the east wall is exposed within an excavation pit, where a tomb was discovered. The northern facade features a rectangular marble door with an ancient brick arch, flanked by two arched windows on either side. The east and north walls showcase mixed masonry, incorporating reused funerary stones and Roman bricks. Approximately one-quarter of the old church, extending from the north to the south, has been repurposed as a museum reception area and an exhibition gallery, while the southernmost end of the old structure remains undetermined. The remaining walls are not plastered with clear indications of previous plastering. Architectural analysis of the church's initial stage suggests a rectangular floor plan, with entrances on the east and north sides, accompanied by two arched windows on the north side and a buried site beneath the structure.

DOCUMENTAZIONE FOTOGRAFICA

Foto Generali     Fotopiano     Prospetto

STRATIGRAFIA VISIBILE	<input type="text" value="5"/>	N° APERTURE SCHEDATE	<input type="text" value="1"/>
TECNICHE MURARIE CAMPIONATE	<input type="text" value="2"/>	N° CAPITELLI SCHEDATI	<input type="text" value="1"/>
PRESENZA DI CHIAVI - TIRANTI	<input type="text" value="0"/>		

ARCATE DI PORTICO	ELEMENTI DI REIMPIEGO	NOTE/MISURAZIONI
N° di Arcate <input type="text" value="3"/>	Yes. Reused funerary stone and Roman bricks... 30xWx06 cm	ARCH MEASUREMENT: • VERTICAL: 3.8 M • HORIZONTAL: 2.35M
Tipo di Arco <input type="text" value="Semi Circular"/>		
N° Pilastri <input type="text" value="0"/>		

Following the photographic documentation, a basic recording of the building is carried out. This includes assigning a Building ID and noting the cadaster number or street number. A detailed description of the building is also recorded, encompassing the materials used and the construction techniques employed. Additionally, precise measurements of the building's dimensions are taken to ensure accurate records.

Figure 25: A basic recording form, for stratigraphy of the Oratorio di San Michele.

The next phase involves the identification, delimitation, and numbering of Stratigraphic Units (SUs). The boundaries of each SU are carefully marked with a line to differentiate them from one another. It's important to note that no line should be used to signify Associated Elements (AE) that are contemporaneous with the wall. The numbering system for these elements begins with 1001 for SUs and 101 for AEs, ensuring a systematic approach to the analysis.

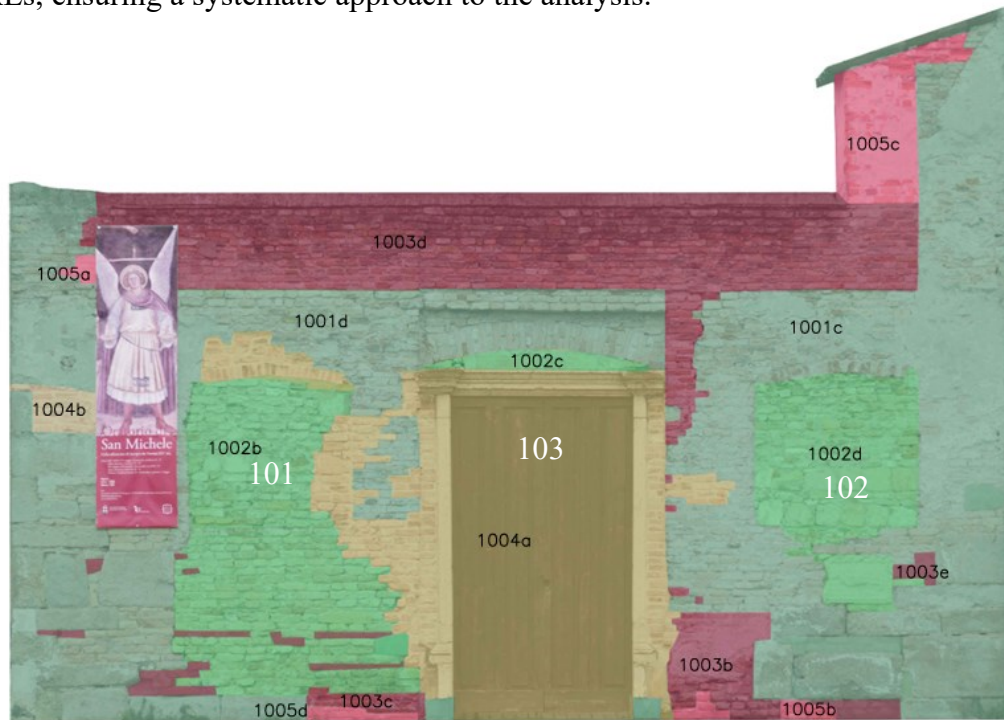


*Figure 26: Identification of Stratigraphic units in the North wall.*

#### **4.4. RESULTS OF THE STRATIGRAPHIC ANALYSIS**

Although the exact age of Oratorio di San Michele remains uncertain, it exhibits a complex architectural evolution marked by the reuse of materials from different periods. This complexity makes it challenging to date the original structure based solely on the morphology of the materials present. To address this, six mortar samples were collected from different locations within the building, guided by a stratigraphic analysis of the remaining walls. Then a detailed analysis of the mortars and binders used in the building's various phases was conducted, providing a more robust dataset to trace its architectural development and structural stability.

This analysis was focused on three key areas of the structure, believed to be the oldest based on the materials used: the northern façade, the eastern wall, and the underground eastern section of an excavation pit. The stratigraphic examination of these areas revealed five distinct phases of construction, identified through careful visual inspection and measurement. This approach helps to piece together the building's historical narrative, offering insights into its construction and the different stages of its development over time.

A. Stratigraphy sequence of North Wall



Figure 27: Orthophoto of North wall.

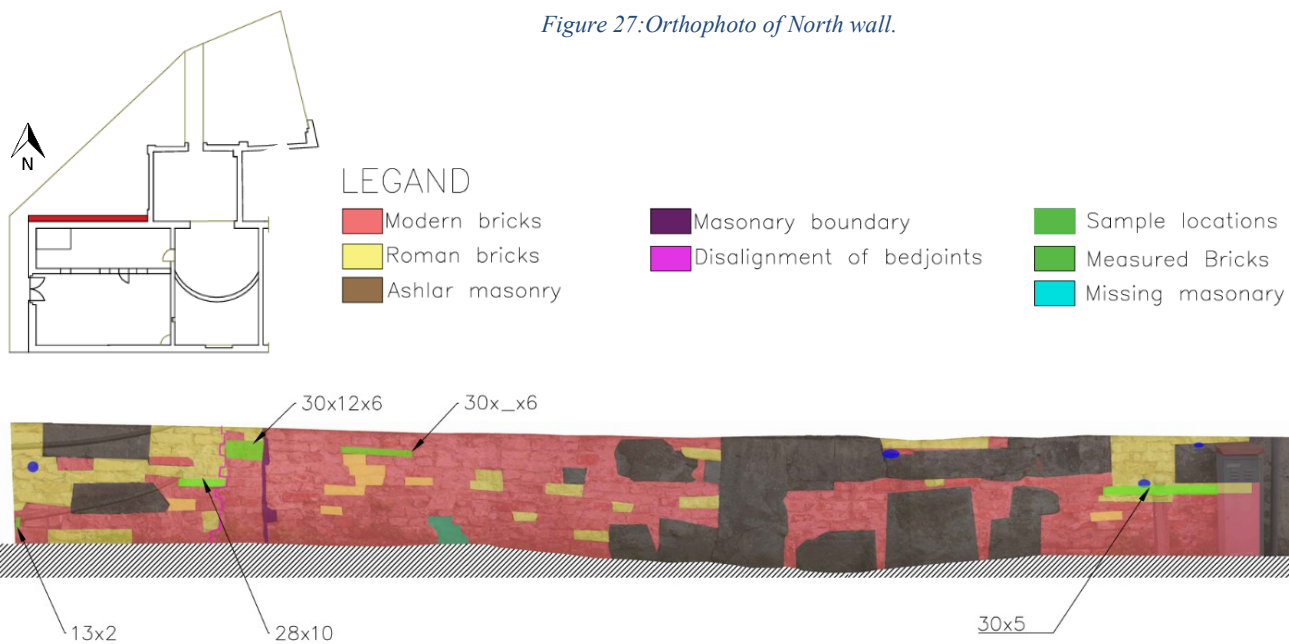


Figure 28: Material study of North wall, all measurements are in cm.

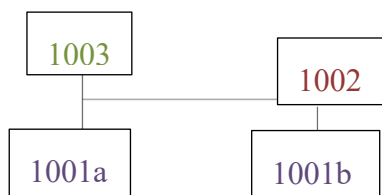


Figure 29: Stratigraphy sequence of North wall.

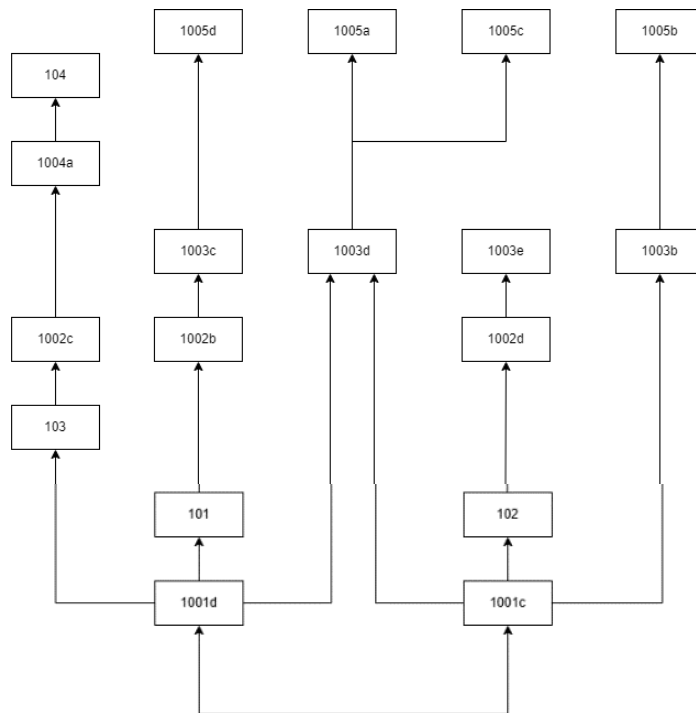


Figure 30: Stratigraphic analysis of North wall.

*B. Stratigraphy sequence of West Wall*



*Figure 32: Orthophoto and the position of the West wall.*



*Figure 33: Stratigraphy Sequence of West wall.*

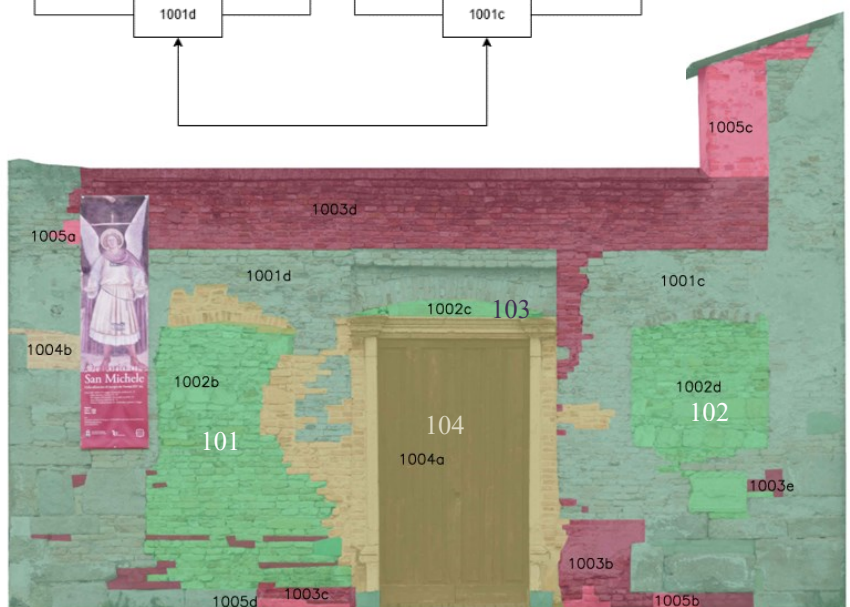


*Figure 31: Stratigraphy Analysis of West wall.*

C. Stratigraphy sequence of North wall in the Excavation pit.

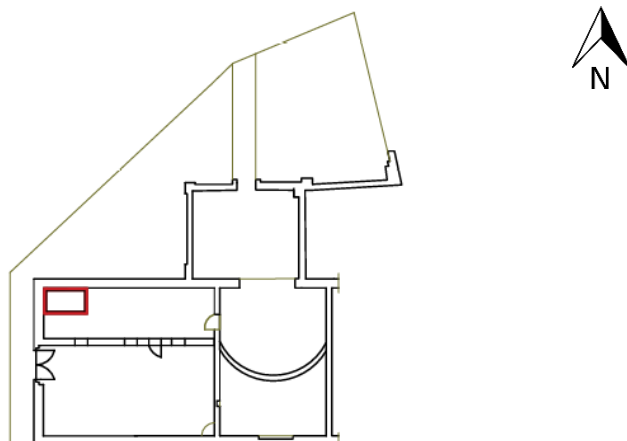


Figure 34: Position of the Northern excavation wall.



Figure 35: Orthophoto of the Northern excavation wall

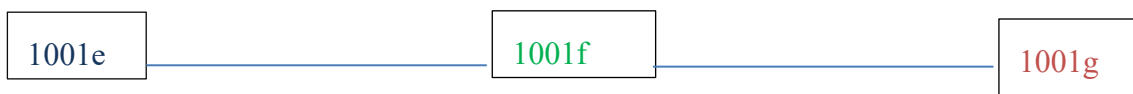


Figure 36: Stratigraphy sequence of Northern excavation wall.



Figure 37: Stratigraphy analysis of Northern excavation wall.

## 4.5. DISCUSSION OF THE STRATIGRAPHIC ANALYSIS

The stratigraphy of remaining walls was somewhat complex with a collage of materials belonging to different phases but mainly five phases were identified based on the shapes, color and characteristics of mortar and the materials.

- ∴ **Phase 01 (1001)** - Phase 1 is identifiable through specific sections in the building: 1001a and 1001b in the north wall, 1001c and 1001d in the west wall, and 1001e, 1001f, and 1001g in the north excavation wall. The defining feature of this phase is the use of mixed masonry, incorporating a variety of materials, including cut stone blocks, bricks and Roman bricks measuring 60x12x6 cm. The reuse of materials, characteristic of the medieval period, reflects the environmental and political challenges of the time. Consequently, Phase 1 is considered the oldest phase of the building.
- ∴ In the north excavation walls, three distinct layers are visible, corresponding to the different functional areas of the wall, such as the foundation (1001g), vertical tomb walls (1001f) and Horizontal joint of the tomb wall (1001e). In both the west and north walls, the boundaries of Phase 01 are defined by the separation from other phases, although the material characteristics remain consistent across these areas. This phase represents the foundational construction of the building, marked by the strategic reuse of materials available during the medieval period.
- ∴ The architectural features in the west wall that belong to Phase 1 include an arched door (103) and two semicircular arched windows (101L, 102R). These windows show signs of collapse at their lower edges, and the door was later modified with a marble upgrade during the fourth phase of the building's development. The damage to these features could have occurred during the Hungarian invasion in 889 or possibly because of the conflict between the Carrara family and the Visconti in 1390. Given that the refilling materials are relatively modern, it is likely that Phase 2, which took place in the 14th century, involved both restoration efforts and renovations aimed at expanding the building.
- ∴ **Phase 02 (1002)** - Phase 02 likely dates to the 14th century and is associated with the expansions and renovations carried out by the Carraresi family. Evidence of this phase can be seen in the north wall as 1002a, and in the west wall as 1002b, 1002c, and 1002d, where refilling work was done around the left window, the door, and the right window. The work during this phase utilized reused materials, including funerary stones and variously sized bricks. A key characteristic of Phase 02 is that it involved hasty refilling, with irregularly shaped bricks and reused materials placed without proper bed joints, suggesting a rushed construction effort.

- ∴ **Phase 03 (1003)** – There is 1003a strata in the north wall and 1003b, 1003c, 1003d, and 1003e strata in the west wall. This phase possibly belongs to renovations after the 18th century. It is obvious that phase three doesn't have any kind of a whitewashed layer on top of it because in 1774, Gaetano Andreis, who became the parish priest in 1774, ordered that the Church of San Michele be completely whitewashed. Tommaso Soranzo, after becoming obscenely aware of this order, ordered that this measure be blocked. By 1792, the church was whitewashed, and in 1808, it ceased functioning as a fortress. These plasters may depict a phase that has extended the walls using new materials to have better stability and suitability for its function.
- ∴ **Phase 04 (1004)** – The main characteristic of this phase is white grouting and regular bricks in regular courses. It is a renovation of the grouting between bricks using a very white mortar that is present in 1004a strata in the West wall along with 401, a marble arched door. The door could have been already there or replaced during this era with new, more regular bricks and mortars following regular courses.
- ∴ **Phase 05 (1005)** – Visible as 1005a, 1005b, 1005c, and 1005d in the west wall, this phase depicts the most recent materials from the building, appearing in bright red colors and unique shapes and sizes that are also visible in the interior fillings of the west wall. 1005c could have been a part of the bell tower as well. These possibly belong to 20th-century restorations around the time it became a UNESCO World Heritage site.



*Figure 38: Reconstruction of Oratorio di San Michele in Sketchup 3D warehouse.*

#### 4.6. CONCLUSION OF THE STRATIGRAPHIC ANALYSIS

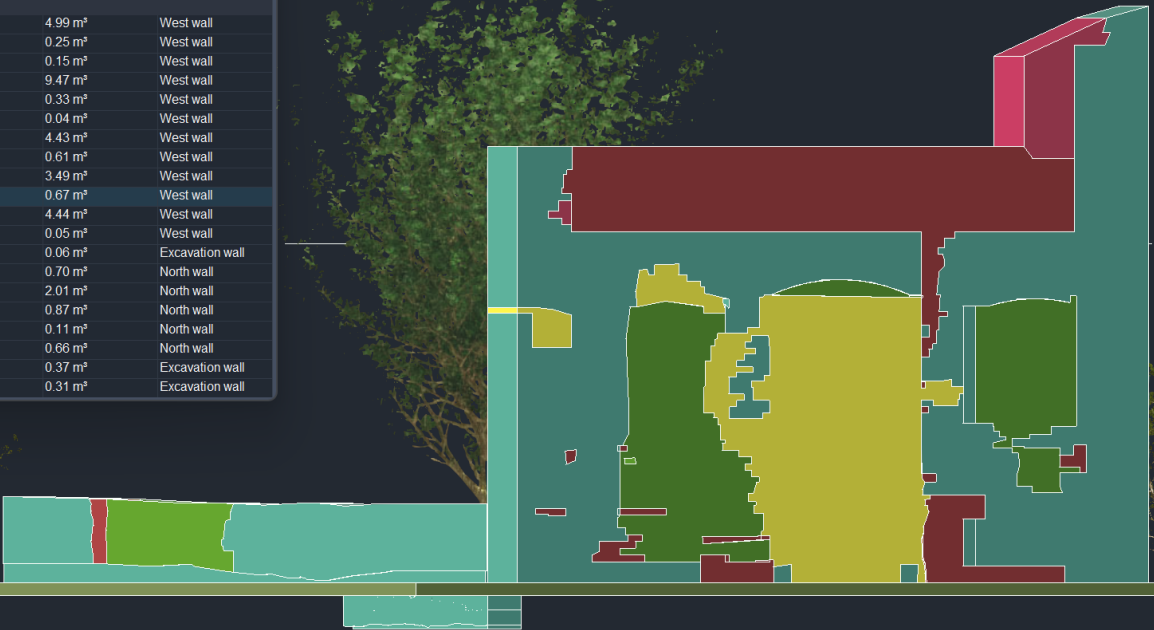
Following the stratigraphy, the oldest stratum suitable for dating the initial structure was identified as 1001, from which a total of six samples were collected. Four samples came from the west excavation wall: SM\_01 from stratum 1001e, SM\_02 and SM\_04 from stratum 1001f, and SM\_03 from stratum 1001g. SM\_05 was collected from stratum 1001c of the west wall, while SM\_06 was taken from stratum 1001a in the north wall. These efforts aimed to identify the most suitable mortar sample for Carbon-14 dating, fulfilling the primary goal of the study.



Final revit file .rvt - Schedule: Wall Material Schedule

<Wall Material Schedule>

A	B	C	D
Type	Area	Volume	Comments
1004	9.42 m <sup>2</sup>	4.99 m <sup>3</sup>	West wall
1004	0.46 m <sup>2</sup>	0.25 m <sup>3</sup>	West wall
1004	0.29 m <sup>2</sup>	0.15 m <sup>3</sup>	West wall
1001	17.87 m <sup>2</sup>	9.47 m <sup>3</sup>	West wall
1003	0.62 m <sup>2</sup>	0.33 m <sup>3</sup>	West wall
1003	0.07 m <sup>2</sup>	0.04 m <sup>3</sup>	West wall
1003	8.36 m <sup>2</sup>	4.43 m <sup>3</sup>	West wall
1003	1.15 m <sup>2</sup>	0.61 m <sup>3</sup>	West wall
1001	6.59 m <sup>2</sup>	3.49 m <sup>3</sup>	West wall
1005	1.26 m <sup>2</sup>	0.67 m <sup>3</sup>	West wall
1002	8.37 m <sup>2</sup>	4.44 m <sup>3</sup>	West wall
1003	0.09 m <sup>2</sup>	0.05 m <sup>3</sup>	West wall
1001	0.11 m <sup>2</sup>	0.06 m <sup>3</sup>	Excavation wall
1001	1.32 m <sup>2</sup>	0.70 m <sup>3</sup>	North wall
1001	3.79 m <sup>2</sup>	2.01 m <sup>3</sup>	North wall
1002	1.64 m <sup>2</sup>	0.87 m <sup>3</sup>	North wall
1003	0.20 m <sup>2</sup>	0.11 m <sup>3</sup>	North wall
1001	1.24 m <sup>2</sup>	0.66 m <sup>3</sup>	North wall
1001	0.70 m <sup>2</sup>	0.37 m <sup>3</sup>	Excavation wall
1001	0.58 m <sup>2</sup>	0.31 m <sup>3</sup>	Excavation wall



# Chapter V: Historic Building Information Modeling

## 5.1. INTRODUCTION TO BIM

- ∴ **Building Information Modeling (BIM)** represents the digital transformation's core in the architecture, engineering, and construction (AEC) industry. Originating from the advancements in early computer-aided design (CAD) technologies during the 1970s and 1980s, BIM began with simple 2D drafting and evolved to include basic 3D modeling. However, these early models lacked the dynamic, "intelligent" capabilities that modern BIM systems encapsulate, which integrate comprehensive data about the properties and functions of building components.
- ∴ The evolution of BIM was significantly influenced by Charles M. Eastman's pioneering work in the late 1970s, particularly his development of parametric modeling. Eastman's research introduced a computational methodology to manipulate design geometry algorithmically using parameters, which laid the foundation for sophisticated BIM processes (Chuck Eastman, 2011). This technique allows for design identities to be defined by malleable properties rather than fixed shapes, enabling the use of visual programming to graphically assemble programs and features.
- ∴ This concept of BIM was revolutionized with the creation of Revit in 2000 by Revit Technology Corporation, co-founded by Leonid Raiz and Irwin Jungreis. Revit was designed to fully exploit BIM capabilities, allowing architects and other building professionals to design in 3D, incorporate 2D annotations, and manage data across the building's lifecycle systematically. After Autodesk acquired Revit Technology Corporation in 2002, Revit was integrated into Autodesk's suite of design tools, establishing it as a cornerstone of BIM applications, although it was not the first software to support BIM methodologies. Today, BIM extends beyond mere 3D spatial modeling to include 4D (time scheduling) and 5D (cost management), which enhances collaboration among stakeholders and improves efficiency and sustainability within the AEC industries. The American Institute of Architects succinctly defines BIM as "a model-based technology linked with a database of project

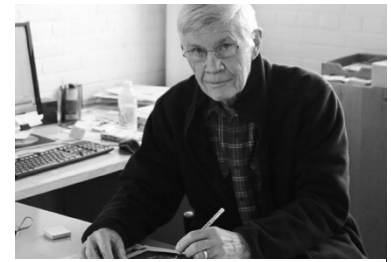


Figure 39: Father of BIM, Charles M. Eastman (Farias, 2020)



Figure 40: Software used for HBIM

(BIM) work process (Rocha, Luis Mateus, Fernandez, & Ferreira, 2020) information" (Chuck Eastman, 2011). This progression from basic CAD to advanced BIM marks a significant evolution in how building projects are planned, designed, and managed, fundamentally transforming practices across the AEC sectors and making Autodesk a leader in BIM, helping the industry achieve better working methods and outcomes.

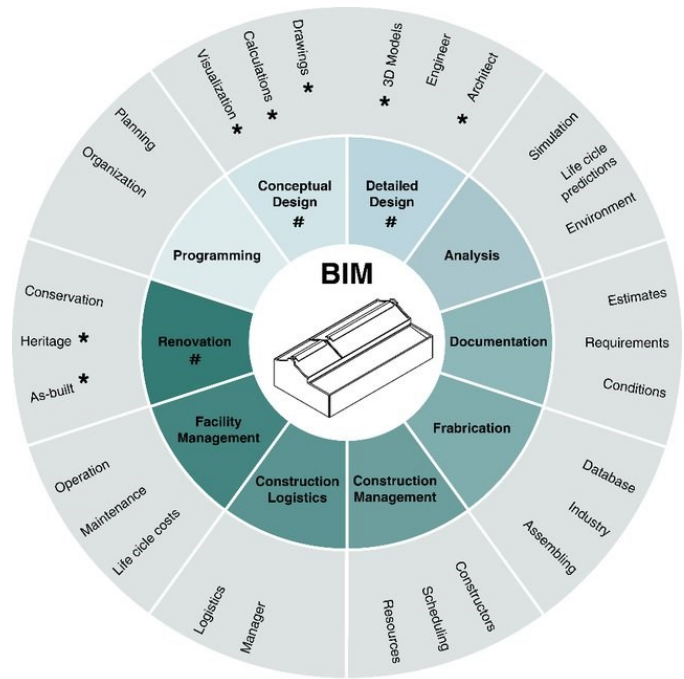


Figure 41: Diagram of a Building Information Modeling (BIM) work process (Rocha, Luis Mateus, Fernandez, & Ferreira, 2020).

∴ **Historic Building information modelling (HBIM)** is a specialized form of BIM adapted for heritage buildings, focusing on maintaining, managing, and restoring historical structures using digital technology. Murphy describes HBIM as a parametric modeling approach that incorporates both the geometrical and attribute data of architectural elements from historical databases (Maurice Murphy, 2009). While standard BIM practices are well-established for modern buildings through uniform procedures, applying BIM to heritage buildings presents unique challenges due to their complex shapes and the detailed surveys required. This results in more extensive data collection, increased costs, and higher time investments. Key concepts in HBIM like modeling tolerance and level of development (LOD) help manage these challenges by defining the precision and detail in the models, which accommodate the irregularities common in historical structures.

∴ **Modeling Tolerance** in HBIM refers to the degree of accuracy to which a model represents the actual physical dimensions and irregularities of a historic structure. Setting appropriate modeling tolerances involves deciding how precisely these

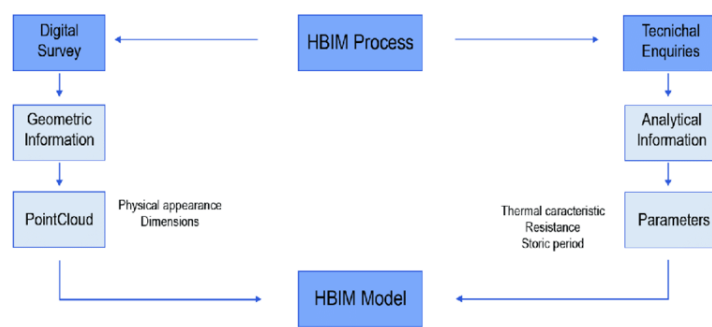


Figure 42: Diagram of a HBIM work process.

irregularities need to be captured in the HBIM model. For example, a high tolerance might be necessary when detailed conservation work is required, where understanding minute details like cracks or unevenness is crucial. Conversely, a lower tolerance might be sufficient for general management or maintenance tasks, where such fine details are less critical to the operations.

- ∴ *Level of Development (LOD)* specifies the detail and accuracy of the information included in the HBIM model at various stages of the project. It defines what elements of a building are to be modeled and how detailed the information should be at each stage of the design, construction, or restoration process. LOD is typically categorized into levels that ascend in detail from basic massing (LOD 100) to highly detailed specifications (LOD 500):
  - LOD 100: The model contains basic massing data about size, shape, location, and orientation.
  - LOD 200: Generic placeholders representing approximate quantities, size, shape, location, and orientation are added.
  - LOD 300: The model has precise architectural details and specific material representations.
  - LOD 400: Includes detailed fabrications, assembly, and construction details.
  - LOD 500: The model reflects the as-built condition, serving as a base for maintenance and operations.
  
- ∴ In historical buildings, higher LODs are often necessary to accurately represent the complex features and craftsmanship of the structure. Each level of development helps stakeholders understand the amount of detail available and ensures that the model meets the specific needs of the project at various phases. The use of Building Information Modeling (BIM) typically streamlines the design and construction process by reducing repetitive tasks through automation and the use of parametric architectural element libraries as well.
  
- ∴ The integration of photogrammetry and laser scanning into the Historical Building Information Modeling (HBIM) workflow offers significant benefits for understanding of a site by capturing its current condition, which is essential for detecting errors, monitoring changes over time, and producing accurate as-built documentation. Photogrammetry and laser scanning are critical in environments where traditional surveying is impractical or too time-consuming, such as on large-scale sites or structures with difficult access. They help to streamline traditional survey processes, reducing repetitive tasks and freeing up time for more critical activities like detailed modeling and analysis. The data from these techniques are compiled into point cloud files that represent the building's detailed geometry.

- ∴ However, effective use of these technologies requires careful consideration of several factors. For photogrammetry, it's essential to have overlapping images with consistent lighting to ensure comprehensive data capture. For laser scanning, considerations include avoiding occlusions and ensuring thorough coverage of the environment to facilitate accurate model construction.



Figure 43: a photogrammetry model of Oratorio di San Michele, using a drone (Talami, 2024).

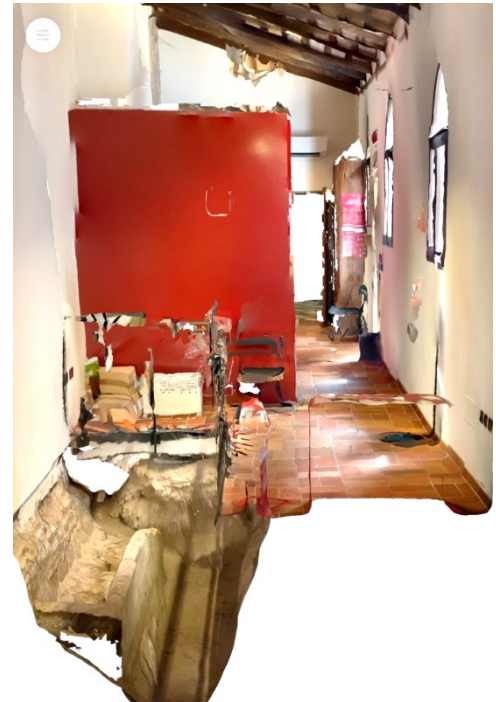


Figure 44: LIDAR Model of a part of the oratorio di San Michele using 3d Scanner app.

- ∴ A growing need to store and share information and models of architectural heritage has prompted scholars to test different ways to approach the HBIM. They still show some limitations, but not so much in the integration between different kinds of data. The case study of the Oratorio di San Michele primarily focuses on integrating the stratigraphy of the remaining walls with the archeometric analysis of binders using Building Information Modelling (BIM).

- ∴ **To Date and to Remodel Early Phases of the Building:** Understanding the chronological development of a building is essential for accurate historical documentation and restoration. Dating allows historians and conservationists to identify the different construction phases, which is crucial for accurate historical interpretation and

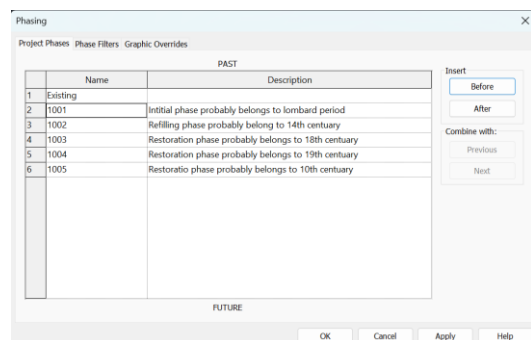


Figure 45: Phasing Tool for Dating and Remodeling Early Phases, AutoCAD Revit.

preservation. This involves the use of techniques like stratigraphic analysis, carbon dating, and other archaeological methods to determine the age of various building components. By remodeling these early phases in a digital environment, such as through Building Information Modelling (BIM), it becomes possible to visualize how the structure evolved over time, providing a clear understanding of its historical context.

- ∴ **To understand Structural Vulnerability:** Knowing the structural weaknesses of a building is critical for ensuring its safety and longevity. Identifying vulnerabilities helps in making informed decisions about necessary reinforcements or other interventions to prevent potential collapse or damage. Structural analysis often involves studying the materials used, the construction techniques, and the current condition of the building. Advanced modeling tools, like finite element analysis (FEA) within a BIM environment, can simulate how the building might respond to various stressors, such as earthquakes, heavy loads, or environmental degradation. This information is crucial for planning reinforcements.

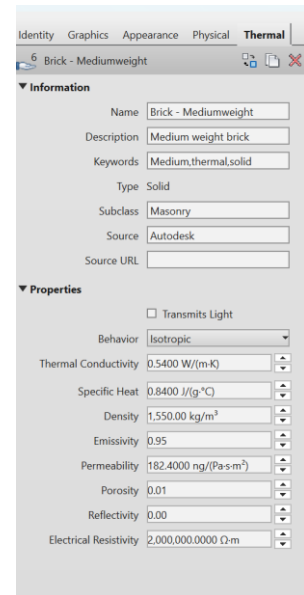
	Name	Case Number	Nature	Category
1	DL1	1	Dead	Dead Loads
2	LL1	2	Live	Live Loads
3	WIND1	3	Wind	Wind Loads
4	SNOW1	4	Snow	Snow Loads
5	LR1	5	Roof Live	Roof Live Loads
6	ACC1	6	Accidental	Accidental Loads
7	TEMP1	7	Temperature	Temperature Loads
8	SEIS1	8	Temperature	Seismic Loads

Figure 46: Structural Analysis Tool for Structural Vulnerability, Auto CAD - Revit

- ∴ **To manage Future Disasters:** A solid understanding of the building's structural integrity and historical evolution is crucial for disaster preparedness. This knowledge allows for the development of contingency plans to protect the building from future disasters like earthquakes, fires, or floods. Disaster management involves creating a detailed risk assessment and emergency response plan based on the building's vulnerabilities. This includes identifying critical areas that require reinforcement, such as load-bearing walls or foundations, and planning for rapid response to mitigate damage in the event of a disaster.
- ∴ **To determine where to add reinforcements:** Reinforcements are often necessary to preserve the structural integrity of historic buildings, especially those that are vulnerable to collapse or degradation over time. Knowing where to add these reinforcements ensures that interventions are effective and minimally invasive. Structural engineers, using tools like BIM, analyze the building's load distribution and material properties to determine the best locations for reinforcements. This might involve adding steel beams, buttresses, or other supports in strategic locations to strengthen the building without altering its historic character.
- ∴ **Sampling for Future Analysis:** Selecting appropriate locations for material sampling is important for ongoing conservation efforts. Samples taken from the building can be

analyzed to determine the composition and properties of materials used, which is crucial for restoration and conservation work. Using BIM and other analytical tools, conservationists can map out the building and select locations that will yield the most informative samples without compromising the structure. These samples can then be analyzed for chemical composition, microstructure, and other properties to inform future restoration efforts.

- ∴ **Material and Mortar Analysis:** Understanding the materials and mortars used in historical construction is key to preserving the authenticity of the building during restoration and repairs. Material analysis typically involves examining the composition and source of building materials, while mortar analysis focuses on the binders and aggregates used. Techniques such as X-ray diffraction (XRD), scanning electron microscopy (SEM), and chemical analysis are often employed. This information can guide the selection of compatible materials for repairs or reconstructions.



*Figure 47: Ability to integrate mechanical, thermal and physical properties to the 3D model, Auto CAD - Revit.*

- ∴ **Determining Mechanical Strength of Construction Techniques:** Understanding the mechanical strength of historical construction techniques is essential for assessing the building's current condition and planning for any necessary reinforcements. This involves testing the mechanical properties of the materials and construction techniques used, such as compression strength, tensile strength, and shear resistance. These tests can be performed on samples or through non-invasive methods. The results are used to assess the building's capacity to withstand various forces, informing decisions about potential reinforcements.
- ∴ **Geolocation of Materials:** Identifying the origin of materials used in construction helps in understanding historical trade routes and sourcing methods, which can be important for historical accuracy in restoration. By analyzing isotopic compositions or using other geological techniques, researchers can often trace the materials back to their original quarries or production sites. This geolocation can be mapped in BIM, providing valuable insights into map the old trade routes and to the historical context of the building's construction too.

Each of these processes contributes to a comprehensive understanding of a historic building, ensuring that conservation efforts are informed, precise, and respectful of the structure's historical significance. Integrating these approaches through BIM and other advanced tools allows for better preservation and management of cultural heritage.

## 5.2. METHODOLOGY OF BIM ANALYSIS

The creation of Building Information Model (BIM) for the Oratorio di San Michele faced significant challenges due to the lack of a measured drawings. However, since the main goal was to analyze the key stratigraphy of the building, the focus was narrowed down to three selected walls, making the task more manageable. The detailed methodology for this process is outlined below.

- I. *Data Collection:* The initial phase of data collection and preparation commenced with the acquisition of photographs of selected walls using a Leica Camera. These images were subsequently processed with Adobe Photoshop to generate orthophotos, which serve as precise, scaled representations of the building's surfaces.



Figure 48: 3D scanner app in iOS used for LIDAR of Oratorio di San Michele

In addition to the orthophotos, historical plans of the Oratorio di San Michele were gathered to serve as reference materials. To address any gaps in measurement data, a measured drawing was produced utilizing a Milesee Laser Scanner for reference in Auto CAD. To further document the existing physical structure of the building, laser scanning technology (LIDAR-Light Detection and Ranging) was employed. A 5th generation iPad Pro equipped with the application called 3D Scanning App was utilized to scan the entire building, encompassing the remaining walls as well as both the exterior and interior spaces. This process generated a detailed digital record of the building's current condition.

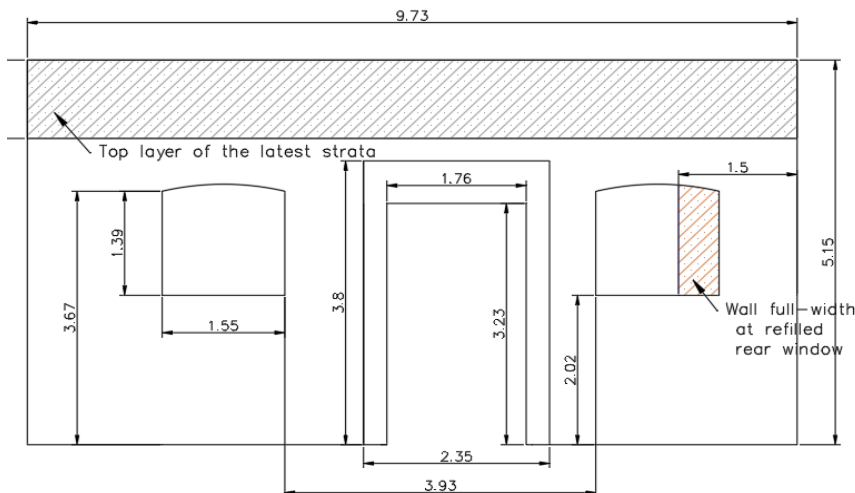


Figure 49: Autocad drawing of the measurements of the West wall, measured by Milesee Laser scanner with a 2mm +/- precision. All measurements are in Meters.



- II. Tracing to Revit: A crucial aspect of the process involved aligning the laser scan data with the orthophotos to ensure integration within a common coordinate system, essential for creating a unified and cohesive model in the BIM software. This was followed by importing the orthophotos and the historical map into the BIM software Revit to trace building's layout and features. The tracing process was meticulously executed by importing PDFs and images of floor plans, along with the point cloud data retrieved from LIDAR scanning, into the modeling to ensure accurate alignment with precise dimensions.
- III. A In the process of historical annotation of the BIM model, historical construction phases were created using Revit's Phase tool and documentation capabilities. A PDF document containing the orthophoto of the walls with stratigraphy was scaled to real size and used as reference material. The point cloud models were not used for stratigraphy segmentation as they did not render properly. To cut an irregular shape into the wall, the following steps were executed: Component > Model In-Place was selected under the Architecture tab, with "Walls" designated as the category. In the Family Editor, Void Forms from the Create tab was chosen, and Void Extrusion was used to sketch the required shape. The void was then aligned and positioned within the wall. The Cut tool under the Modify tab was applied to subtract the void from the wall. The process was completed by exiting the in-place family mode.
- IV. Structural Analysis: The primary goal was to identify sample locations and integrate data from mortar analysis into the wall stratigraphy. A wall material schedule was created in Revit, focusing on five specific areas, each highlighted with different colors for clarity. To generate this schedule, the process began by navigating to the View tab and selecting Schedules > Schedule/Quantities. "Walls" was chosen as the category, and relevant fields such as Material: Name, Material: Area, and Material: Volume were added to the schedule properties. The finalized schedule provided a detailed overview of the materials used in the walls, along with their respective areas and volumes, and was subsequently placed on a sheet or exported for further analysis.
- V. Export: The BIM model was finalized, ensuring all elements were accurately represented and fully integrated with the historical data. A final validation was conducted by cross-referencing the model with all available data sources to guarantee precision. The model was then exported in multiple formats, including 3D views, PDFs, and PNGs, for inclusion on a website to enhance the study's interactivity and to complement the mortar analysis.

### 5.3. RESULTS OF BIM ANALYSIS



Figure 50: Data tracing from LIDAR models.

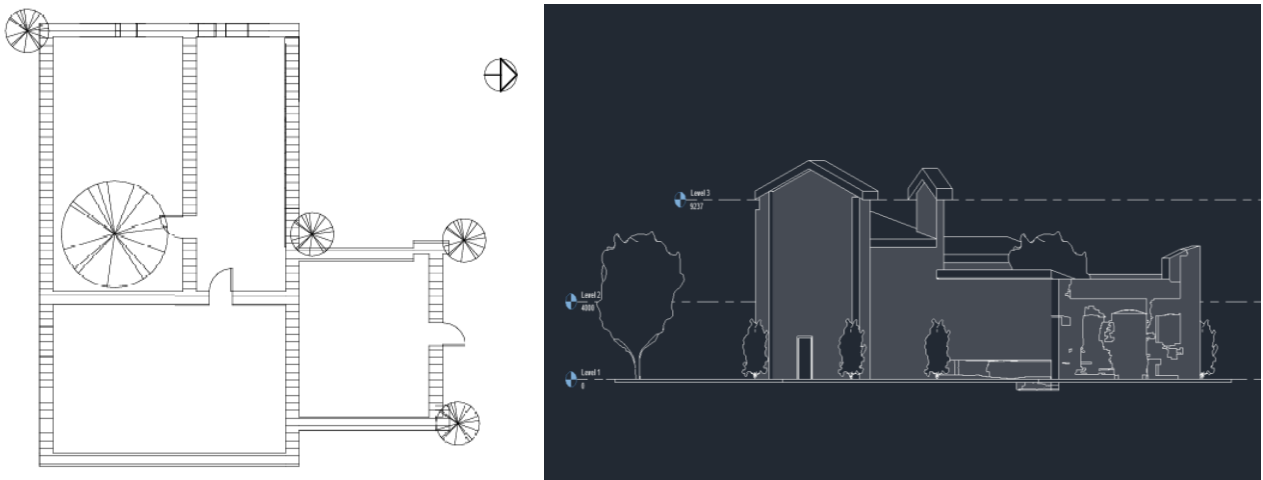
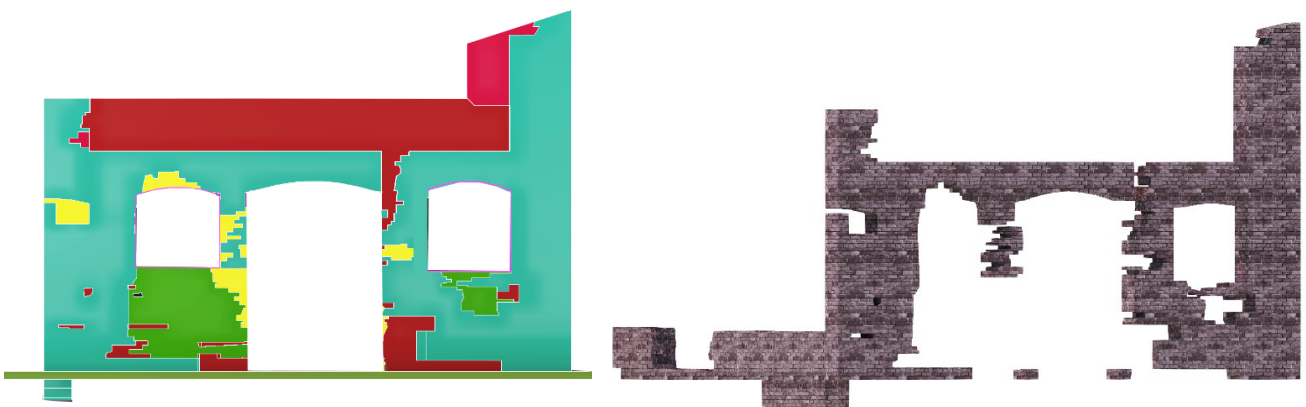


Figure 51: Creating the model based on the floor plan.



Phasing

Phase Filter Show Previous

Phase 1001

Project Phases Phase Filters Graphic Overrides

PAST

	Name	Description
1	Existing	
2	1001	Intitial phase probably belongs to lombard period
3	1002	Refilling phase probably belong to 14th century
4	1003	Restoration phase probably belongs to 18th century
5	1004	Restoration phase probably belongs to 19th century
6	1005	Restoratio phase probably belongs to 10th century

Figure 52: Using the Phasing feature to visually observe different stratigraphy of all the walls together.



Figure 53: Using unique colors to symbolize different stratas from the oldest to most recent as 1001 to 1005.



Figure 54: Creating the oldest to most recent construction phases as different stratigraphies.

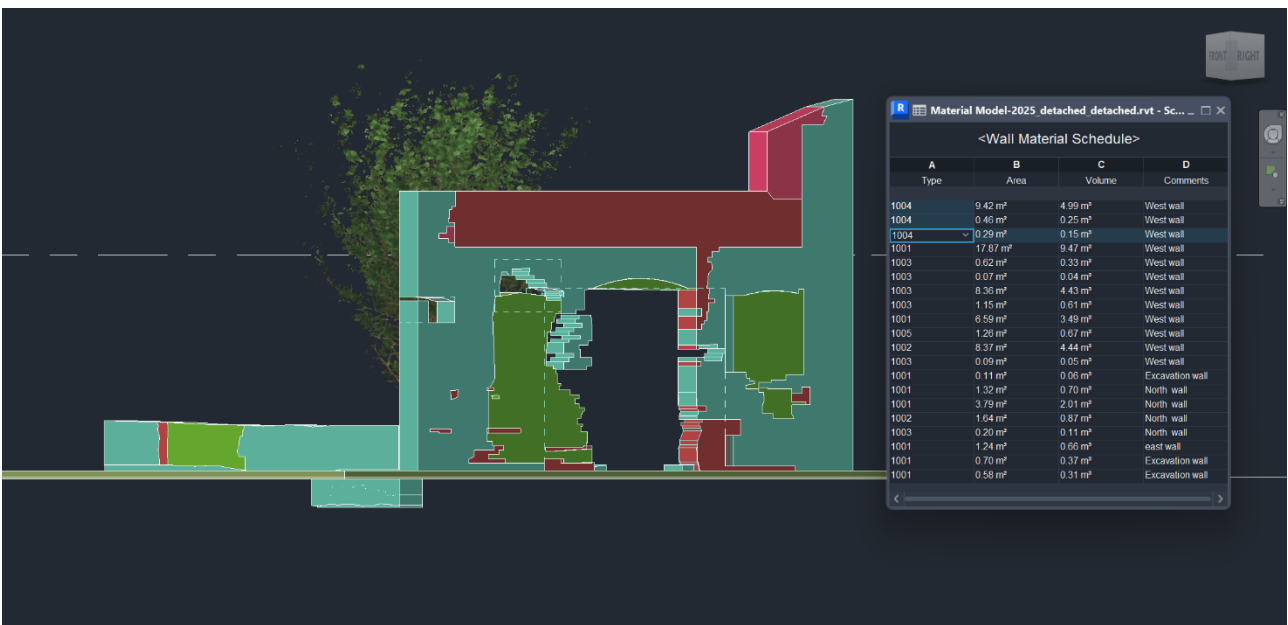


Figure 55: Using parametric modeling and wall scheduling feature to calculate the volume and the area of each stratigraphy of Oratorio di San Michele.

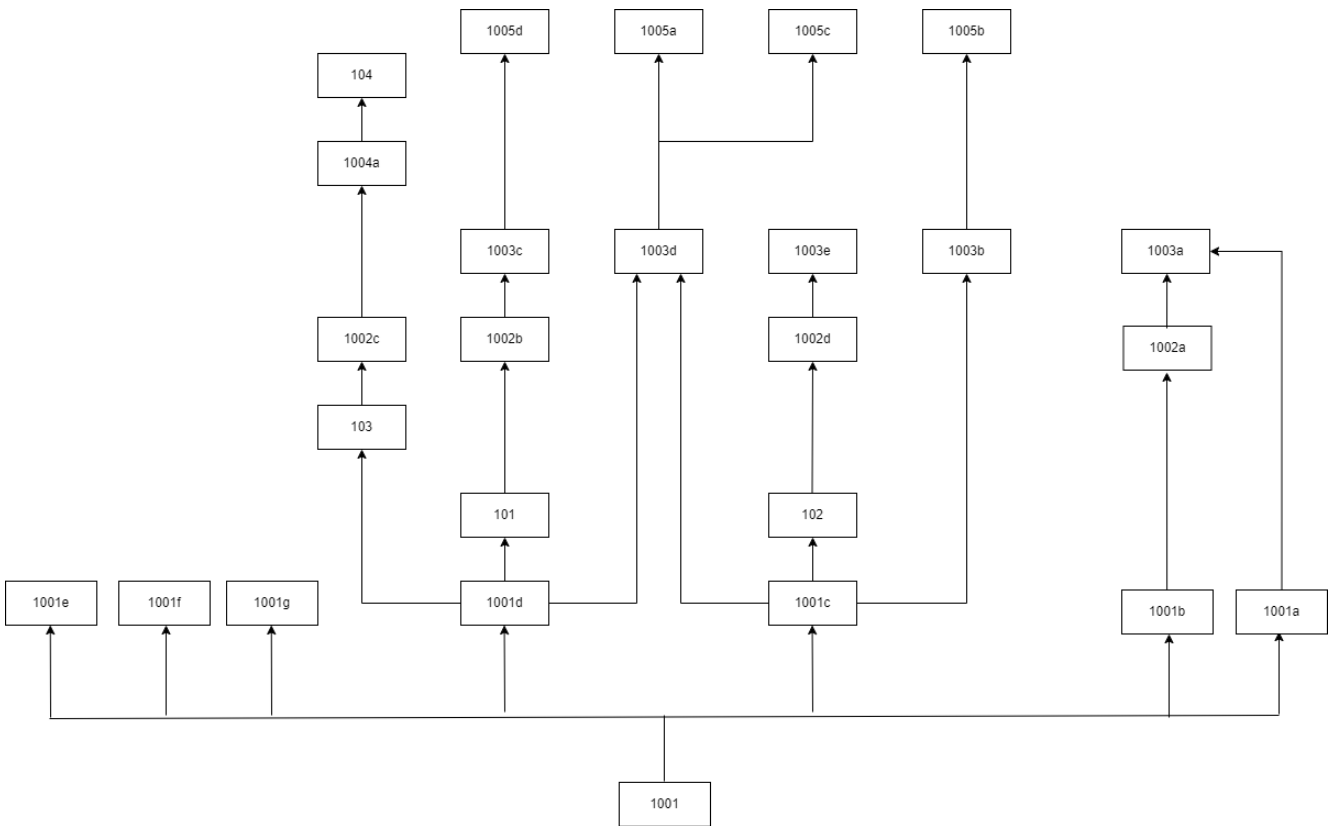
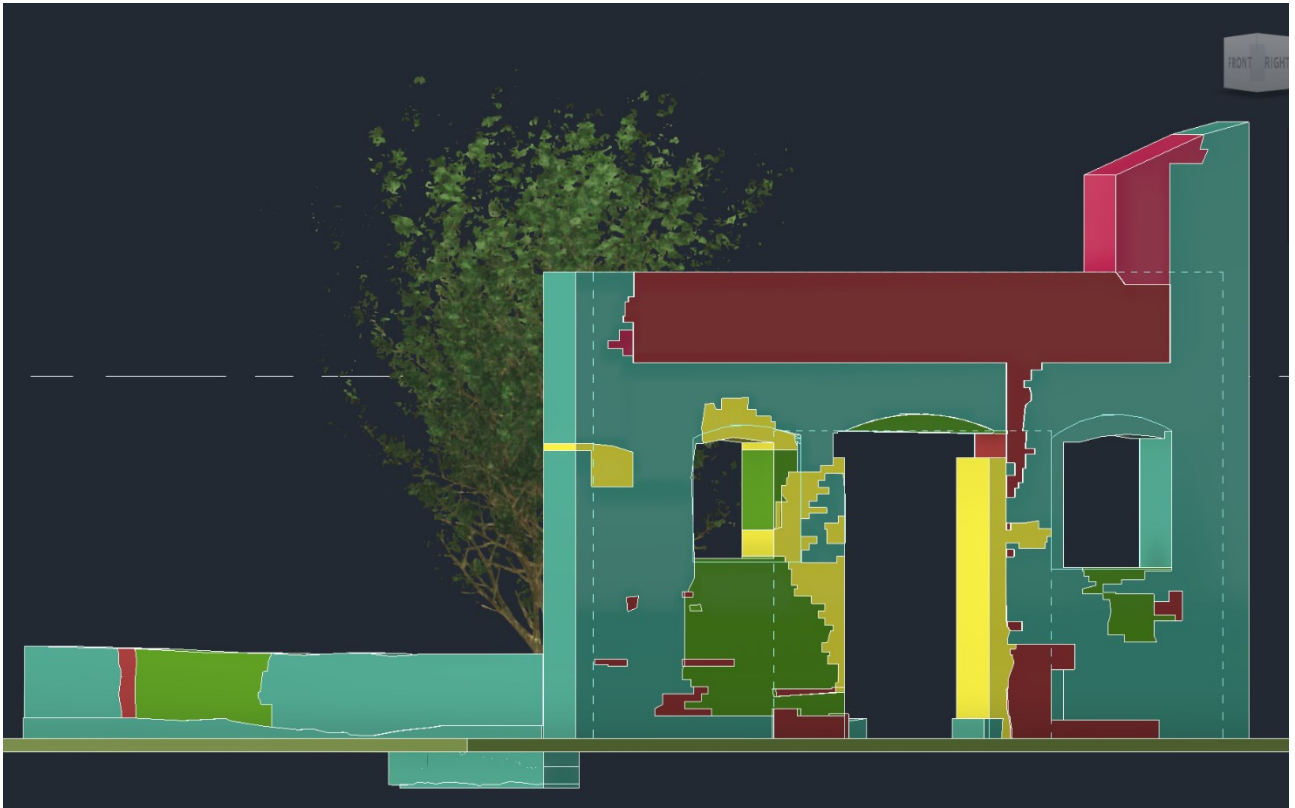


Figure 56: The final Stratigraphy sequence covering all the remaining walls.

Stratigraphy unit	Description	Area	Volume	Position	Harris Matrix Ref.
1004	Repointing (whitish mortar)	2.15 m <sup>2</sup>	1.14 m <sup>3</sup>	North wall	1004a
1004	Repointing (whitish mortar)	0.46 m <sup>2</sup>	0.25 m <sup>3</sup>	North wall	1004a
1004	Repointing (whitish mortar)	0.29 m <sup>2</sup>	0.15 m <sup>3</sup>	North wall	1004b
1001	Original wall	17.87 m <sup>2</sup>	9.47 m <sup>3</sup>	North wall	1001c
1003	Replaced Restoration	0.61 m <sup>2</sup>	0.32 m <sup>3</sup>	North wall	1003c
1003	Replaced Restoration	0.07 m <sup>2</sup>	0.04 m <sup>3</sup>	North wall	1003c
1003	Extended Restoration	8.36 m <sup>2</sup>	4.43 m <sup>3</sup>	North wall	1003d
1003	Replaced Restoration	1.15 m <sup>2</sup>	0.61 m <sup>3</sup>	North wall	1003b
1001	Original wall	6.60 m <sup>2</sup>	3.50 m <sup>3</sup>	North wall	1001d
1005	Modern Restoration	1.26 m <sup>2</sup>	0.67 m <sup>3</sup>	North wall	1005c
1002	Irregular Refill	4.28 m <sup>2</sup>	2.27 m <sup>3</sup>	North wall	1002b
1003	Replaced restoration	0.09 m <sup>2</sup>	0.05 m <sup>3</sup>	North wall	1003e
1001	Original wall- Foundation	0.11 m <sup>2</sup>	0.06 m <sup>3</sup>	Excavation wall	1001e
1001	Original wall	1.33 m <sup>2</sup>	0.70 m <sup>3</sup>	east wall	1001
1001	Original wall	3.79 m <sup>2</sup>	2.01 m <sup>3</sup>	east wall	1001b
1002	Irregular Refill	1.64 m <sup>2</sup>	0.87 m <sup>3</sup>	east wall	1002
1003	Replaced restoration	0.20 m <sup>2</sup>	0.11 m <sup>3</sup>	east wall	1003
1001	Original wall	1.24 m <sup>2</sup>	0.66 m <sup>3</sup>	east wall	1001a
1001	Original wall-Foundation	0.70 m <sup>2</sup>	0.37 m <sup>3</sup>	Excavation wall	1001g
1001	Original wall-Foundation	0.58 m <sup>2</sup>	0.31 m <sup>3</sup>	Excavation wall	1001f
102-103	Original Cut for windows	5.26 m <sup>2</sup>	2.79 m <sup>3</sup>	North wall	101&102
104	Original Cut for the door	7.34 m <sup>2</sup>	3.89 m <sup>3</sup>	North wall	104

Figure 57: Final BIM model of oratorio di San Michele with architectural elements and stratigraphical relationships referred to the Harris Matrix diagram of the stratigraphy sequence.

<Wall Material Schedule>				F5				
A	B	C	D	A	B	C	D	
Type	Area	Volume	Comments	Stratigraphy	Area	Volume	Wall location	
1004	9.42 m <sup>2</sup>	4.99 m <sup>3</sup>	West wall	1	1004	9.42 m <sup>2</sup>	4.99 m <sup>3</sup>	West wall
1004	0.46 m <sup>2</sup>	0.25 m <sup>3</sup>	West wall	2	1004	0.46 m <sup>2</sup>	0.25 m <sup>3</sup>	West wall
1004	0.29 m <sup>2</sup>	0.15 m <sup>3</sup>	West wall	3	1004	0.29 m <sup>2</sup>	0.15 m <sup>3</sup>	West wall
1001	17.87 m <sup>2</sup>	9.47 m <sup>3</sup>	West wall	4	1001	17.87 m <sup>2</sup>	9.47 m <sup>3</sup>	West wall
1003	0.62 m <sup>2</sup>	0.33 m <sup>3</sup>	West wall	5	1001	17.87 m <sup>2</sup>	9.47 m <sup>3</sup>	West wall
1003	0.07 m <sup>2</sup>	0.04 m <sup>3</sup>	West wall	6	1003	0.62 m <sup>2</sup>	0.33 m <sup>3</sup>	West wall
1003	8.36 m <sup>2</sup>	4.43 m <sup>3</sup>	West wall	7	1003	0.07 m <sup>2</sup>	0.04 m <sup>3</sup>	West wall
1003	1.15 m <sup>2</sup>	0.61 m <sup>3</sup>	West wall	8	1003	8.36 m <sup>2</sup>	4.43 m <sup>3</sup>	West wall
1001	6.59 m <sup>2</sup>	3.49 m <sup>3</sup>	West wall	9	1003	1.15 m <sup>2</sup>	0.61 m <sup>3</sup>	West wall
1005	1.26 m <sup>2</sup>	0.67 m <sup>3</sup>	West wall	10	1001	6.59 m <sup>2</sup>	3.49 m <sup>3</sup>	West wall
1002	8.37 m <sup>2</sup>	4.44 m <sup>3</sup>	West wall	11	1005	1.26 m <sup>2</sup>	0.67 m <sup>3</sup>	West wall
1003	0.09 m <sup>2</sup>	0.05 m <sup>3</sup>	West wall	12	1002	8.37 m <sup>2</sup>	4.44 m <sup>3</sup>	West wall
1001	0.11 m <sup>2</sup>	0.06 m <sup>3</sup>	Excavation wall	13	1003	0.09 m <sup>2</sup>	0.05 m <sup>3</sup>	West wall
1001	1.32 m <sup>2</sup>	0.70 m <sup>3</sup>	North wall	14	1001	1.32 m <sup>2</sup>	0.70 m <sup>3</sup>	North wall
1001	3.79 m <sup>2</sup>	2.01 m <sup>3</sup>	North wall	15	1001	3.79 m <sup>2</sup>	2.01 m <sup>3</sup>	North wall
1002	1.64 m <sup>2</sup>	0.87 m <sup>3</sup>	North wall	16	1002	1.64 m <sup>2</sup>	0.87 m <sup>3</sup>	North wall
1003	0.20 m <sup>2</sup>	0.11 m <sup>3</sup>	North wall	17	1003	0.20 m <sup>2</sup>	0.11 m <sup>3</sup>	North wall
1001	1.24 m <sup>2</sup>	0.66 m <sup>3</sup>	North wall	18	1001	1.24 m <sup>2</sup>	0.66 m <sup>3</sup>	North wall
1001	0.70 m <sup>2</sup>	0.37 m <sup>3</sup>	Excavation wall	19	1001	0.70 m <sup>2</sup>	0.37 m <sup>3</sup>	Excavation wall
1001	0.58 m <sup>2</sup>	0.31 m <sup>3</sup>	Excavation wall	20	1001	0.58 m <sup>2</sup>	0.31 m <sup>3</sup>	Excavation wall
1001	0.11 m <sup>2</sup>	0.06 m <sup>3</sup>	Excavation wall	21	1001	0.11 m <sup>2</sup>	0.06 m <sup>3</sup>	Excavation wall

Figure 58: Exporting area and volume data from Revit to Microsoft EXCEL.

#### **5.4. DISCUSSION OF BIM ANALYSIS**

Autodesk Revit's Building Information Modeling (BIM) is a prominent method for visual parametric modeling of selected stratigraphy of a single wall, yet it is not the only tool capable of such tasks. ArchiCAD also supports parametric BIM with a strong focus on architecture, while Blender and Free CAD provide non-parametric BIM solutions that offer flexibility in design processes without strict parametric constraints. Despite the focus on stratigraphy, Revit's BIM model is adept at calculating the structural stability of walls by integrating the differing mechanical properties of bricks used across various construction phases. Future enhancements could include calculating the mechanical strength of each stratum within the model, thus enriching our comprehension of the individual mechanical and thermal behaviors of each stratum. Additionally, implementing a Masonry Quality Index and conducting seismic vulnerability tests using sonic pulses on appropriate stratigraphy layers could further augment the research value, with all such assessments being facilitated and referenced within the BIM framework. Autodesk Revit augments Finite Element (FE) analysis through its precise modeling capabilities and seamless integration with structural analysis tools via various plugins. This integration supports automatic updates and efficient data transfers, ensuring that FE analyses are continually synchronized with the most recent architectural designs. Furthermore, Revit aids in the visualization and documentation of analysis results, fostering effective collaboration among all project stakeholders.

#### **5.5. CONCLUSION OF BIM ANALYSIS**

Overall, integrating stratigraphy with BIM can be seen as the initial step in a series of potential studies. This method is likely to be more effective in large-scale buildings and especially beneficial when employed in a multidisciplinary approach involving structural engineers, archaeologists, artists, reconstructors, conservationists, geologists, and material scientists. This collaborative approach facilitates an excellent documentation of Oratorio di San Michele with a comprehensive understanding of historical structures, enhancing both conservation and restoration efforts.



# Chapter VI: Archaeometry of Mortars

## 6.1. INTRODUCTION TO MORTAR

A mortar is a composite material composed of a binder and fine aggregates, primarily used as an adhesive in masonry to bond bricks and stones. Typically supplied in powder form, mortar becomes a fluid paste when mixed with water, allowing it to be molded, shaped, or applied to surfaces. This paste naturally hardens under standard environmental conditions. In construction, binders play crucial roles, including forming structural components, enhancing the strength of buildings by linking structural and architectural elements, and improving waterproofing to protect masonry surfaces from environmental damage. Instead of using pure binder paste, aggregates like quartz are often used along with the paste to minimize volume changes during hardening, thereby reducing shrinkage effects. The aggregate plays a crucial role in mitigating macro-cracking during the drying process of the binder/water mixture, increasing the bulk modulus of the composite, and enhancing the overall volume of the binder. When the aggregate has a particle size within the sand range (typically 0.6 to 0.8 mm), the binder/aggregate/water mixture is termed 'mortar.' Depending on the mineral composition of the binder, these mixtures can be classified as lime mortars, natural hydraulic lime mortars, magnesian lime mortars, gypsum mortars, or clinker mortars. Lime mortars and gypsum mortars are particularly prevalent in archaeological contexts and still much used for small-volume applications such as wall plastering and repointing.

Type of binder	Starting material	Appx. <i>T</i> of firing (°C)	Reactive material product	Reaction process	
Binders based on carbonate	Lime plaster	limestone	Quicklime (CaO) Slaked lime (Ca(OH) <sub>2</sub> )	aerial carbonation	
	Hydraulic Lime plaster	limestone	Slaked lime + pozzolan	pozzolanic reaction	
	Natural Hydraulic Lime plaster	limestone + clays/volcanic glass	800–1000	Natural hydraulic lime	hydration reaction
	Magnesian plaster	dolomite	Slaked magnesia-lime (Ca(OH) <sub>2</sub> ) (Mg(OH) <sub>2</sub> )	aerial carbonation	

*Figure 59: Binders based on carbonates, their nature and reaction processes. (Artioli, Secco, & Addis, 2019)*

During ancient and medieval times, many binders were derived from carbonates, such as calcite and dolomite. These binders can be categorized based on their chemical compositions and the primary reaction processes that occur when mixed with water. The pyro-technological production process creates a reactive material that stabilizes during setting and hardening. The primary



differences between binder types arise from the nature of the initial material, which dictates the chemical reaction pathway, and the firing temperature, which influences the binder's quality and reactivity.

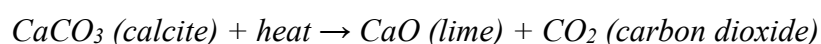
Lime-based binders gain strength through aerial carbonation, hydration and pozzolanic reactions. Aerial carbonation involves the absorption of CO<sub>2</sub> from the air, forming carbonates like calcium carbonate, while pozzolanic reactions involve the dissolution of alumino-silicate phases, leading to the precipitation of hydrated phase of calcium-silicate-hydrate (C-S-H). In magnesian binders, pozzolanic reactions involve the dissolution of alumino-silicate phases, leading to the precipitation of hydrated phase in form of magnesium-silicate-hydrate (M-S-H). Hydraulic binders, including those forming M-S-H phases, are capable of hardening underwater contributing to the mechanical strength and durability of the binder.

The mechanical strength of a mature binder largely depends on the recrystallization of these reaction products within the matrix and the interlocking of newly formed crystal phases. The microstructure, including the size, shape, and orientation of these crystal phases, is critical in determining the material's physical and engineering properties. As the binder sets, it transforms into a material entirely composed of recrystallized reaction products. A fully carbonated lime paste solidifies into a material consisting solely of fine calcite crystals, while a magnesian lime paste produces a material containing both calcium carbonate and magnesium carbonate, as well as M-S-H phases (Artioli, Secco, & Addis, 2019).

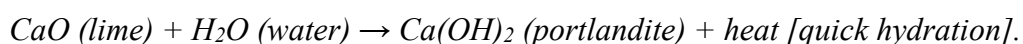
### † **Composition & Properties of Lime based Mortars**

The first artificial binders used by mankind during the 7th and 8th millennia BC were limestone and gypsum-based plasters mainly because they were relatively simple to prepare. For lime plasters, the key reactive compound is quicklime, which is obtained by burning limestone. Traditionally, the burning of carbonates (limestones, dolomites, travertine, marbles, but also shells and corals) is performed in limekilns, which are massive furnaces sometimes several meters high, charged from above with decimeter- to meter-sized blocks of limestone, and then fired for days by adding wood or charcoal to the combustion chamber at the base (Oates, 1998; Williams, 2004).

- I. The process involves heating limestone (calcium carbonate, CaCO<sub>3</sub>) to a temperature sufficient to decompose it into lime (calcium oxide, CaO) and carbon dioxide (CO<sub>2</sub>). This chemical reaction is the foundation of lime production:



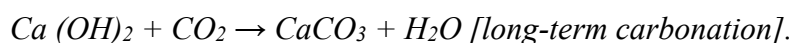
- II. The hydration of lime to form portlandite:



After the limestone is converted to quicklime, it is ground into a fine powder, however, rather unstable in normal humidity conditions and tends to hydrate quickly to portlandite. This powder is then mixed with water in a process known as slaking, which forms portlandite (calcium hydroxide, Ca (OH)<sub>2</sub>). Depending on the water-to-solid ratio, the resulting mixture can be either a slurry (more liquid) or a paste (more solid). If the CaO powder is mixed with an exact (i.e. stoichiometric) amount of water (lime/water=75.7/24.3=3.12 by weight) the product is a fine dry powder, and the process is called 'dry hydration' because there is exactly the right amount of water required to produce portlandite. If the CaO powder is mixed with excess water then a smooth paste is obtained in a slurry form, and the process is referred to as 'lime slaking'. The portlandite paste (slaked lime or lime putty) can then be used as a binder and an architectural component (filler, adhesive, cracks sealer).

The production of quicklime requires careful control of temperature. The ideal temperature for converting limestone to lime is around 850°C, although the reaction can occur at slightly lower temperatures under reducing conditions (lack of oxygen). However, lime kilns typically operate at temperatures between 920-1000°C to speed up the decarbonation process. This high-temperature environment accelerates the chemical reaction but must be carefully controlled. If the temperature is too high, it can lead to the formation of "dead-burned" lime, which is unreactive and unsuitable for construction purposes ( (Ruiz-Agudo, 2009).

- III. After the application the paste dehydrates slowly and reacts with atmospheric CO<sub>2</sub> producing a hard material composed of microcrystalline calcite. When kinetics of carbonation are slow so that in recent samples the reaction is not complete and residual crystals of portlandite may be observed(Van Balen, 2005) . The carbonation of portlandite over the long term to form calcite:



The quality of the binder is influenced by several factors, including the composition, porosity, and impurity content of the fired limestone, as well as the maximum firing temperature, the temperature-time profile during firing, and the slaking conditions. To produce lime, the carbonate material (usually limestone) should ideally be made up almost entirely of calcium carbonate (CaCO<sub>3</sub>). This purity is important because it influences the behavior of the lime during and after the firing process. If the carbonate contains flint (a form of silica) or a significant amount of clays (which contain alumina and silica), these impurities can react during the firing process. At the high temperatures used in lime

kilns, these impurities can react with calcium to form aluminosilicate compounds. These reactions are key because the resulting materials have properties that differ from pure lime. These aluminosilicate compounds are hydraulic in nature, meaning they can set and harden under water, unlike pure lime, which requires air to carbonate and harden. This property is what defines natural hydraulic lime (NHL). When carbonate materials used to produce lime contain magnesium, typically from magnesian calcite or dolomite, the resulting product is known as magnesian or dolomitic lime. During the firing process, magnesium forms periclase (MgO) in addition to the lime (CaO). Unlike calcium oxide, which quickly reacts with water to form portlandite (Ca(OH)<sub>2</sub>), periclase rehydrates much more slowly, eventually forming brucite (Mg(OH)<sub>2</sub>) (Blauer-Bohm & Jagers, 1997).

As the lime paste hardens, the structure of the material evolves, making it crucial to understand these changes when studying ancient lime mortars, especially in archaeological contexts.

When analyzing unconsolidated archaeological layers, by examining size (typically range in size from 0.1 to 2.0 mm), texture, and mechanical properties of the carbonate particles scientists can identify whether the calcite present in the sample originated from lime.

Optical microscopy allows researchers to closely examine the texture and composition of ancient lime mortars, helping to determine the nature of the calcite. Especially to distinguish calcite that formed naturally through geological processes from calcite that originated from the carbonation of portlandite. This distinction is important because it can influence interpretations of the archaeological findings, such as understanding the original materials used and the methods of construction employed. (Pecchioni, Fratini, & Cantisani, 2014)

Calcium nodules/ Lime lumps can form in one of three ways:

- ∴ Residues of Unburned Geological Carbonate: Sometimes, the limestone used to make the lime might not be fully calcined (burned), leaving behind unburned carbonate, which can appear as calcite nodules in the mortar.
- ∴ In-homogeneously Slaked Lime Putty: During the slaking process, where quicklime is mixed with water to form lime putty, if the mixture is not uniform, some areas might form lumps of portlandite (a form of calcium hydroxide). These lumps can later convert into calcite as they carbonate over time.
- ∴ Reprecipitated Late Calcite: After the mortar has set, calcite can form from dissolved calcium hydroxide (from the lime) that reprecipitates into nodules within the mortar (Hughes, Leslie, & Callebaut, 2001).

Calcite nodules are important for several reasons. They help in identifying ancient mortars, determining the original ratio of binder to aggregate (which is the mixture of lime and sand or other materials in the mortar), and in some cases, they are used in radiocarbon dating to estimate the age of the mortar. Properly identifying the origin of these calcite nodules is critical because errors can lead to skew the analysis of the binder-to-aggregate ratio or result in inaccurate radiocarbon dating, which could mislead researchers about the age and construction methods of the ancient structure.

Distinguishing between lime-derived and natural calcite is important for correctly interpreting ancient mortars, especially when using techniques like radiocarbon dating. Methods such as FTIR, luminescence analysis, stable isotope fractionation, and micromorphological features help researchers make this distinction by analyzing the physical and chemical properties of the calcite (Artioli, Secco, & Addis, 2019).

## 6.2. DATING MORTARS USING <sup>14</sup>C TECHNIQUE

In order to radiocarbon (<sup>14</sup>C) date a building structure such as a wall, several components of the mortar can be employed, such as (1) its binder and lime lumps, which were formed by the absorption of atmospheric CO<sub>2</sub> during the carbonation phase, (2) charcoal particles representing a relic of the calcination process, and (3) shell fragments eventually present among the aggregate particles. There are different ways of preparing and purifying mortars for radiocarbon dating. Cryo2Sonic 2.0 is one of these methods, focusing on isolating the datable lime binder from the mortar while removing unwanted contaminants like geological carbonates. The process includes several steps as follows:

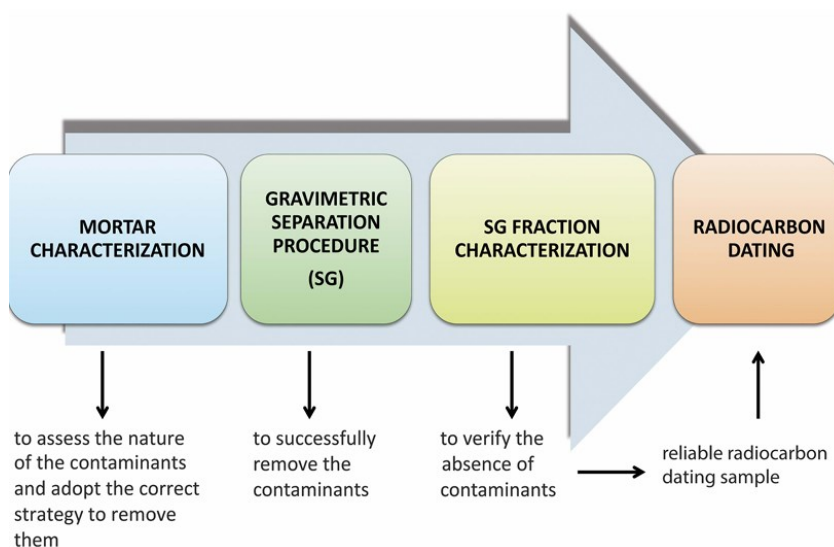


Figure 60: The steps of Cryo2sonic version 2.0 (v.2.0) (Addis, et al., 2019).

The protocol consists of four steps: (1) mortar characterization, (2) gravimetric separation treatment, (3) characterization of the obtained powder, and (4) <sup>14</sup>C dating of the powder that is composed by pure lime binder devoid of any contaminants.

The first step of this method is to identify and understand the nature of its contaminants. The characterization step primarily focuses on identifying datable components like lime binder, lime lumps, charcoal particles, and shell fragments, and detecting contaminants such as geological carbonates or improperly prepared lime that could alter the <sup>14</sup>C dating signal. Various techniques,

including Colorimetry, X-ray Diffraction (XRD), Scanning Electron Microscopy with Energy Dispersive Spectroscopy (SEM-EDS), and Optical Microscopy, are employed to verify the types of

### DATEABLE MORTAR MATERIALS

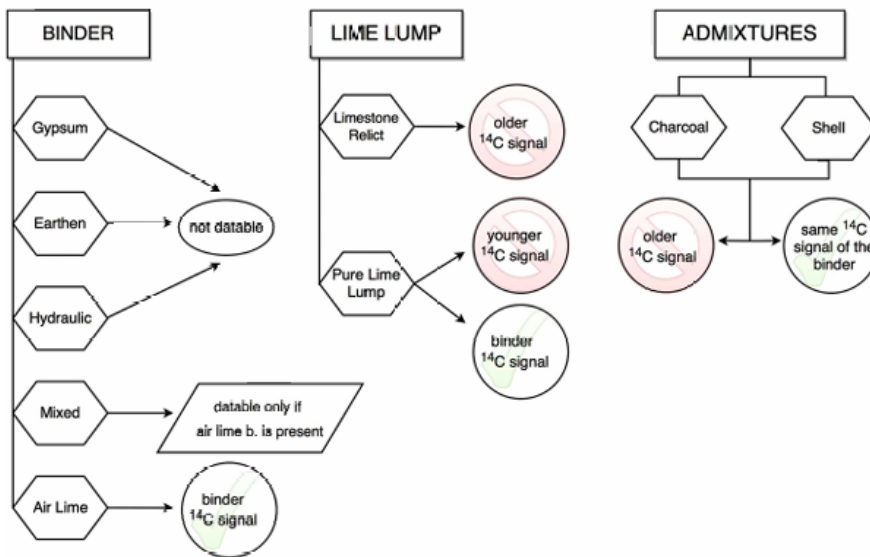


Figure 61: Flow chart of the identification of dateable materials within the mortars and their possible contaminations.

Types of binder: gypsum– hearten–hydraulic (since no carbonate is present, they are not <sup>14</sup>C dateable); mixed (dateable only if a lime binder is present); and air lime (dateable). Types of lime lumps: limestone relict (source of dead carbon that could contaminate the lime binder <sup>14</sup>C signal), pure lime lump (depending on the lump setting time, its <sup>14</sup>C signals could reflect either the binder setting time or a younger time). Types of admixtures: charcoal and shell (their <sup>14</sup>C dating accuracy varies depending if they were contemporary to the time of the wall construction or not) ( Addis, et al., 2019).

binders, filtering out all except those based on air lime or mixed with a significant amount of lime suitable for <sup>14</sup>C dating.

The nature of lime lumps is assessed using optical and cathodoluminescence spectroscopy to ascertain their dateability or potential as contaminants. Petrographic analysis checks for geological carbonate aggregates, significant sources of "dead carbon" that can skew <sup>14</sup>C results. Additionally, this process helps identify minerals like hydrotalcite that can trap modern CO<sub>2</sub> and alter the original <sup>14</sup>C signal, potentially leading to inaccurate dating.

The characterization also includes assessing the porosity of the mortar to understand if secondary calcite has crystallized within the binder, influencing dating results due to later recrystallization processes. This comprehensive evaluation of both organic and inorganic components determines their suitability and accuracy for radiocarbon dating, ensuring the reliability of the dating results by fine-tuning the separation and preparation procedures based on the specific characteristics of each mortar sample ( Addis, et al., 2019).

### MINERALO-PETROGRAPHICAL CHARACTERIZATION: MORTAR DATING CONTAMINANTS

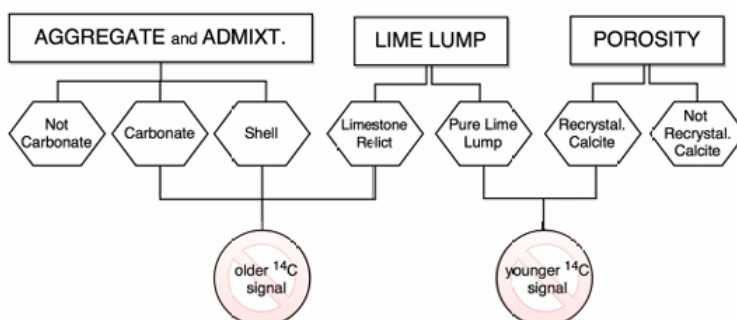


Figure 62: Flow chart of the most common mortar contaminants.

Carbonate aggregates and limestone relict (source of dead carbon); shell fragments that could have an older <sup>14</sup>C signal than the binder, pure lime lump that could harden after the binder; and recrystallized calcite that crystallize after the binder ( Addis, et al., 2019).



# Chapter VII: Methodology

## 7.1. ACTION PLAN OVERVIEW

The primary objective of the archaeometric analysis of mortars is to determine the age of the Oratorio di San Michele by identifying the best candidate sample for radiocarbon ( $^{14}\text{C}$ ) dating. The process of sampling and drawing conclusions in the archaeometric analysis of mortars was guided by Professor Michele Secco, with all the lab work conducted under his supervision in the Department of Geoscience laboratories. To achieve this, the samples selected for analysis must be representative of the oldest strata of the building. By focusing on these older layers, we aim to isolate the mortar sample with the most favorable mineralogical characteristics that will support accurate absolute dating. Through detailed mineralogical characterization, we can thoroughly assess and rank the samples, ensuring that the oldest and most suitable mortar is selected for radiocarbon dating. Let's break down the process to systematically evaluate and rank these samples.

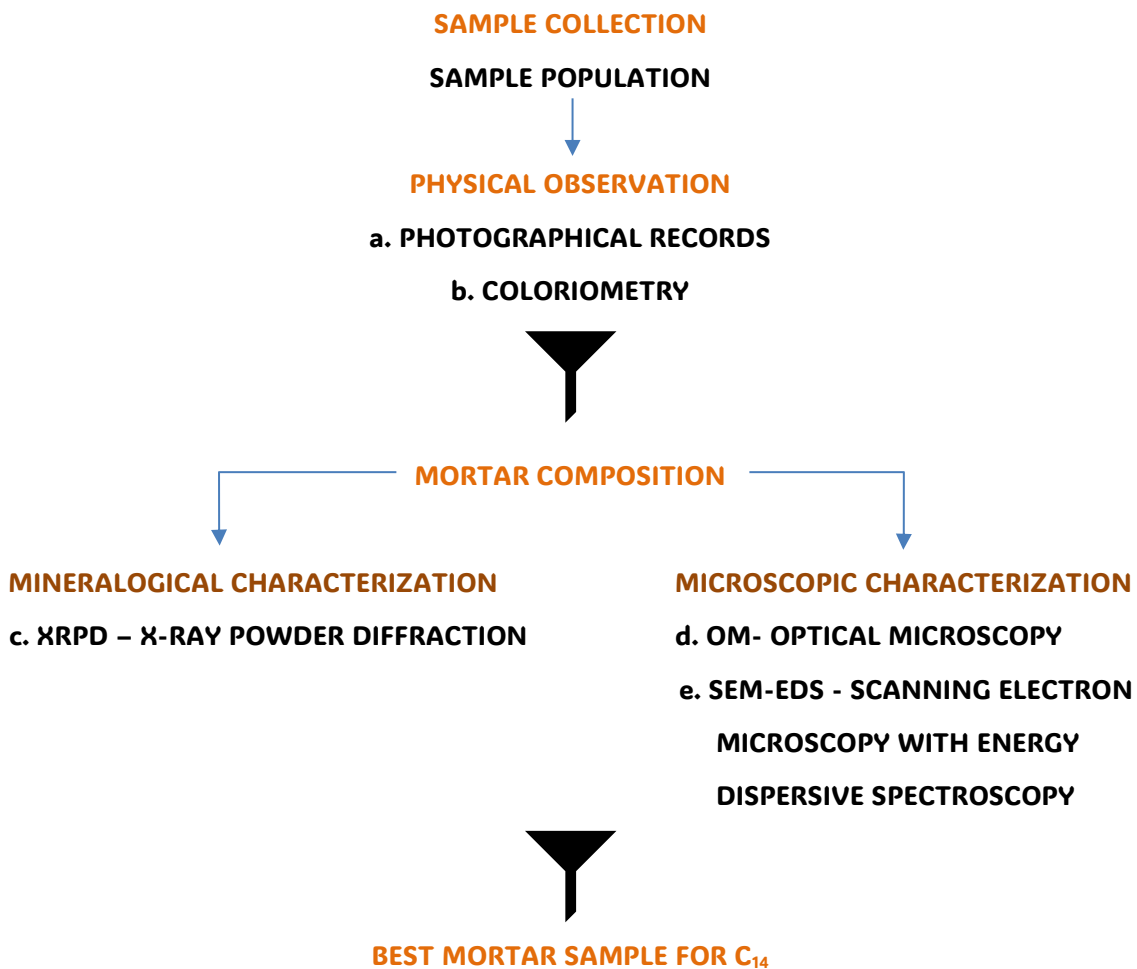


*Table 1- Overview of Methodology .*

## † Sample Population

- ∴ Method of Collection: Prior to extraction, detailed photographs were taken of each sample site, capturing both the broader surrounding area and the precise location of the sample. These photographs were labeled to ensure accurate documentation of the sample site's appearance before and after extraction. Samples were carefully collected using a chisel and hammer, focusing on the extended edges of mortar joints from various locations. The extracted samples were then placed in labeled zip-lock bags, with each bag numbered for subsequent laboratory analysis.

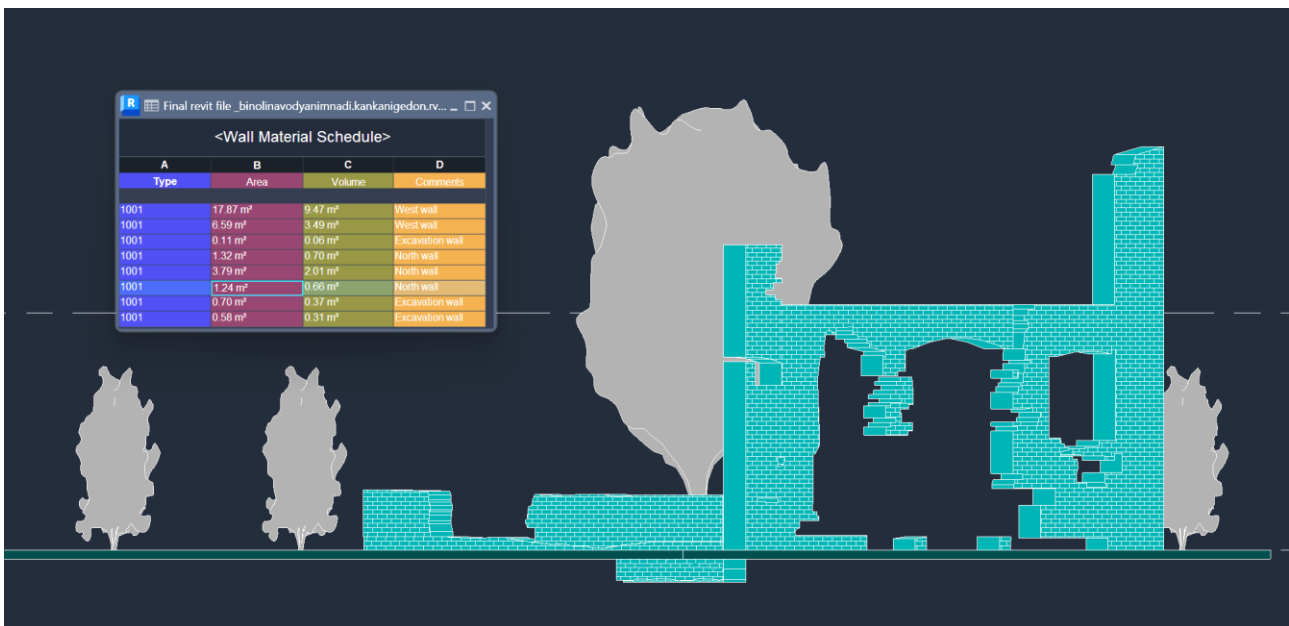


Figure 63: Strata 1001 of remaining walls at Oratorio di San Michele.

- ∴ How Sample Locations were decided: The goal of the archaeometry analysis is to determine the structure's age by identifying the most suitable mortar samples for C14 analysis. To achieve this, we focused on the oldest, undisturbed strata of the building, specifically targeting original components. Emphasis was placed on the 1001 strata and mainly on the underground foundation areas uncovered in recent excavations, as these are most likely to contain the original materials needed for accurate dating.
- ∴ Four samples, labeled SM\_01, SM\_02, SM\_03, and SM\_04, were collected from the inner surface of the foundation of the North wall, located in the excavation pit. This part of the building is considered the least contaminated within the overall stratigraphy. Sample SM\_05 was taken from the West wall, and SM\_06 was collected from the North wall. These samples from different walls are being compared to understand the relationship between the strata across the building and to determine if these sections originated from the same period.



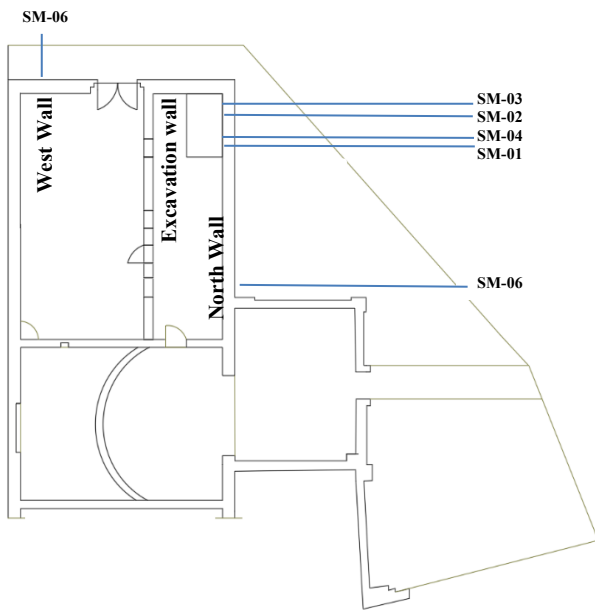


Figure 64: Plan view of the sample locations.



Figure 65: 3D view of the sampling locations.

Sample No:	Strata	Structural function	Construction Techniques
SM_01	1001f	Mortar Bed for the Tomb	<ul style="list-style-type: none"> <li>∴ Irregular large bricks+ Bedding mortar</li> <li>∴ The bedding mortar extrudes perpendicularly from the wall, extending towards the tomb slabs.</li> </ul>
SM_02	1001g	Head joint mortar	<ul style="list-style-type: none"> <li>∴ Regular bricks+ Bedding mortar</li> <li>∴ Last bed joint on the bricks before the flooring</li> </ul>
SM_03	1001f	Bed joint mortar	∴ Regular bricks + Bedding mortar + homogeneous structure
SM_04	1001f	Brick foundation	∴ Regular bricks + Bedding mortar + homogeneous structure
SM_05	1001c	Ashlar and brick joint	∴ Regular cut stones+ mortar joint bricks
SM_06	1001a	Ashlar and brick joint	∴ Regular cut stones+ mortar joint bricks

Table 2-Sample population of the study.

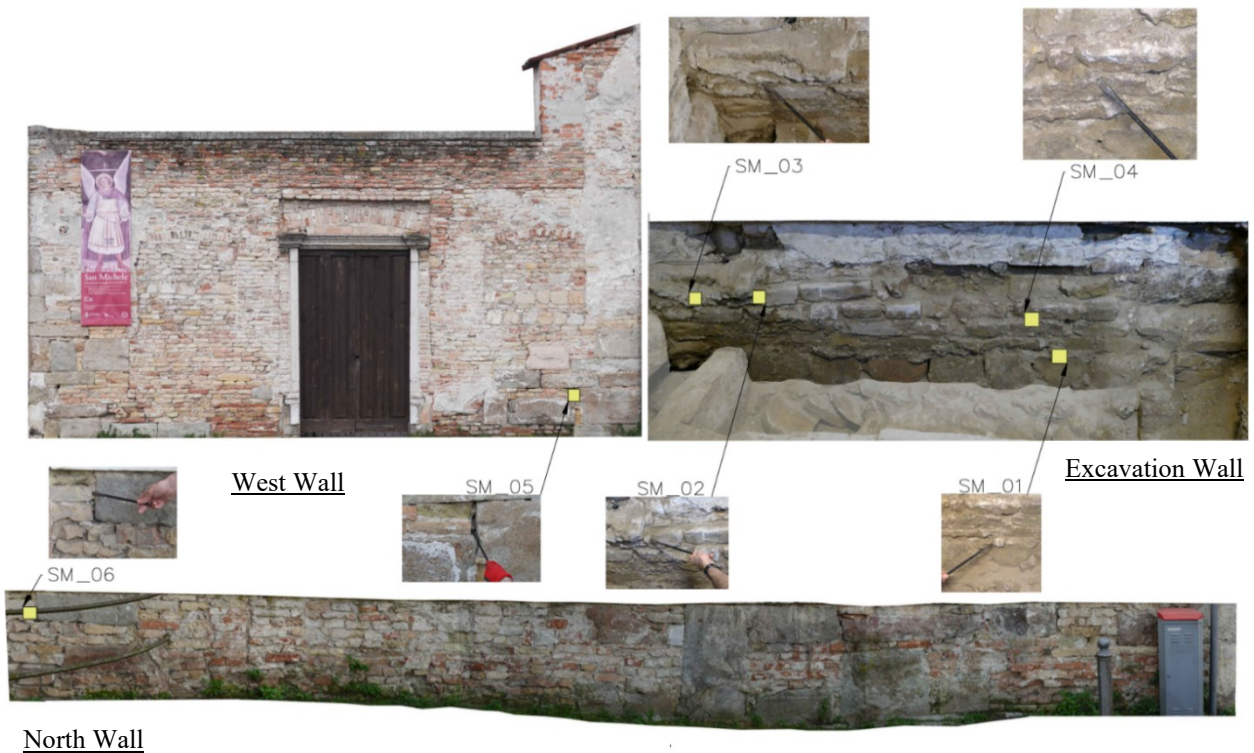


Figure 66:2D Views of the sampling Locations.

## 7.2. PHOTOGRAPHICAL RECORDS

This process involved documenting the macro characteristics of the mortars, including their texture, color, and overall appearance. Photographic recording is utilized to capture detailed images of the samples, providing a visual record that can be referenced throughout the analysis.

### † SM\_01

Sample 01 exhibits a gray-colored mortar characterized by a coarse texture and a thick, crumbly consistency, indicative of its robust nature. A well-composed blend with a balanced ratio of sand and lime-based binder, suitable for foundational purposes. Noteworthy inclusions such as shells, minor wood fragments, and calcite, along with aggregates measuring around 5mm, contribute to its heterogeneous composition. The presence of gravel particles within the sand aggregate further enhances its structural integrity. Overall, Sample 01 exemplifies a meticulously crafted mortar with attributes conducive to enduring structural support, reflecting the craftsmanship and resourcefulness of ancient builders.



*Figure 67: Sampling process of SM\_01.*

### † SM\_02

Sample 02 exhibits a coarse-textured, thick gray mortar. The presence of 1mm diameter voids on its surface suggests loose aggregates/ shells/ calcite inclusions. The mortar contains crushed gravel particles larger than 3mm, alongside shells, enhancing its structural integrity. Like Sample 01, Sample 02 utilizes a lime-based binder. Despite the voids, it is characterized by a wetter state that may be attributed to its positioning. Voids could have been left by

vegetable material, mostly straw or grass, added when the mortar was prepared to prevent shrinkage and cracking of this first layer of mortar while it was setting.

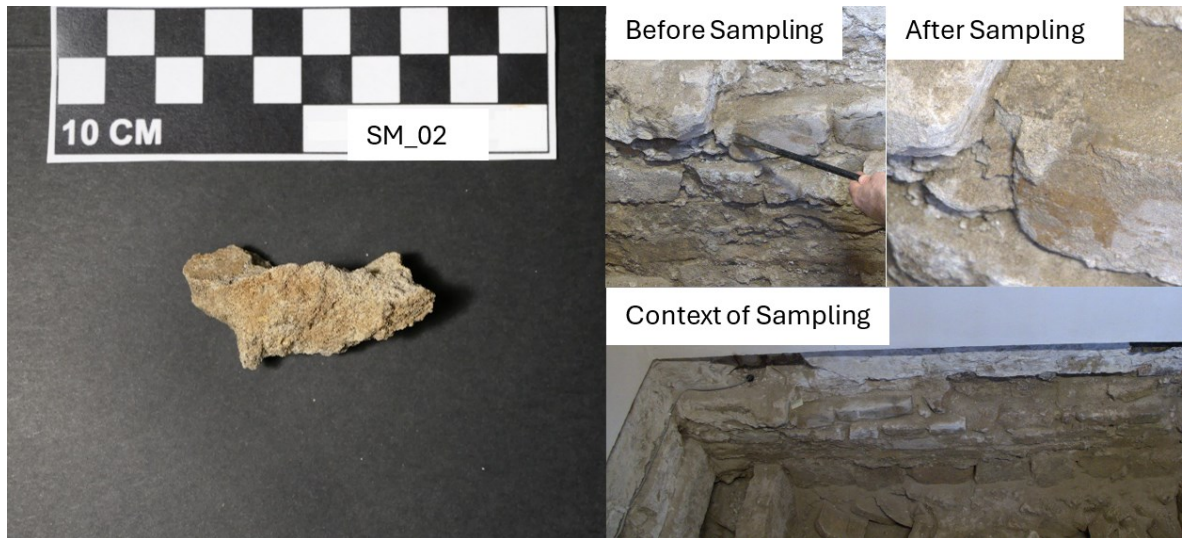


Figure 68: Sampling Process of SM\_02.

#### † SM\_03

Sample 03 exhibits a whitish mortar with a coarse texture and a lightweight, thick consistency. The inclusion of a terracotta piece measuring nearly 9mm adds diversity to its composition, indicating a mixture of materials. Composition reflects varied proportions of lime-based binder and aggregates making it less homogeneous. The outer surface shows lime washing, confirming the use of lime as a binder. With aggregates comprising sand, gravels and terracotta, Sample 03 showcases material versatility, suggesting adaptability for various construction contexts.

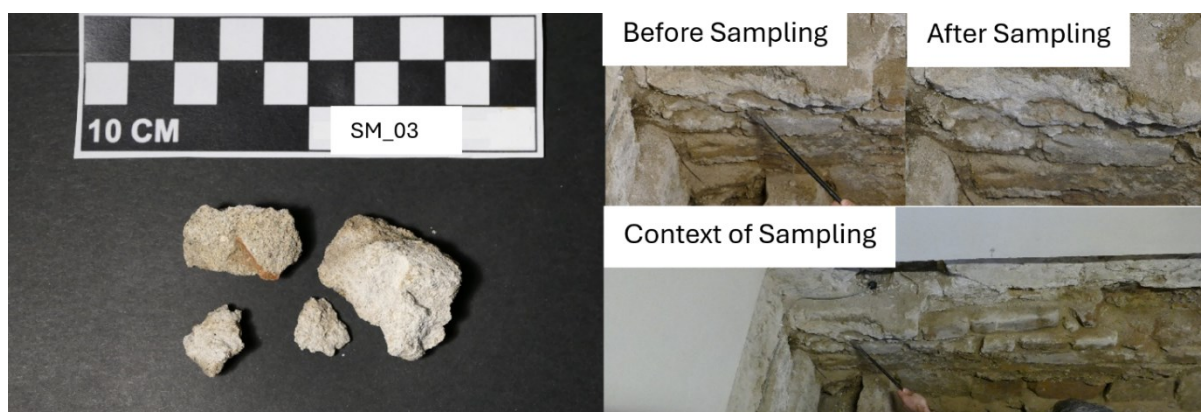


Figure 69: Sampling process of SM\_03.

#### † SM\_04

Sample 04 is characterized by a brownish-gray mortar exhibiting a coarse texture and thick consistency, indicative of its robust structural potential. Notably, the presence of a terracotta piece larger than 1cm, along with aggregates, contributes to its heterogeneous composition.

The variable proportions of lime-based binder and aggregates can be observed. The inclusion of sand, terracotta, and limestone grains within the aggregate highlights the material diversity.

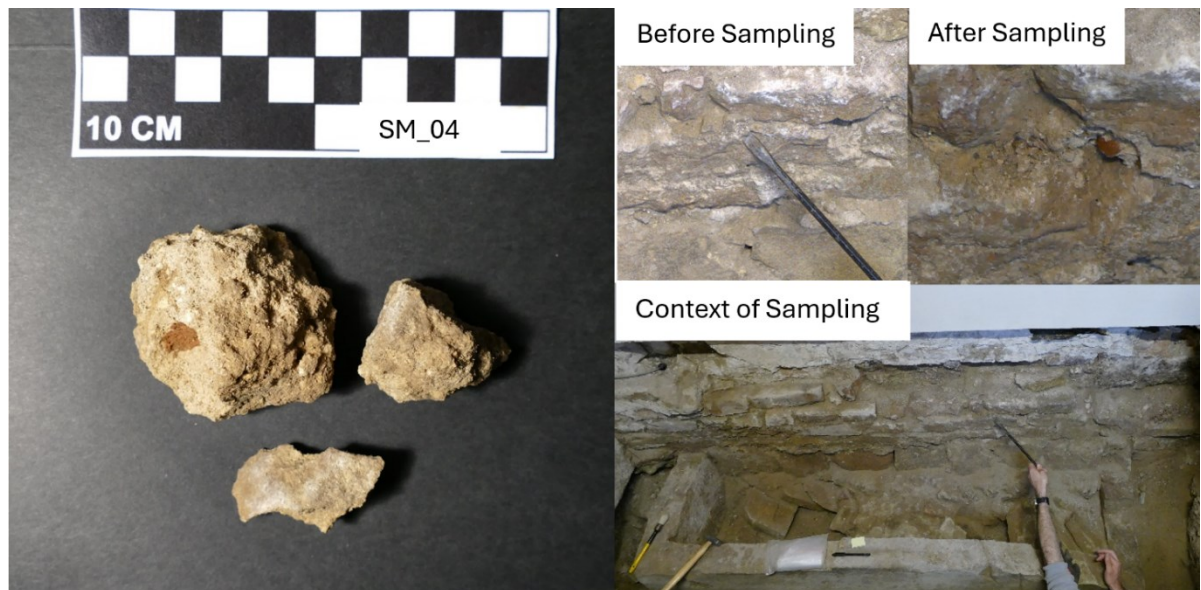


Figure 70: Sampling process of SM\_04.

† SM\_05

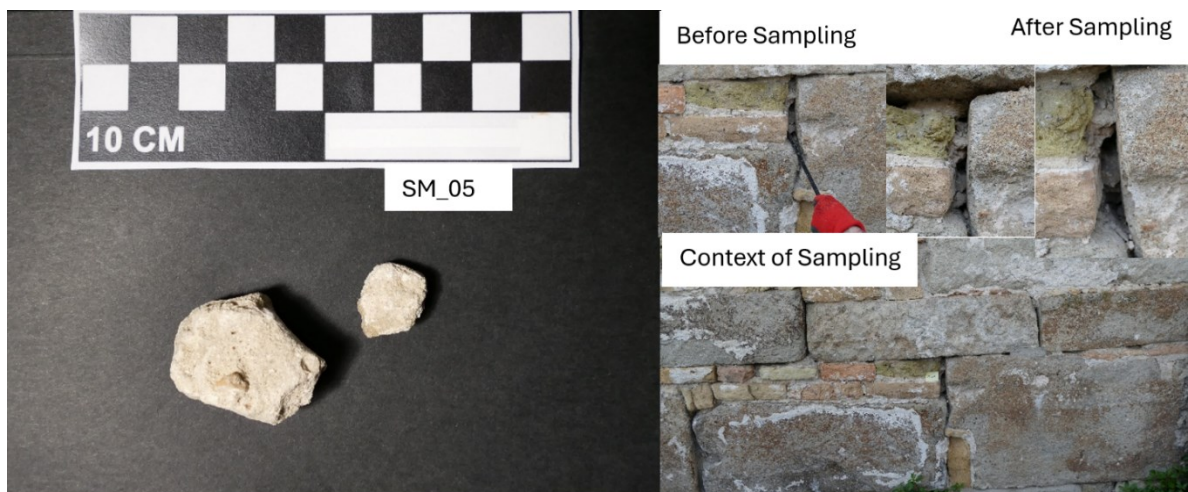


Figure 71: Sampling Process of SM\_05.

Sample 05 features a whitish mortar with a dry and sandy texture, containing terracotta pieces around 3mm in size as aggregates. The mortar is lightweight and easily breakable, with a higher proportion of calcite compared to aggregates and sand. Constituted of a lime-based binder, it demonstrates versatility in construction applications. Small fragments of tile or brick were presumably added for the hydraulic qualities they would contribute, making the mortar more resistant to damp.

† SM\_06

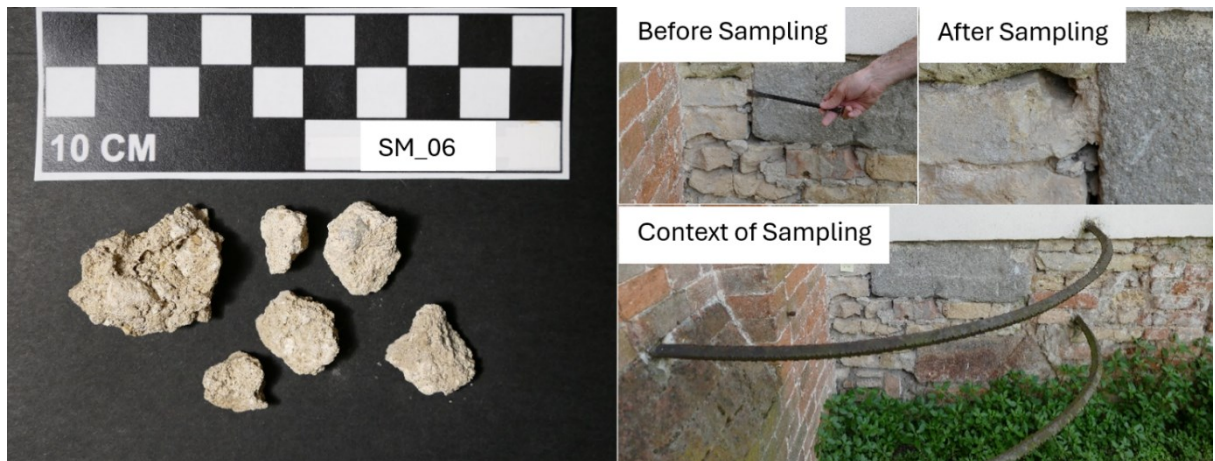


Figure 72: Sampling Process of SM\_06.

Sample 06 displays a whitish mortar with a dry, sandy, and powdery texture, characteristic of a lightweight composition. Notably, gravel pieces around 3mm in size serve as aggregates, contributing to its structural integrity. Analysis reveals a composition that is easy to break and less cohesive, with an excess of sand. In this lime-based binder no terracotta is visible to the naked eye.

### 7.3. COLORIMETRY

Colorimetry is performed to measure and quantify the color attributes of the mortar. This technique involves the use of a colorimeter to obtain precise color values, which can indicate the presence of specific materials, such as different types of lime or aggregates. The data collected during this phase serves as a foundational reference for subsequent analyses, helping to identify variations in composition and state of preservation across different samples.

- I. The measurements were conducted on the mortar in its powdered state, which ensures a uniform mixture of binders and aggregates. No additional sample preparation was necessary as the powdered mortars were already prepared for X-ray powder diffraction (XRPD) analyses. It is important to note that the color measurements were taken on the powder without adding zinc oxide to avoid altering the actual color values of the samples.
- II. The collection of color data for each of the 49 samples was executed using a PCE-XXM 30 colorimeter from PCE-Instruments. This device features a D/8 SCI measurement angle, an 8 $\emptyset$  aperture, and a wavelength range from 400 to 700 nm. Each sample required less than a minute to measure, with color values recorded in the *Lab*\* color space.

## 7.4. (XRPD): X-RAY POWDER DIFFRACTION

Mineralogical characterization is conducted using X-ray Powder Diffraction (XRPD). XRPD is an analytical technique that identifies crystalline phases within the mortar by measuring the diffraction pattern of X-rays passing through the sample. The diffraction pattern is unique to each mineral, allowing for precise identification of the minerals present. The output from XRPD is a diffractogram, which displays peaks corresponding to specific minerals. This data is critical for understanding the raw materials used in the mortar, such as the types of lime or pozzolanic additives. Knowing the mineralogical composition helps in determining the technological choices made during the mortar's production and provides clues about the environmental and geological sources of the materials. The procedure followed for XRPD analysis is as follows.

- I. Sample selection for XRD: The analysis was initiated by selecting a representative homogeneous fraction of all six mortar samples, which included both the matrix and the aggregates for a comprehensive evaluation.
- II. Grinding: The initial stage in preparing the mortar sample began with a coarse grinding phase. A suitable fraction was selected and extracted from the main sample using a screwdriver and dental tools. This fraction was then crushed with a hammer to create a coarsely ground powder. This powder was subsequently stored in plastic containers for XRPD and as testimonial samples for further processing. In the first round of grinding, the coarse powder was pulverized using a Retsch mixer mill MM 400 using a plastic jar with zirconia grinding. During this stage, 15 mL of the sample was processed for 5 minutes, which resulted in a powder with a granulometry of approximately 50 microns. The second round of grinding, or micronization, was conducted using a McCrone XRD-mill to achieve finer granularity. Here, the powder was reduced to a granulometry of about 5 microns. To ensure even mixing and to prevent particle agglomeration, a homogeneous portion of this ground sample was mixed with 15 mL of ethanol and ground for an additional 5 minutes at a working speed of 75%. After grinding, the mixture of ethanol and powder was left to dry for 24h on a watch glass, preparing it for the subsequent analytical procedures.



Figure 73: Grinding tools and the Grinded samples.



Figure 74: RD Mill McCrone.

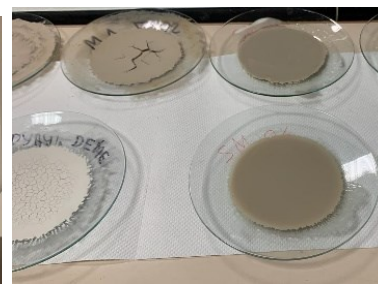
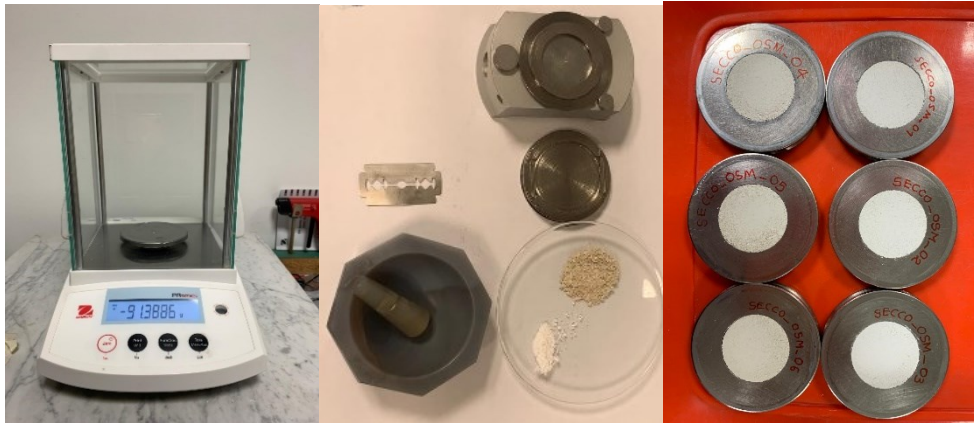


Figure 75: Fine grinded sample with ethanol on watch glasses for drying.



*Figure 76: Analytical Balance and the Tools used for mixing and backloading the samples.*

- III. In the preparation of samples for X-ray diffraction (XRD) analysis, zinc oxide is added to the mixture to enhance the detection and identification of amorphous content within the samples. Amorphous materials, unlike crystalline structures, do not produce sharp diffraction peaks, so including zinc oxide helps in contrasting these differences, thus facilitating more precise analysis. The precise weighing of zinc oxide is 0.2 grams with 0.8 grams of sample with a precision of  $\pm 0.0004\text{g}$ , totaling 1 gram. Operations were conducted using an analytical balance, which is designed to measure small mass in the sub-milligram range. A micro-spatula was used for transferring and mixing small quantities of powder without loss, while the pestel was essential to break down any clumps that might have formed during the drying or initial mixing stages. This ensures that the powder mixture remains homogenous, which is crucial for consistent XRD results. The back-loading technique was employed to place the mixture in the sample holder, carefully packing the powder into the holder from behind, promoting a random orientation of particles. This technique helps to achieve a more isotropic sample distribution, which is vital for obtaining accurate and representative diffraction data.
- IV. X-Ray Diffraction Measurement: To conduct the X-ray powder diffraction (XRPD) analysis, the prepared samples were examined using a PANalytical X'Pert PRO diffractometer, configured in Bragg-Brentano geometry. This setup utilized a cobalt X-ray tube paired with an X'Celerator detector, optimizing the detection process under specific conditions: the radiation was set to CoK $\alpha$ , the voltage at 40 kV, and the current at 40 mA. The diffractometer was programmed to cover a  $2\theta$  range of  $3\text{-}85^\circ$  with a step size of  $0.02^\circ$  and each step accumulating counts for 100 seconds. Following the XRPD measurements, the mineral phases detailed quantitative analysis, the Rietveld refinement was applied using Topas software, allowing for precise determination of the crystalline structures within the samples. To further enhance our understanding and identify the most suitable sample for carbon-14 dating, Principal Component Analysis (PCA) was conducted using the results. This statistical method



helped clarify which samples exhibited characteristics most conducive to accurate  $^{14}\text{C}$  dating, based on their mineralogical composition.

## 7.5. (OM): OPTICAL MICROSCOPY



*Figure 77: The Instruments used to create the thin sections for Optical Microscopy.*

Microscopic characterization involves both Optical Microscopy (OM) and Scanning Electron Microscopy coupled with Energy Dispersive Spectroscopy (SEM-EDS). OM allows for the examination of thin sections of the mortars under a microscope to observe the texture, grain size, and distribution of the components. This technique provides visual data on the physical structure of the mortars, which can be indicative of the mixing techniques and conditions under which the mortars were applied and cured. The thin sections preparation for the OM analysis was conducted as follows:

- I. Sample preparation began by selecting the most representative side of the solid mortar sample. This side is then ground to a smooth finish using a laboratory grinder with 1200 sandpaper grains, ensuring that any surface irregularities are minimized to obtain a 180 degrees flat surface without any voids. Once grinding is complete, the samples are thoroughly washed to remove any residual grinding debris and impurities. After washing, the samples were dried using an air compressor. This step effectively removes moisture, preparing the samples for the embedding process. Each sample was then put on top of a heated table to dry with their labels for several hours. This controlled heating helps extract any residual moisture from the samples, which is essential for successful resin embedding.
- II. Prepare the epoxy resin following specific mix ratios and handling procedures to ensure optimal consistency and bonding properties. The resin is then carefully poured over flat

surface of the samples in the containers using a dropper to eliminate any air bubbles. The resin used in this case is Araldite 2020A and Araldite 2020 B. Mixing proportion was 10:3 as for every 100 parts of the resin (2020A), 30 parts of the hardener (2020B) were used. Once the resin is poured, the samples are placed inside a vacuum chamber and subjected to three vacuum cycles. These cycles consist of the placement of samples under vacuum (at 0.8 bar) for some minutes depending on the response of the sample. This process is done to extract all possible air inside the sample. To prepare thin samples, blocks of cured epoxy were initially cut to dimensions of 30 x 45 mm using a diamond saw. The surfaces of these blocks were then gritted with diamond grit, followed by smoothing with 400 and 600 grit abrasive papers. The smoothed blocks were dried on a hot plate. Each block was then glued to pre-heated glass holders using approximately 2 grams of resin, ensuring a gradual placement of the glass to avoid the formation of bubbles. The samples were left to dry overnight on a gluing bench. Subsequently, the samples were re-cut to a thickness of approximately 600 microns using a diamond saw. The thickness of the sample blocks was further reduced to about 30 microns using a grinding machine. The final thickness of the thin sections was evaluated by measuring different points with a comparator, first assessing the glass and then various areas of the section. Areas not meeting the 30-micron thickness were manually ground using powdered silicon carbide mixed with water. The effectiveness of this grinding was inspected under an optical microscope by observing the interference colors of quartz. The final steps involved polishing the surface of the sections with an automatic polisher.

- III. Once the preparation of the sections is complete, the samples are then ready for examination using the Leica DM750 P Polarized Light Microscope (PLM) equipped with a FLEXACAM C1 integrated digital camera, utilizing objectives of 1.6X, 4X, and 10X in transmitted light (TL) mode with a resolution of 4000dpi. The analysis of thin sections is conducted at various magnifications to meticulously assess each sample at multiple levels of detail and ImageJ software was used to measure the aggregate sizes.

## **7.6. (SEM & EDS): SCANNING ELECTRON MICROSCOPY & ENERGY DISPERSIVE SPECTROSCOPY**

SEM-EDS provides a deeper inspection, magnifying samples to the nanometer level. The SEM captures detailed images of the mortar's microstructure, while the EDS module conducts point-specific analyses of the elemental composition. This comprehensive approach allows for the identification of various aggregates and secondary materials, such as repair compounds or modifications resulting from environmental exposure.

I. For SEM-EDS, each of the six samples underwent a preparation process that involved coating the thin sections (initially examined via optical microscopy) with a fine layer of gold using the Quorum Q150R rotary pumped coater via a sputtering method. This gold coating enhances the spatial resolution of the images due to gold's conductive properties.



Figure 78: Quorum Q150R Rotary pump Coater used for gold coating.

II. Following this, the samples were individually examined with the Coxem EM-30 plus tabletop SEM at an acceleration voltage of 20 kV. Observations were made at varying magnifications using secondary electrons to gather chemical data from the samples, and semi-quantitative elemental compositions were determined through EDS analysis.

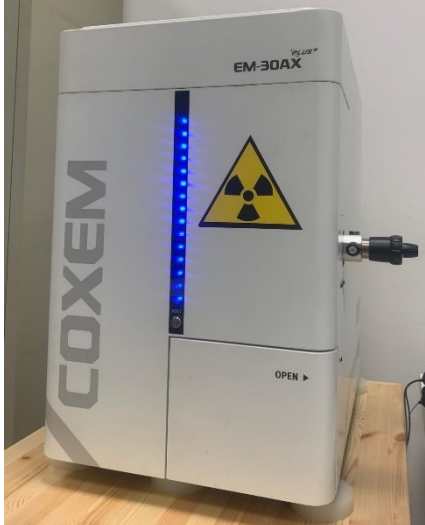
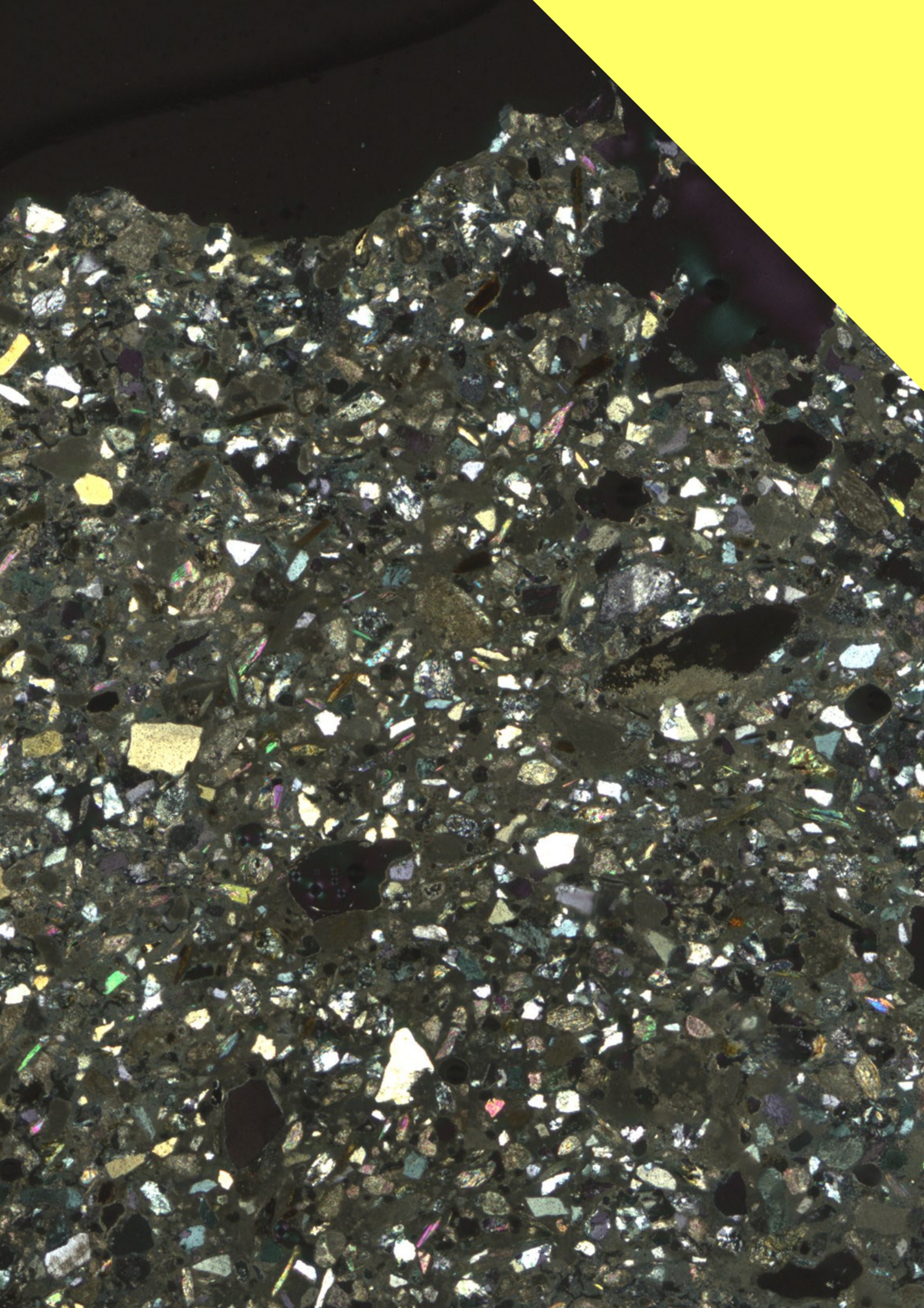


Figure 79: COXEM EM-30AX + SEM.

The collected data—including diffractograms from XRPD, micrographs from OM and SEM, and elemental maps from EDS—are integrated to create a comprehensive profile of each mortar. This detailed profile is instrumental in pinpointing the exact materials and construction techniques employed, shedding light on the technological methods of the period. Additionally, this analysis aids in evaluating the mortar's performance attributes such as strength, permeability, and resistance to environmental degradation, crucial for assessing the structure's long-term resilience and selecting the most suitable sample for  $^{14}\text{C}$  testing.



# Chapter VIII : Results

## 8.1. COLORIMETRY RESULTS

Sample	L*	a*	b*	Color	R	G	B
SM_01	84.9	1.6	7.6		221	210	198
SM_02	87.6	1.3	7.8		229	218	205
SM_03	84.8	1.3	8.0		221	210	197
SM_04	84.8	1.9	9.5		223	210	194
SM_05	85.2	1.9	9.7		224	211	195
SM_06	87.9	1.6	9.3		231	219	203

Table 3: Colorimetry results on the powder form of the mortar samples.

The colorimetry results of the six mortar samples (SM\_01 to SM\_06) are represented by three key values: L\*, a\*, and b\*. These values describe the color of each sample in the CIELAB color space, a color space defined by the International Commission on Illumination (CIE).

L\*: Lightness value, ranging from 0 (black) to 100 (white).

a\*: Red/Green value, where positive values indicate red and negative values indicate green.

b\*: Yellow/Blue value, where positive values indicate yellow and negative values indicate blue.

Additionally, the color representation in RGB (Red, Green, Blue) is also provided for each sample, giving a practical visualization of the color.

- ∴ Sample 06 is the lightest in terms of *lightness* ( $L^*$ ) with a value of 87.9, while Sample 01 is the darkest with an  $L^*$  value of 84.9. Samples 02 and 03 have an average  $L^*$  of 86.2, and Samples 04 and 05 have an average  $L^*$  of 85.0, falling in between.
- ∴ Regarding the *red/green* ( $a^*$ ) values, Samples 04 and 05 have the strongest red tint with an  $a^*$  value of 1.9, whereas Samples 02 and 03 have the weakest with an  $a^*$  value of 1.3.
- ∴ In terms of the *yellow/blue* ( $b^*$ ) values, Samples 04 and 05 are the most yellowish with  $b^*$  values of 9.5 and 9.7 respectively, Sample 01 is the least yellowish with a  $b^*$  value of 7.6, and Sample 06 has a significant yellow tint with a  $b^*$  value of 9.3, though less than Samples 04 and 05.
- ∴ Overall, considering the *RGB values*, Sample 06 is the lightest and potentially most neutral in color (RGB: 231, 219, 203), while Sample 01 is darker with a more pronounced grayish tint (RGB: 221, 210, 198). Samples 02 and 03 are lighter than Sample 01 but darker than Sample 06, with an average RGB of 225, 214, 201. Samples 04 and 05 are the most yellowish among all the samples, with an average RGB of 223.5, 210.5, 194.5.

## 8.2. X-RAY POWDER DIFFRACTION (XRPD) RESULTS

The XRPD patterns from a total of 06 mortar samples were analyzed both qualitatively and quantitatively. Mineral phases were identified using X'Pert HighScore Plus software, while quantitative analyses were performed using the Rietveld method through Topas software from Bruker. The quantitative values obtained from these analyses are presented in the following table.

Sample	Calcite	Hydrocalumite	Hydrotalcite	Dolomite	Quartz	Albite	Microcline	Muscovite	Clinochlore	Hematite	Ilmenite	Amorphous
SM_01	38.20	1.87	0.00	4.73	17.17	4.49	2.07	5.65	2.26	0.44	0.15	22.97
SM_02	28.35	0.57	0.00	10.03	25.05	7.98	2.23	7.58	2.79	0.44	0.28	14.26
SM_03	24.62	2.31	0.17	8.61	26.39	8.08	2.29	6.83	3.14	0.52	0.19	16.84
SM_04	44.88	0.64	0.00	13.62	15.23	5.33	2.61	2.59	1.36	0.45	0.27	13.03
SM_05	37.90	0.38	0.00	16.99	15.49	5.39	2.81	2.88	1.66	0.59	0.18	15.73
SM_06	34.19	0.00	0.00	14.94	24.55	8.35	3.80	4.01	2.21	0.58	0.20	7.17

Table 4: XRPD results on Powder form of mortar samples.

### 8.2.1. COMPOSITION ANALYSIS

Each sample contains varying percentages of several minerals. These mineral percentages explain the composition of the mortar samples.

- ∴ *Calcite*: The primary component, suggesting the use of lime in the mortar.
- ∴ *Hydrocalumite and Hydrotalcite*: Present in some samples, indicating possible pozzolanic reactions.
- ∴ *Dolomite*: Found in varying amounts, suggesting dolomitic lime or dolomite aggregates and their reactivity in the binder matrix.
- ∴ *Quartz*: Common in all samples, indicating sand or other siliceous aggregates.
- ∴ *Albite and Microcline*: Feldspar minerals indicating the presence of specific types of sand or aggregates.
- ∴ *Muscovite*: A mica mineral, suggesting the use of specific geological materials.
- ∴ *Clinochlore, Hematite, Ilmenite*: Various other minerals contributing to the overall composition.
- ∴ *Amorphous phase*: Non-crystalline components, possibly from unreacted lime or other binder materials.

### 8.2.2. REACTION PHASES

The presence of calcite as the dominant component across all samples indicates the primary binder is lime. The presence of hydrocalumite and hydrotalcite in some samples suggests pozzolanic reactions, where silica and alumina from aggregates react with lime to form additional binder

phases. The presence of quartz, feldspars, and other minerals points to the use of natural sand or crushed stone aggregates.

### 8.2.3. CONSTRUCTION TECHNOLOGY

The use of lime (calcite) as the primary binder, along with the presence of quartz and feldspar minerals, suggests the manufacturing of a traditional lime mortar. The variations in dolomite content might indicate the use of dolomitic lime or the inclusion of dolomite-rich aggregates. The presence of pozzolanic phases in some samples suggests the use of materials that would react with lime to enhance the mortar's durability and strength, or that para-pozzolanic reaction happened during the reaction phases.

### 8.2.4. SAMPLE CLUSTERING

Clusters will be based on the similarities in their mineralogical compositions, which can be influenced by the raw materials proportions, compositions and the reaction phases precipitated during the mortar preparation.

- ∴ SM\_01: This sample is predominantly composed of calcite (38.20%) and amorphous materials (22.97%). The presence of hydrocalumite (1.87%) indicates the presence of AFm phases, suggesting a binder matrix with high pozzolanic activity, producing non-crystalline C-S-H and M-S-H phases.
- ∴ SM\_02 and SM\_03: These samples have lower calcite content (28.35% and 24.62%, respectively) but are richer in silicate sand and quartz (25.05% and 26.39%, respectively). The presence of hydrocalumite (0.57% and 2.31%) and hydrotalcite (0.00% and 0.17%) indicates noticeable pozzolanic reactions, suggesting a shift towards silicate-based aggregates.

The moderate calcite and high quartz content indicates a consistent source of lime and similar aggregate in SM\_01, SM\_02 and SM\_03, highlighting the only difference as SM\_01 having a well reacted, prominent pozzolanic reaction.

- ∴ SM\_04 and SM\_05: These samples are rich in calcite (44.88% and 37.90%) and dolomite (13.62% and 16.99%) with a reduced presence of AFm phases (hydrocalumite at 0.64% and 0.38%), reflecting a fatter binder matrix with carbonate aggregates. They have higher calcite and moderate quartz, indicating more lime usage and potentially different sources of aggregates or proportions.

- ∴ SM\_06: This sample has high calcite (34.19%) and dolomite content (14.94%), with no evident pozzolanic reactions (absence of hydrocalumite and hydrotalcite), signifying a binder matrix dominated by aerial reaction. The lower amorphous content (7.17%) also supports the lack of pozzolanic activity. It stands alone with high quartz and balanced mineral composition, indicating a distinct source or preparation method.

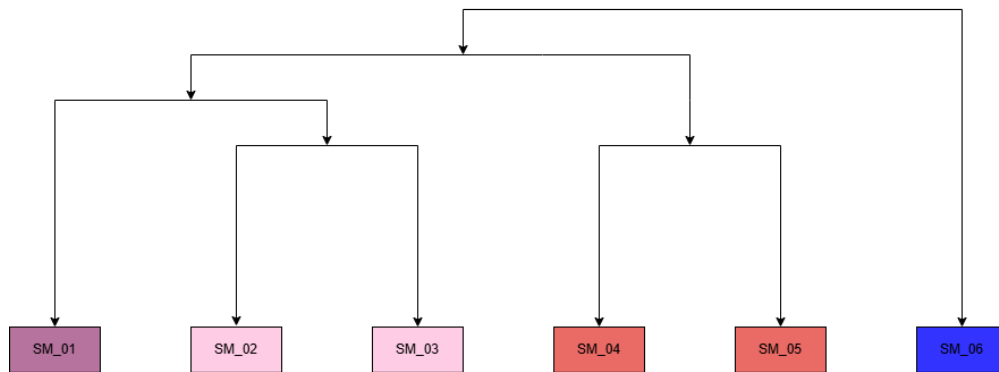


*Table 5: Clustering of mortar samples based on XRPD Data.*

### 8.3. OPTICAL MICROSCOPY (OM) RESULTS

The observation of the thin sections under the polarized light microscope was done on six samples from each sample location representing all the remaining walls. Similar characteristics such as binder type, composition and the size of aggregates of the binder fraction provided insights to filter out the oldest and more suitable sample for the <sup>14</sup>C dating. The aggregate sizes were measured using the IMAGE J software. Three types of images are taken to compare the unique features as follows, brightfield images in reflection mode, plane polars mages in transmission mode and crossed polars images in transmission mode. Brightfield microscopy is a technique that displays the true colors of a sample by directly illuminating it and capturing light transmitted through it. This method often reveals the natural colors of the sample, although these can be enhanced by dyes or stains applied during preparation. On the other hand, transmission microscopy enhances the visibility of transparent specimens by giving at the same time useful information on the petrographic characteristics of constituents. Each of these techniques highlights different aspects of the sample, making them valuable for various applications in scientific and medical imaging.



### 8.3.1. SAMPLE 01 - OPTICAL MICROSCOPY SCANS

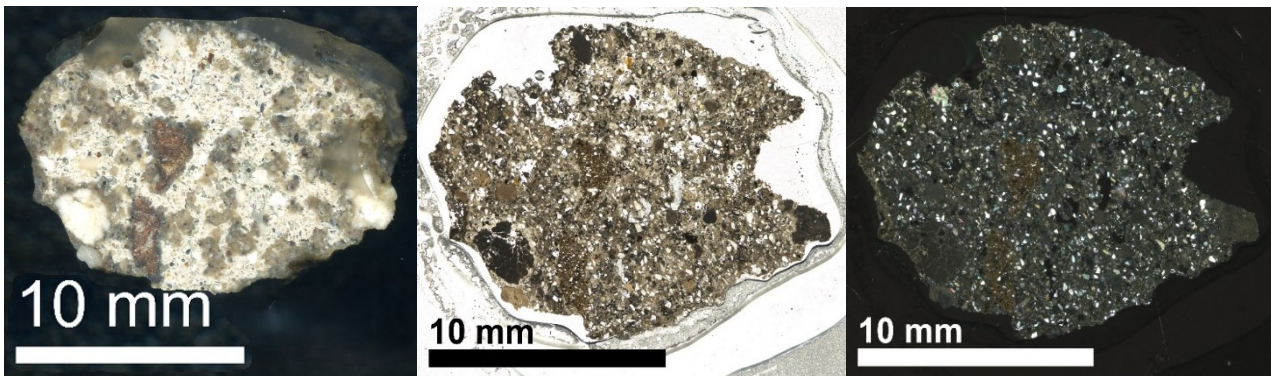
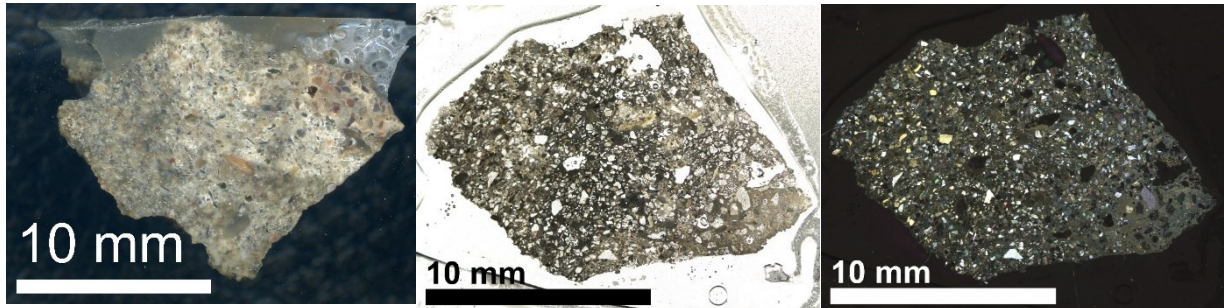


Figure 80: Brightfield image, plane polars transmission image and crossed polars transmission image of SM\_01.

- ∴ Binder Composition: The mortar sample (SM\_01) features a fat white binder phase, indicative of a lime-rich composition, with a fine aggregate fraction. The binder appears heterogeneous, displaying varying degrees of birefringence under polarized light microscopy. Brighter regions within the binder suggest areas of higher birefringence, likely resulting from the carbonation of the lime paste, while darker regions may indicate the presence of hydrated aluminosilicate phases. Additionally, the binder's structure ranges from sparitic to microcrystalline (micritic), reflecting its complex and varied nature. The presence of lime lumps, visible as almost white patches, further supports the lime-rich composition. These lumps, remnants of incompletely slaked lime, are characteristic of traditional lime mortars and can influence the mortar's durability and structural properties.
- ∴ Reaction Rims: The darker binder matrix observed in the sample suggests the occurrence of para-pozzolanic reactions. These reactions may have occurred due to the interaction of the lime binder with siliceous materials within the aggregate, leading to the formation of reaction rims. The presence of these rims indicates a chemical interaction between the binder and certain aggregate particles, contributing to the overall strength and longevity of the mortar.
- ∴ Aggregate Characteristics: The mortar contains a diverse array of aggregates, including medium to coarse gravels and fine sands, exhibiting a bimodal distribution. The sand fraction appears to have been sourced from the Bacchiglione River, as indicated by its composition. The aggregates include quartz and other minerals, with the mean aggregate dimension around 0.243 mm, primarily represented by mica, while the maximum dimension reaches 3.028 mm, likely from argillite. The presence of carbonate minerals, such as dolomite and calcite, is also noted. The aggregates are well-distributed within the binder, contributing to the mortar's structural integrity. Lime lumps, measuring up to 2.5 mm, are dispersed throughout the sample and are indicative of historical construction techniques where the lime was not fully slaked before mixing with the aggregates. The lime lumps, while potentially beneficial for the

mortar's strength, could also introduce weaknesses if they were too numerous or unevenly distributed.

### 8.3.2. SAMPLE 02 OPTICAL MICROSCOPY SCANS



*Figure 81: Brightfield image, plane polars transmission image and crossed polars transmission image of SM\_02.*

- ∴ Binder Composition: The binder in SM\_02 is also lime-based, with relevant non-birefringent areas relating to the occurrence of hydrated aluminosilicates. The texture is more uniform compared to SM\_01, with fewer visible lime lumps, suggesting a more thoroughly mixed or slaked mortar. The binder displays a fine micritic structure with some spitic regions, indicating variable carbonation. The presence of finer lumps within the binder might suggest the use of more processed lime or a different mixing technique compared to SM\_01.
- ∴ Reaction Rims: Like SM\_01, reaction rims are present, though they seem less pronounced, indicating potentially fewer pozzolanic reactions or a lower reactivity of the aggregate materials with the binder. The overall chemical reactivity within the sample might be lower, possibly reflecting different environmental conditions or a different lime composition.
- ∴ Aggregate Characteristics: SM\_02 exhibits a more homogeneous aggregate distribution, with a maximum aggregate size of around 1 mm and a mean size of 0.243 mm. The aggregates are finer overall, with fewer coarser particles, suggesting a different sourcing or sieving process for the sand. The aggregates include a significant amount of silicates, and their linear distribution within the binder indicates a well-processed mix. The absence of larger particles might suggest that SM\_02 was used in a finer bedding layer or in a context where a smoother, less textured mortar surface was required.

### 8.3.3. SAMPLE 03 OPTICAL MICROSCOPY SCANS

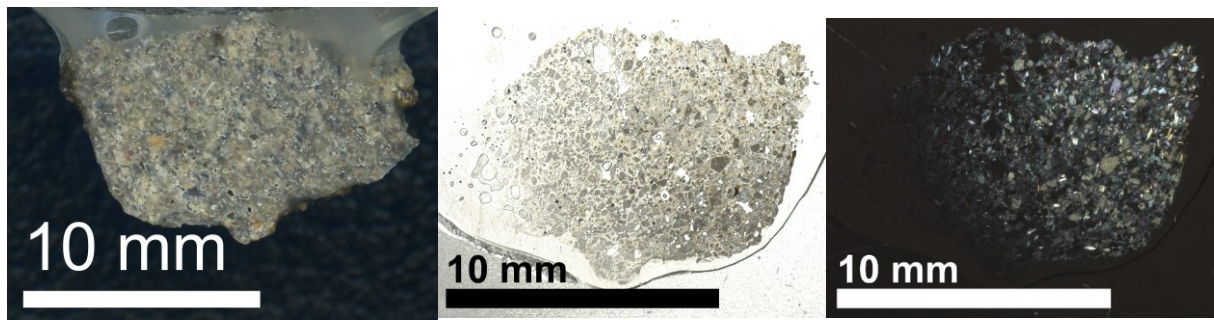


Figure 82: Brightfield image, plane polars transmission image and crossed polars transmission image of SM\_03.

- ∴ Binder Composition: Both SM\_02 and SM\_03 have a finely textured binder, which indicates a similar approach in the mortar mix, with less to no lime lumps compared to SM\_01 and SM\_02. The fine micritic structure in both samples suggests that these mortars were optimized for similar functions, possibly in the same phase of construction or in layers requiring a finer finish.
- ∴ Reaction Rims: SM\_03, like SM\_02, displays several areas characterized by low to null birefringence due to pozzolanic reaction, which indicates an active interaction between the lime binder and the siliceous materials in the aggregate. This reaction suggests that both samples were exposed to similar environmental conditions or that they were designed to enhance the durability of the structure through pozzolanic activity.
- ∴ Aggregate Characteristics: The aggregate characteristics of SM\_02 and SM\_03 are quite similar, with mean aggregate dimensions of 0.243 mm and maximum dimensions close to each other (0.255 mm for SM\_03). This suggests a consistent selection of aggregate material, likely sourced from the same location or prepared using similar sieving methods.

### 8.3.4. SAMPLE 04 OPTICAL MICROSCOPY SCANS

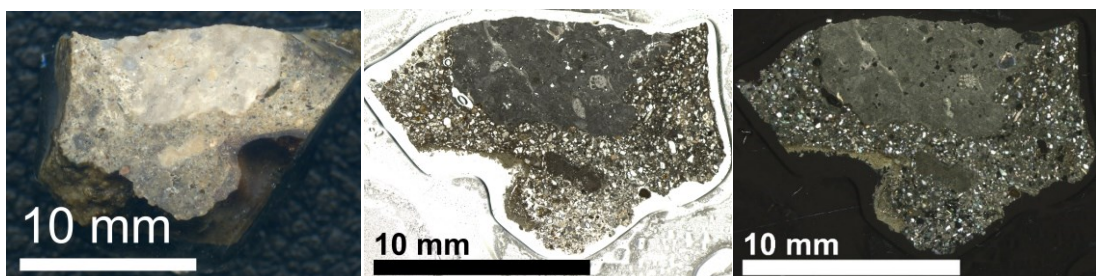


Figure 83: Brightfield image, plane polars transmission image and crossed polars transmission image of SM\_04.

- ∴ Binder Composition: The binder in SM\_04 appears to be lime-based, like the other samples, but it exhibits a distinct heterogeneous texture. This sample contains a lime lump sized at

0.436 mm, relatively smaller compared to those found in SM\_01, but still relevant. This evidence may suggest that the lime was not fully slaked before use, which is a characteristic evidenced also in sample SM\_01.

- ∴ Reaction Rims: The presence of reaction rims around aggregates in SM\_04 indicates past chemical interactions, like what is seen in SM\_01 and SM\_02 but less prominent, suggesting slightly less reactivity or that it was exposed to different environmental conditions.
- ∴ Aggregate Characteristics: The aggregates in SM\_04 are characterized by a mean size of 0.600 mm, with the presence of a centimeter-sized limestone aggregate. This is a significant contrast to SM\_02 and SM\_03, where the aggregates are finer and more uniform, with mean sizes around 0.243 mm and maximum dimensions generally below 1 mm. SM\_04's coarser aggregates suggest a more structural role for this mortar, possibly in a foundational layer or a context where greater strength was required, whereas SM\_02 and SM\_03 were likely used in finishing layers where smoothness was key.

#### 8.3.5. SAMPLE 05 OPTICAL MICROSCOPY SCANS

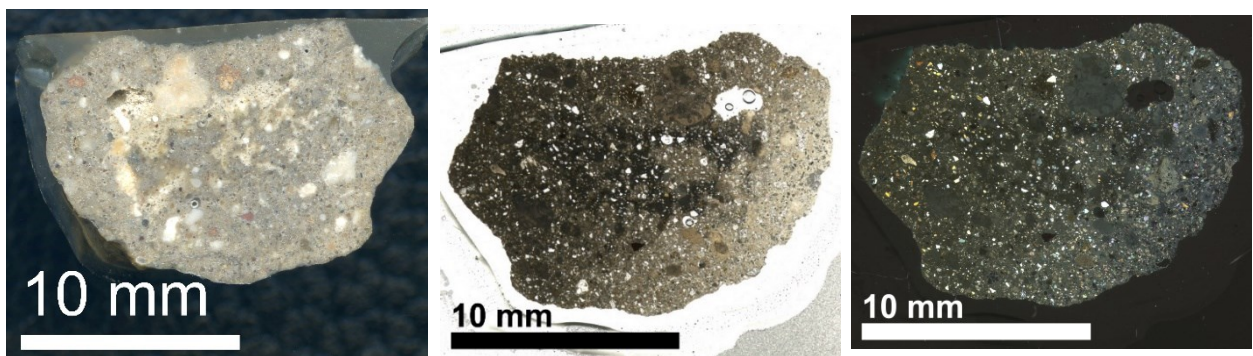


*Figure 84: Brightfield image, plane polars transmission image and crossed polars transmission image of SM\_05.*

- ∴ The binder in SM\_05 contains multiple lime lumps, with sizes of 0.435 mm, 0.315 mm, and 0.335 mm. This indicates that the lime was not fully slaked before mixing, like what has been observed in SM\_01 and SM\_04, suggesting a traditional preparation technique, possibly aimed at enhancing the mortar's workability or strength. The binder's texture appears relatively coarse, reflecting a composition that balances the inclusion of lime lumps with a generally finer matrix, aligning more closely in terms of binder heterogeneity.
- ∴ SM\_05 displays significant reaction rims, second only to SM\_01. These reaction rims indicate active chemical processes, such as pozzolanic reactions, occurring between the lime binder and the siliceous aggregates. The prominence of these rims suggests that SM\_05 was designed to be durable, possibly with a focus on strengthening the bond between binder and aggregates.

- ∴ The aggregates in SM\_05 have a mean size of 0.146 mm, with a prominent aggregate reaching 1.321 mm. The aggregate distribution suggests a mixture that is both varied and carefully selected, like SM\_04 but with slightly finer mean aggregate sizes. The presence of large lime lumps alongside these aggregates suggests that SM\_05 was intended for a structural role, providing both strength and some degree of refinement aligning with its sampling locations, the West wall faced that bared a window with regular stone blocks. Comparing sample SM\_01 with the pair of samples SM\_04 and SM\_05, the latter are fatter, having big lumps and a coarser aggregate fraction. While SM\_01 is more reacted.

### 8.3.6. SAMPLE 06 OPTICAL MICROSCOPY SCANS

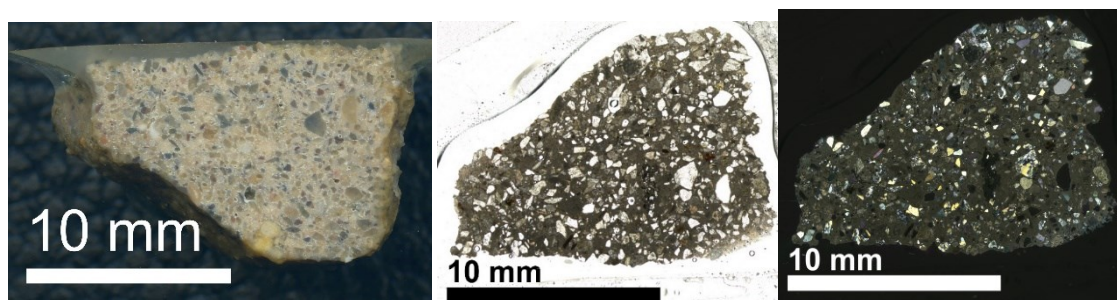


Figure 85: Brightfield image, plane polars transmission image and crossed polars transmission image of SM\_06.

- ∴ The binder in SM\_06 appears to be dense and uniform, surrounding a significant number of aggregates. The relatively fine texture of the binder, with fewer visible lime lumps, suggests a well-mixed mortar, potentially indicating a more refined or controlled preparation method. The overall consistency of the binder points towards a mix intended for strength and durability, likely used in structural applications where the uniformity of the binder was crucial. Compared to SM\_01, SM\_04, and SM\_05, which exhibit more heterogeneous binders with visible lime lumps, SM\_06 stands out for its more uniform binder. SM\_06's higher aggregate content suggests a need for greater structural integrity, and possibly a mortar of a newer construction phase.
- ∴ The absence of reactive phases suggests that SM\_06 was designed to have a more stable and less reactive mortar composition, which aligns with the uniformity of the binder.
- ∴ SM\_06 is characterized by a high aggregate content with a mean aggregate dimension of 0.56 mm. The aggregates are well-distributed and consistent in size, suggesting that the mortar mix was carefully prepared with an emphasis on uniformity and structural integrity.

## 8.4. SCANNING ELECTRON MICROSCOPY WITH ENERGY-DISPERSIVE SPECTROSCOPY (SEM-EDS) RESULTS

### 8.4.1. SEM SCANS OF SAMPLE 01

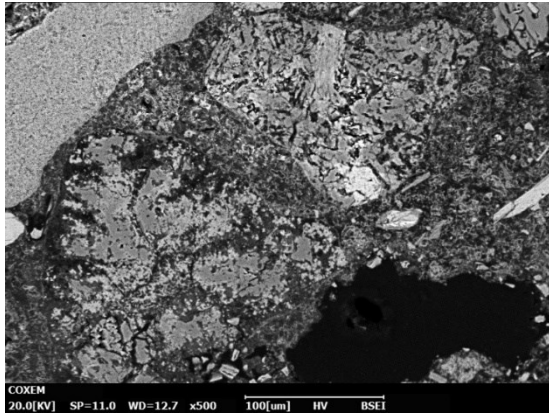


Figure 86: SEM at x500 and WD-12.7 of SM\_01.

The mortar exhibits a dark, complex matrix where pozzolanic reactions dominated. The dissolution of microcrystalline quartz or chert released silicon, while dolostones contributed magnesium, leading to the formation of M-S-H phases within the binder. The interaction between the dissolved silica from quartz or chert and magnesium from dolostones under alkaline conditions resulted in the formation of M-S-H. This process is indicative of dedolomitization within the

alkaline carbonate environment, crucial for the stability and durability of the mortar. The dissolution of silicates, such as those found in quartz or chert, and dolomites is key to the mortar's microstructure. This dissolution not only releases essential ions for M-S-H formation but also affects the overall composition and strength of the binder. The binder is predominantly composed of CaO, SiO<sub>2</sub>, and MgO, with minor contributions from Al<sub>2</sub>O<sub>3</sub> and Fe<sub>2</sub>O<sub>3</sub>. This composition highlights a complex reaction environment where pozzolanic and dedolomitization processes have significantly altered the materials, enhancing the mortar's performance over time.

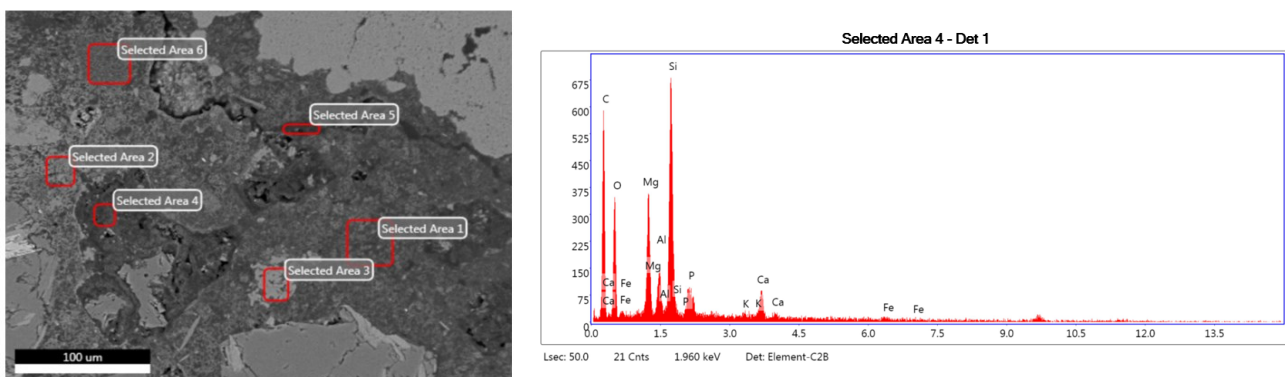


Figure 87: SEM-EDS analysis demonstrating the M-S-H phases and para pozzolanic reactions of SM\_01.

### 8.4.2. SEM SCANS OF SAMPLE 02 & 03

The SEM analysis of Sample 02 and Sample 03 shows comparable results. In Area 8 of SM\_02, a complex matrix rich in calcium oxide (CaO), magnesium oxide (MgO), and silicon dioxide (SiO<sub>2</sub>) is visible. While SM\_03 shares similar characteristics with SM\_02, it additionally reveals an "M-S-H"

phase with a shoe-shaped plagioclase particle in Area 07. This combination indicates a lime-based mortar in which the siliceous and magnesian components of the aggregate reacted to form magnesium silicate hydrates (M-S-H). The presence of M-S-H phases is particularly significant as it suggests a strong pozzolanic reaction, which not only enhances the mechanical properties of the mortar but also contributes to its long-term durability. The interaction between calcium carbonate ( $\text{CaCO}_3$ ) and the silicate components leads to a robust and chemically stable structure. This indicates that the mortar was carefully formulated, possibly using local materials rich in magnesium and silica, to create a durable and resilient binding material suitable for the construction's long-term preservation.

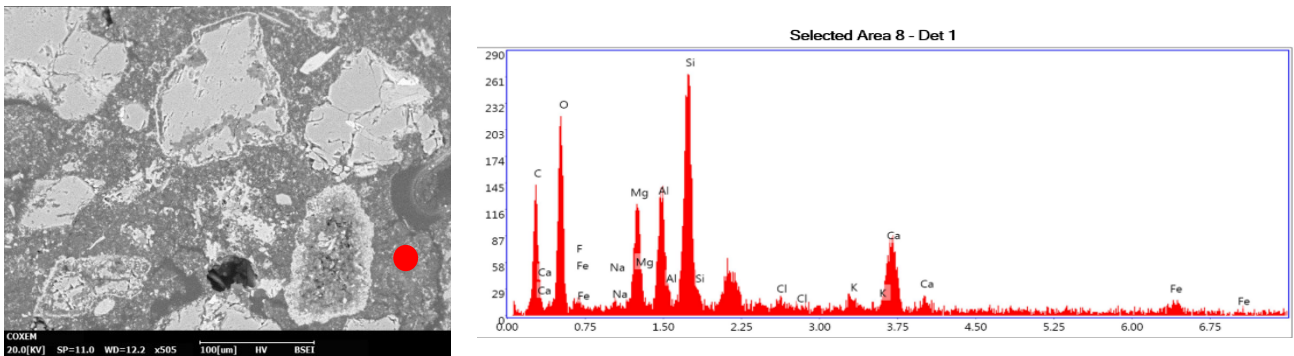


Figure 88: SEM -EDS Analysis of SM\_02 demonstrating the presence of an association of anthropogenic carbonates and M-(A)-S-H phases.

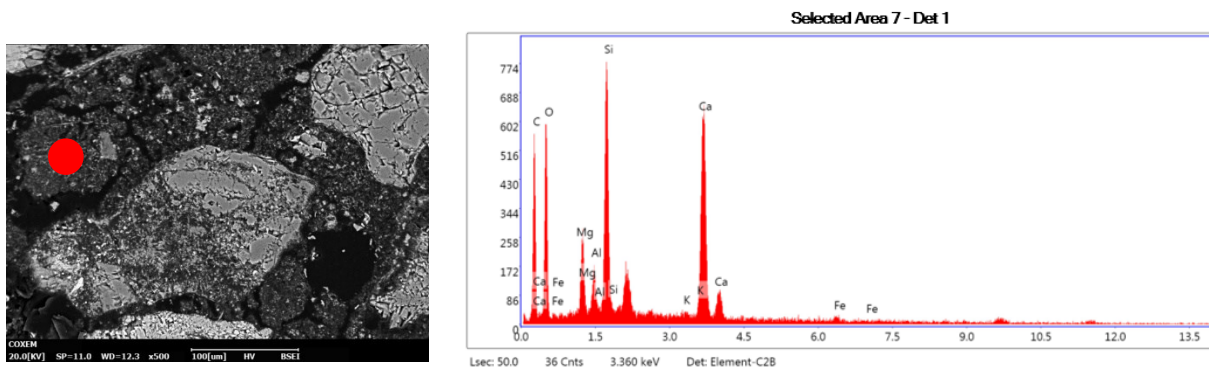


Figure 89: SEM-EDS analysis of SM\_03 demonstrating M-S-H phase with shoe shaped plagioclase particle.

#### 8.4.4. SEM SCANS OF SAMPLE 04 & SAMPLE 05

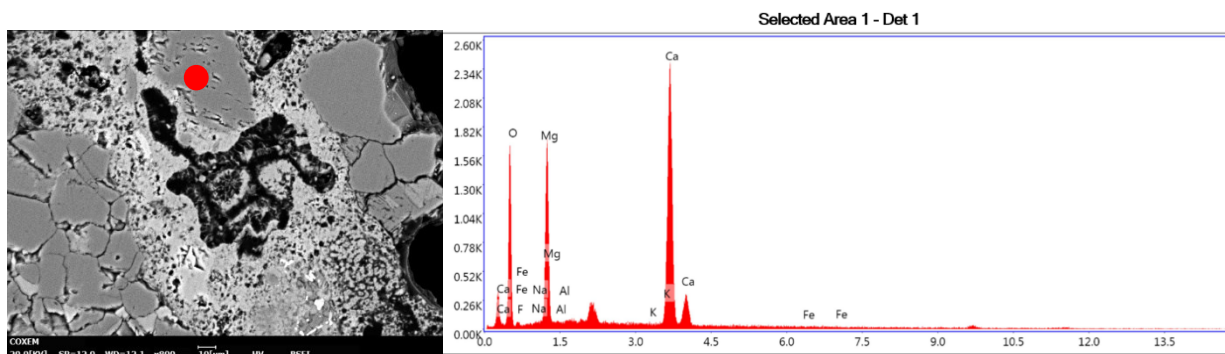


Figure 90: SEM -EDS of SM\_04 demonstrating the preservation of dolomite.

The Energy Dispersive X-Ray Spectroscopy (EDS) spectrum reported above of SM\_04, is related to a clast of dolostone aggregate with the typical Ca/Mg ratios expected for such mineral. The clast doesn't show any trace of interfacial dissolution due to dedolomitization processes, as observed in the previous samples. This indicates excellent preservation of dolomite in this material.

The absence of pozzolanic and para-pozzolanic reaction processes, along with the preservation of dolomite, suggests that the dolomite components did not chemically interact within the binder matrix, which indeed resulted mainly Ca-based, as indicated by the EDS spectrum reported below from SM\_05. Such findings suggest a structurally focused use of the mortar, relying heavily on the binding properties of lime, characteristic of earlier construction methods before the development of advanced mortar technologies based on the utilization of hydraulic binders. The analysis underscores the challenges in accurately quantifying such ancient material compositions due to their complex degradation and preservation states.

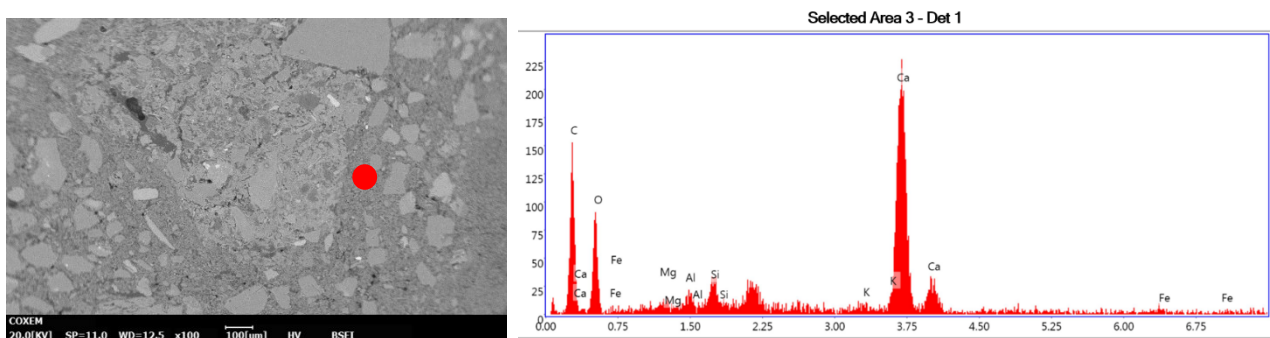


Figure 91: SEM -EDS of SM\_05 demonstrating the lime-based nature of the binder and the absence of para-pozzolanic reactions.

#### 8.4.6. SEM SCANS OF SAMPLE 06

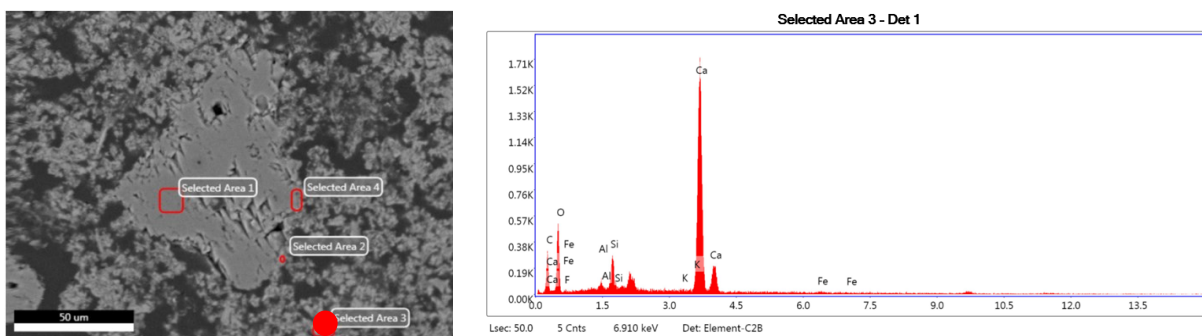


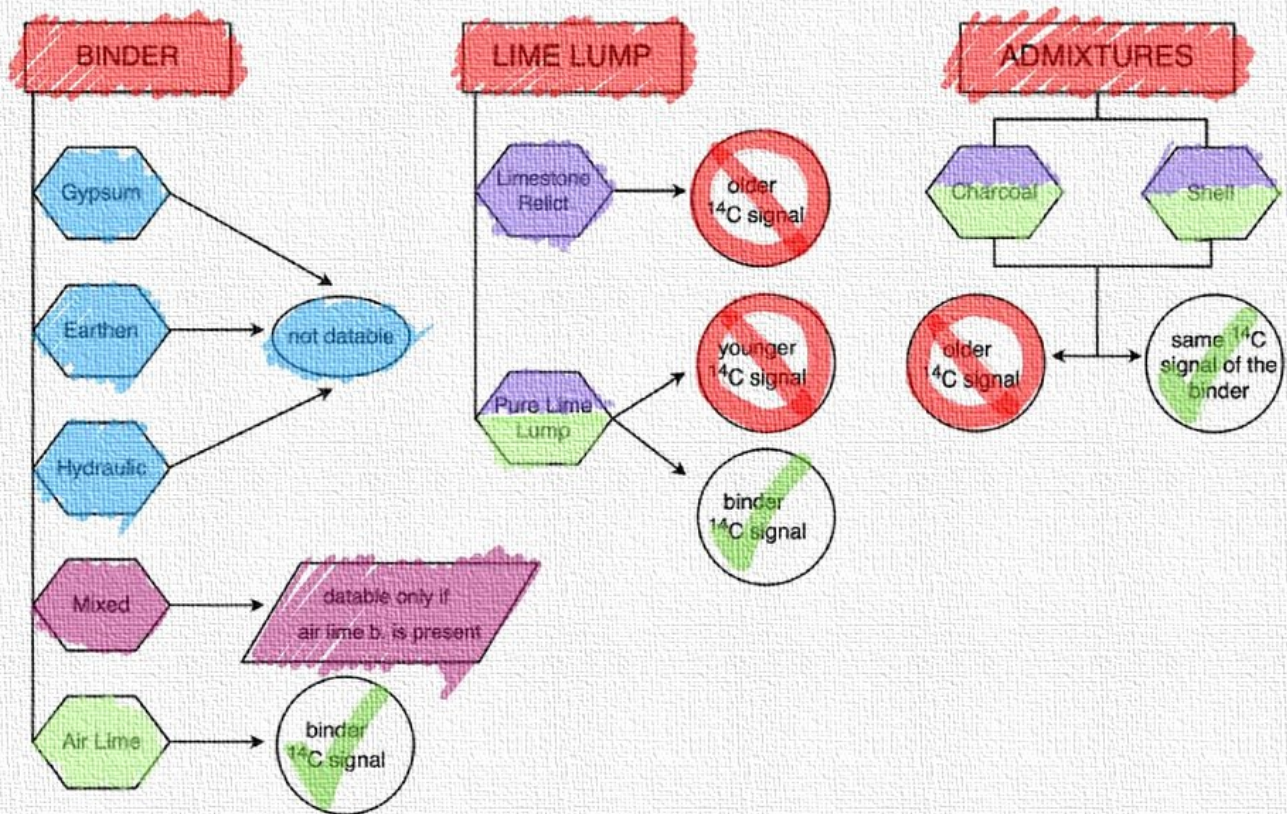
Figure 92: SEM-EDS of SM\_05 highlighting Calcic Composition, indicating an Aerial Reaction with No Evidence of M-S-H or Para-Pozzolanic Reactions.

The EDS spectrum of Area 3 of SM\_06 reveals a calcium-rich composition, indicating the mortar underwent an aerial lime carbonation reaction, where the setting and hardening of the mortar are primarily due to the reaction of lime with atmospheric carbon dioxide (CO<sub>2</sub>), forming calcium carbonate (CaCO<sub>3</sub>).

The absence of M-S-H or para-pozzolanic reactions, as seen in SM\_04 and SM\_05, suggests the mortar relied solely on traditional lime carbonation rather than hydraulic binding processes.



# WHAT ARE THE DATABLE MORTAR MATERIALS ?



( Addis, et al., 2019)

# Chapter IX: Discussion

## 9.1 INTERPRETATION OF COLORIMETRY DATA

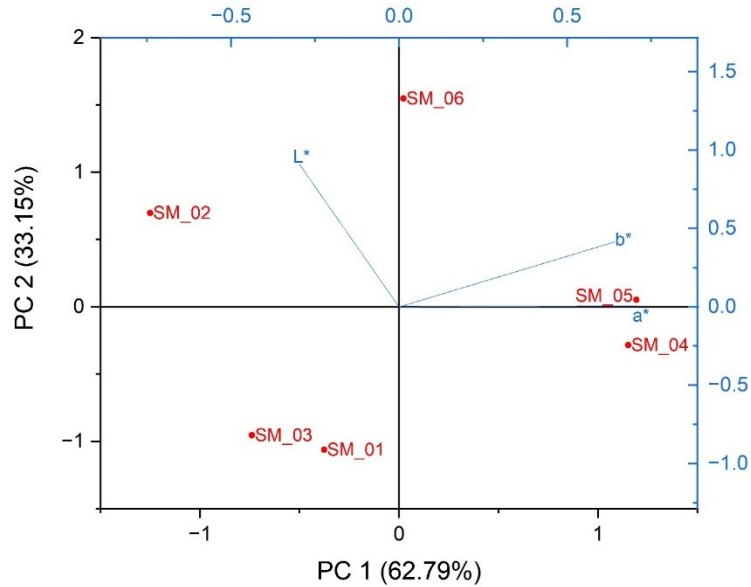


Figure 93: PCA of Colorimetry data for powdered form of mortar samples.

The biplot of the PCA (principal component analysis) performed on the colorimetry analysis of mortar samples is reported in the figure above, with PC1 (Principal Component 1) and PC2 (Principal Component 2) representing 95.94% of total variance in the data. Abbreviations: The blue vectors ( $L^*$ ,  $a^*$ ,  $b^*$ ) represent the original variables, with  $L^*$  indicating lightness,  $a^*$  the red-green color coordinate and  $b^*$  the yellow-blue color coordinate.

The PCA of the colorimetry data for the analyzed mortar samples reveals distinct groupings and relationships among the samples based on their color characteristics. Here's a detailed analysis of these groupings:

- *SM\_01 and SM\_03*: These samples are positioned close to each other in the lower left quadrant, with low scores on both PC1 and PC2. Indicating that they share similar characteristics.
- *SM\_02*: This sample stands alone in the upper left quadrant, indicating unique colorimetric properties characteristics with high PC2 and low PC1 scores.

Despite some variations, such as SM\_01 having closer colorimetric properties to SM\_03 other than SM\_02, they exhibit significant similarity, aligning well with XRPD-QPA results.

- *SM\_04 and SM\_05*: These samples are found near each other in the lower right quadrant, suggesting comparable properties with high PC1 and low PC2 scores. Their close positioning

indicates strong similarities in their color attributes, which agrees with the XRPD-QPA analysis.

- SM\_06: Positioned in the upper right quadrant, SM\_06 exhibits distinct characteristics with high scores on both PC1 and PC2. Its unique position highlights its differences in colorimetric properties from the other samples, suggesting a unique mineralogical composition.

This comprehensive analysis underscores the consistency with XRPD-QPA results, providing a clear understanding of the medieval mortar samples.

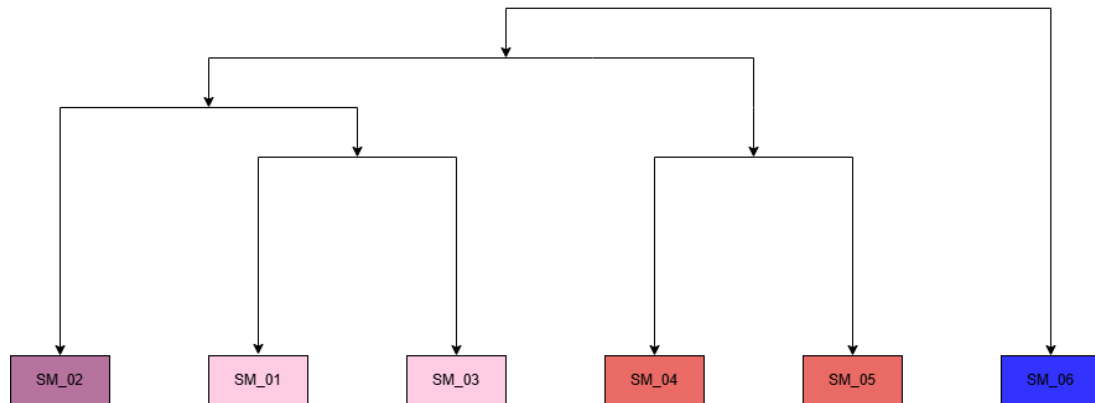


Figure 94: Clustering of the mortar samples based on the colorimetry data.

## 9.2 INTERPRETATION OF X-RAY POWDER DIFFRACTION DATA

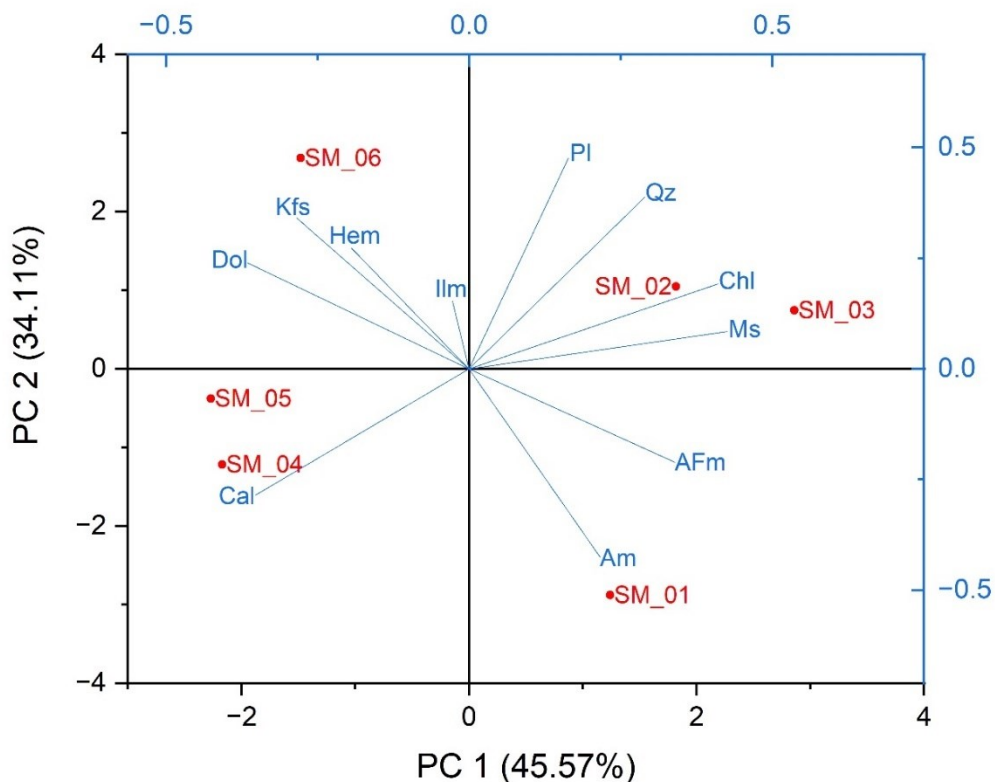


Figure 95: PCA of X-R-P-D Data.

The biplot of the PCA (principal component analysis) performed on the mineralogical profiles obtained from the analyzed bulk samples is reported in the figure above: The first two components have been plotted, representing 69.68% of the total variance. Abbreviations: Cal- calcite, Dol- dolomite, Kfs- K-feldspar (Potassium feldspar), Hem- hematite, Ilm-Ilmenite, Pl-plagioclase, Qz- quartz, Chl-chlorite, Ms-Muscovite, AFm- AFm phases (Alumina-ferrite monosulfate), Am - Amorphous material. The PCA results reveal distinct groupings and relationships among the mortar samples based on their mineralogical profiles.

**SM\_01** positioned in the lower right quadrant of the PCA biplot, is characterized by a mineralogical composition rich in amorphous material (Am) and AFm phases. The binder matrix exhibits a high pozzolanic reaction, leading to the formation of non-crystalline reaction products such as C-S-H (Calcium Silicate Hydrate) and M-S-H (Magnesium Silicate Hydrate) phases. This sample shows a significant pozzolanic activity within the binder matrix, with less emphasis on crystalline minerals, suggesting that the reactions are primarily driven toward the formation of amorphous and AFm phases.

**SM\_02 and SM\_03**, both positioned in the lower right quadrant of the PCA biplot, exhibit a mineralogical composition that is lower in calcite and richer in silicate minerals, with quartz constituting approximately 25% of the content. These samples also have a lower presence of carbonate aggregates like dolomite. The binder matrix shows evident pozzolanic reactions, suggesting that the significant amount of silicate sand is contributing to these reactions. The predominant aggregates in these samples are rich in silicate sand, highlighting the use of quartz as a significant aggregate material.

**SM\_04 and SM\_05**, located in the lower left quadrant, exhibit a mineralogical composition rich in calcite and dolomite with a detectable presence of AFm phases. The binder matrix in these samples is notably "fatter," indicative of a substantial calcite presence. This is further complemented by the use of dolomite as a significant aggregate, enhancing the samples' richness in carbonate minerals. The combination of calcite and dolomite, along with the distinct binder characteristics, underscores the unique composition and potential reactivity of these samples.

**SM\_06**, situated in the upper left quadrant, is characterized by a mineralogical composition that is high in calcite and dolomite but notably lacks pozzolanic compounds. The binder matrix in this sample is primarily composed of carbonate aggregates, reflecting the absence of pozzolanic reaction. This dominance of calcite and dolomite aggregates defines the overall composition and

structural attributes of the sample, emphasizing the significant presence of carbonate minerals without the influence of pozzolanic components.

### 9.3. INTERPRETATION OF OPTICAL MICROSCOPY DATA

In the context of Carbon-14 ( $^{14}\text{C}$ ) dating for archaeological mortar samples, optical microscopy plays a vital role in determining the suitability of these samples based on their microstructural characteristics. The key objective is to minimize the presence of geological carbon, which originates from older carbon sources, such as the limestone used in lime production. This geological carbon can skew the dating results, presenting an older age than the actual archaeological usage of the mortar.

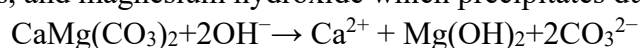
**SM\_02 and SM\_03** both samples exhibit a fine, homogeneously mixed, micritic structure across the binder matrix but they are unsuitable for  $^{14}\text{C}$  dating due to the effects of de-dolomitization. The dissolution of dolomite after the alkali-carbonate reaction in the binder matrix has resulted in the incorporation of geological carbon, making these samples unreliable for accurate  $^{14}\text{C}$  dating.

Conversely, **SM\_06**, although potentially good for  $^{14}\text{C}$  dating due to the absence of alkali-carbonate reactions, is likely a more recent restoration mortar. Its distinct characteristics compared to the other samples suggest it was applied in a later restoration phase, which may influence its suitability for accurately dating the original construction.

On the other hand, **SM\_01** is unsuitable for  $^{14}\text{C}$  dating due to the high level of de-dolomitization in the dolostone aggregate and the significant para-pozzolanic reaction observed. In contrast, **SM\_04** and **SM\_05** are identified as the best samples for dating. While comparable to the older samples (**SM\_01**, **SM\_02**, and **SM\_03**), they do not exhibit any de-dolomitization processes and are primarily composed of carbonated lime, making them more reliable for obtaining accurate  $^{14}\text{C}$  dates.

In conclusion, for archaeological studies where accurate  $^{14}\text{C}$  dating is essential, and the minimization of geological carbon is crucial, **SM\_04 and SM\_05** are recommended due to their mostly carbonated lime-based composition of binder matrices. These samples are most likely to yield reliable and accurate dating outcomes, providing a robust basis for chronological reconstructions associated with archaeological sites.

*The dissolution of dolomite in alkali-rich environments and its impact on  $^{14}\text{C}$  dating:* Dolomite, scientifically referred to as calcium magnesium carbonate ( $\text{CaMg}(\text{CO}_3)_2$ ), undergoes a chemical reaction with hydroxide ions in aqueous solutions, leading to the decomposition of dolomite into calcium ions that may remain in solution or precipitate as calcium carbonate depending on environmental conditions, and magnesium hydroxide which precipitates due to its lower solubility.



This reaction also releases carbonate ions into the solution. In the context of  $^{14}\text{C}$  dating, the carbonate ions originating from this process include ancient, non-radioactive carbon from geological sources, which alters the original amount of radioactive  $^{14}\text{C}$  ( $N_0$ ) in mortar samples. This results in dilution of the radioactive carbon, leading to inaccuracies in dating that render the sample seemingly older than it is.

The influence of aggregate size in this chemical behavior is notable, as studies such as (Katayama, 2009) demonstrate that fine dolomitic limestone aggregates, similar in size to sand, typically show signs of dedolomitization, thereby altering the chemical composition of the aggregates. Conversely, larger sand-sized particles of argillaceous dolomitic limestone exhibit a different reaction pattern, occasionally producing alkali-silica reaction by reacting with the alkaline components of the mortar. This demonstrates how the size of the aggregates can influence the specific chemical reactions observed within the mortar matrix.

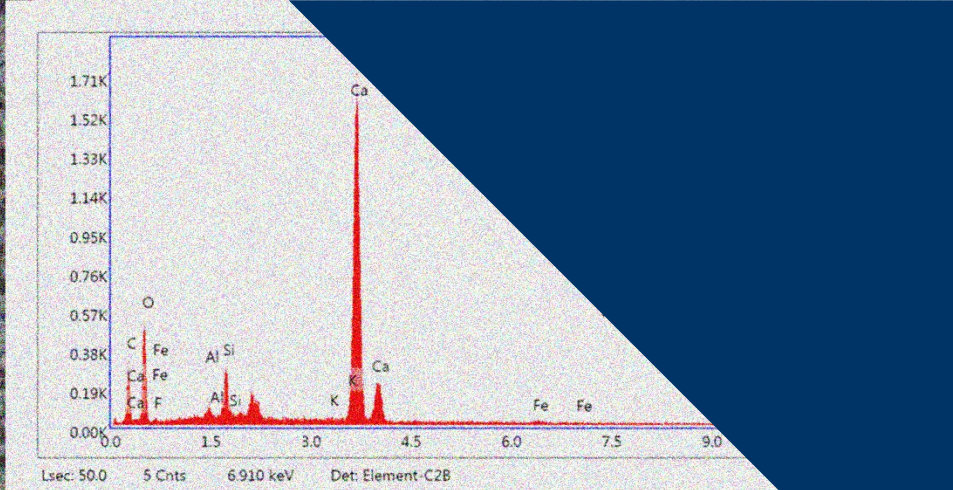
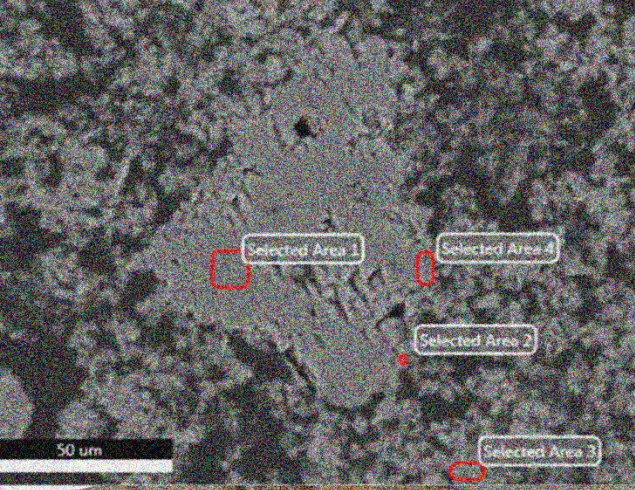
#### 9.4. INTERPRETATION OF SEM-EDS DATA

**Sample SM\_04** and **SM\_05** exhibit characteristics that make them suitable for  $^{14}\text{C}$  dating. The analysis for **SM\_04** shows a preservation of dolomite with low levels of secondary reactions, suggesting a minimal interaction within the binder matrix that would introduce geological carbon. The absence of strong pozzolanic or para-pozzolanic reactions indicates that the dolomite components are stable, with the geological carbon impact likely being low. This makes **SM\_04** a potentially good candidate for accurate  $^{14}\text{C}$  dating.

Similarly, **SM\_05** shows a high percentage of magnesium oxide (MgO) and calcium oxide (CaO) in the dolomite aggregates, indicative of a well-preserved dolomitic structure. The SEM-EDS results suggest that the dolomite content is stable, indicating reliable mineral preservation. This stability suggests minimal chemical alteration, which is ideal for  $^{14}\text{C}$  dating as it implies the preservation of the original carbon content necessary for accurate results.

Conversely, **SM\_06**, despite showing a significant presence of dolomite, indicates a different scenario. The SEM-EDS spectrum features high levels of calcium (Ca) and magnesium (Mg) but also shows minimal secondary mineral formations. This preservation of primary material composition, with low secondary reactions, implies minimal alteration due to pozzolanic reactions, which could have otherwise introduced geological carbon. Therefore, **SM\_06** also presents a good substrate for  $^{14}\text{C}$  dating due to the retained integrity of its original carbon content, but its characteristics significantly different from the other samples allow to hypothesize its origin from a more recent construction phase.

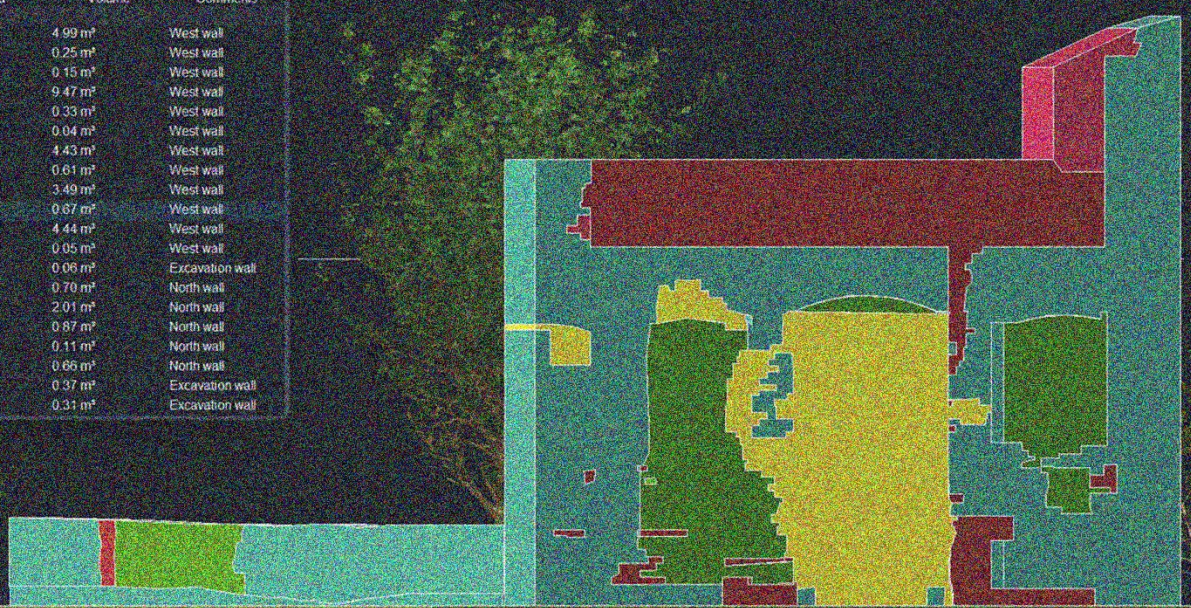
**SM\_01, SM\_02, and SM\_03**, however, are less ideal for  $^{14}\text{C}$  dating based on their SEM-EDS profiles. These samples show extensive signs of chemical reactions, such as the formation of magnesium silicate hydrate (M-S-H) phases and evidence of strong pozzolanic reactions, which are indicative of significant interaction with geological carbon sources. Such interactions suggest that these samples have incorporated older carbon from their limestone origins, making them unsuitable for providing accurate  $^{14}\text{C}$  dating results.



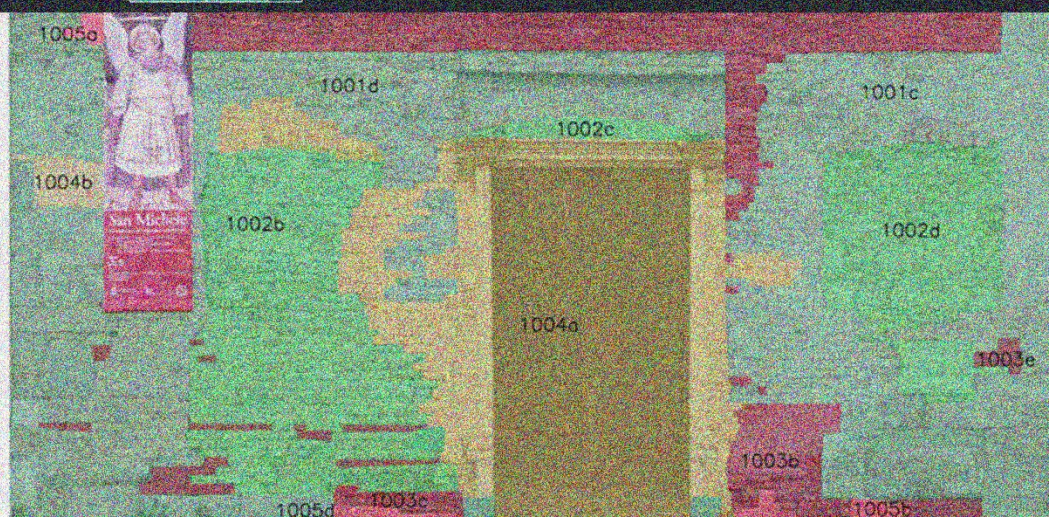
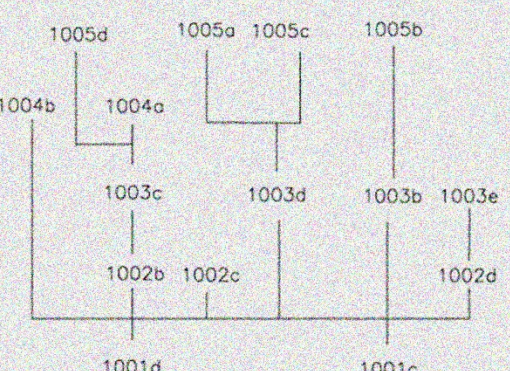
Final revit file .rvt - Schedule: Wall Material Schedule

<Wall Material Schedule>

A	B	C	D
Type	Area	Volume	Comments
1004	9.42 m <sup>2</sup>	4.99 m <sup>3</sup>	West wall
1004	0.46 m <sup>2</sup>	0.25 m <sup>3</sup>	West wall
1004	0.29 m <sup>2</sup>	0.15 m <sup>3</sup>	West wall
1001	17.87 m <sup>2</sup>	9.47 m <sup>3</sup>	West wall
1003	0.62 m <sup>2</sup>	0.33 m <sup>3</sup>	West wall
1003	0.07 m <sup>2</sup>	0.04 m <sup>3</sup>	West wall
1003	8.36 m <sup>2</sup>	4.43 m <sup>3</sup>	West wall
1003	1.15 m <sup>2</sup>	0.61 m <sup>3</sup>	West wall
1001	6.59 m <sup>2</sup>	3.49 m <sup>3</sup>	West wall
1005	1.26 m <sup>2</sup>	0.67 m <sup>3</sup>	West wall
1002	8.37 m <sup>2</sup>	4.44 m <sup>3</sup>	West wall
1003	0.09 m <sup>2</sup>	0.05 m <sup>3</sup>	West wall
1001	0.11 m <sup>2</sup>	0.06 m <sup>3</sup>	Excavation wall
1001	1.32 m <sup>2</sup>	0.70 m <sup>3</sup>	North wall
1001	3.79 m <sup>2</sup>	2.01 m <sup>3</sup>	North wall
1002	1.64 m <sup>2</sup>	0.87 m <sup>3</sup>	North wall
1003	0.20 m <sup>2</sup>	0.11 m <sup>3</sup>	North wall
1001	1.24 m <sup>2</sup>	0.66 m <sup>3</sup>	North wall
1001	0.70 m <sup>2</sup>	0.37 m <sup>3</sup>	Excavation wall
1001	0.58 m <sup>2</sup>	0.31 m <sup>3</sup>	Excavation wall



Phase 02 (green) Phase 05 (red)  
Phase 03 (yellow)





# Chapter X: Conclusion

Analyzing each technique separately provides a clear understanding of which samples are best suited for ( $^{14}\text{C}$ ) dating based on specific attributes highlighted through different analytical methods. Here are the best suggestions from each technique:

Technique	Best Suggestions	Supporting Facts
PCA of Colorimetry Data	SM_04 and SM_05	<b>SM_04 and SM_05</b> are found near each other in the lower right quadrant, indicating strong similarities in color attributes. This grouping suggests that these samples have comparable properties, possibly relating to similar binder compositions that are consistent and stable, traits desirable for $^{14}\text{C}$ dating.
PCA of X-Ray Powder Diffraction Data	SM_04 and SM_05	<b>SM_04 and SM_05</b> appear in the lower left quadrant, showing a mineralogical composition rich in calcite and dolomite with considerable presence of AFm phases. The substantial presence of calcite and dolomite enhances their richness in carbonate minerals, which could mean a more stable and less reactive composition ideal for $^{14}\text{C}$ dating.
SEM-EDS Analysis	SM_04, SM_05, SM_06	<b>SM_04 and SM_05</b> exhibit characteristics favorable for $^{14}\text{C}$ dating, primarily due to the preservation of dolomite with low levels of secondary reactions and stable mineral preservation. These traits suggest minimal interaction within the binder matrix that would introduce geological carbon, making them excellent candidates for accurate $^{14}\text{C}$ dating. <b>SM_06</b> also shows promising results due to its minimal secondary mineral formations and

		preservation of primary material composition, indicating little to no pozzolanic reaction and a low likelihood of geological carbon interference. Even if this sample is potentially datable it is likely of another construction phase due to its significantly different characteristic.
Optical Microscopy Data	SM_04 and SM_05	The minimization of geological carbon is crucial for <sup>14</sup> C dating. <b>SM_04 and SM_05</b> are recommended as their binder matrices presents a mostly carbonated lime-based composition.

*Table 6-Summary of Best sample candidate for <sup>14</sup>C from each technique followed.*

Incorporating the significance of sample locations and their specific functions within the structure adds crucial context to understanding the suitability of each sample for (<sup>14</sup>C) dating based on SEM-EDS analysis. The sample origins and their roles within the building critically influence their compositional attributes and subsequent reactivity, which in turn affects their potential for accurate <sup>14</sup>C dating.

**SM\_02 and SM\_03** were retrieved from the bedding mortar, primarily used between bricks, where the primary role is structural stability. These samples show a high fraction of silicates that catalyze alkaline reactions, typical of materials exposed to constant environmental interactions. **SM\_01**, differing in function as a filling mortar over the tomb, contains similar high silicate content, facilitating alkaline reactions conducive to geological carbon incorporation from limestone origins. Thus, **SM\_01, SM\_02, and SM\_03** are unsuitable for <sup>14</sup>C dating due to their significant content of geological carbon.

In contrast, **SM\_04 and SM\_05**, also used as filling mortars, possess a 'fatter' composition designed to enhance carbonation reactions rather than pozzolanic reactions. This characteristic, coupled with a lower silicate content, makes them more suitable for <sup>14</sup>C dating. Their composition minimizes the likelihood of geological carbon contamination, thus preserving the integrity of the original carbon materials crucial for accurate dating.

**SM\_06** stands out due to its substantial dolomite content and indications of minimal pozzolanic activity. This sample's preservation of the primary mortar composition, evidenced by low levels of secondary reactions, confirms its suitability for yielding accurate <sup>14</sup>C dating results. Although it is not suitable to date the origin of Oratorio di San Michele as it shows different characteristics, likely related to a more recent construction phase.

These insights into the functional distinctions and compositional differences, illuminated by their specific applications within the structure, are pivotal. **SM\_04 and SM\_05** are recommended for  $^{14}\text{C}$  analysis due to their minimal interference from geological carbon and the preservation of original carbon content. Conversely, **SM\_01, SM\_02, and SM\_03** should be avoided for  $^{14}\text{C}$  dating due to their predisposition to incorporate older carbon sources, which would likely yield misleading  $^{14}\text{C}$  dates. **SM\_06** should be avoided, despite the absence of geological carbon, as the sample likely belongs to a later restoration phase.

Incorporating archeometric data of mortars into Building Information Modeling (BIM) further enhances the practicality and utility of BIM in managing historical and archaeological sites. Archeometric analysis, which involves the scientific study of materials and artifacts, provides critical insights into the age, composition, and historical context of mortars used in construction. By integrating this data into the BIM model, professionals can achieve a deeper understanding of the building materials' historical aspects and their implications on the building's structural integrity and conservation needs. Integrating archeometric data enables more precise diagnostics of the mortar condition, such as degradation patterns and potential failure points. This integration aids in the formulation of more accurate and effective restoration and maintenance plans. For heritage conservation, understanding the original materials and methods used in historical structures is crucial. BIM, enriched with archeometric data, allows conservationists to replicate original building materials closely, ensuring that restoration efforts are sympathetic to the original design and materials. BIM provides a centralized platform for managing vast amounts of data. Incorporating archeometric data into BIM makes this information readily accessible to architects, engineers, conservationists, and project managers, facilitating better decision-making and collaboration. Archeometric data contribute to a more comprehensive lifecycle analysis of the building materials. In BIM, this data can be used to monitor the long-term behavior of mortars under various environmental conditions and loading scenarios, predicting future deterioration and planning preventive measures. Using BIM as a repository for both contemporary and historical data creates opportunities for educational outreach and research, promoting a deeper understanding of traditional building techniques and their evolution over time.

riato di antichi affreschi  
sede della Cappella  
Chiesa di S. Michele che si vede  
Padova dalla Fabbriceria del Torrefino  
da dell'Isola Formiggioli



Riviera di San Mio

Scala di Millimetri 5/10

# Chapter XI: References

- Addis, A., Secco, M., Marzaioli, F., Artioli, G., Arnau, A. C., Passariello, I., . . . Brogiolo, G. (2019). Selecting the Most Reliable 14C Dating Material Inside Mortars: The Origin of the Padua Cathedral. *Radiocarbon, Vol 61, Nr 2,*, p 375–393.
- Amorim, C. E. (September 2018). Understanding 6th-century barbarian social organization and migration through paleogenomics. . *Nature Communications*, , 3547.
- Artioli, G., Secco, M., & Addis, A. (2019). The Vitruvian legacy: mortars and binders before and after the Roman World. *EMU Notes in Mineralogy*, (pp. Vol. 20, Chapter 4, 151–202). Padova.
- Barzon, A. (1955). Padova cristiana. In A. Barzon, *Padova cristiana* (p. Padova cristiana). Padova.
- Bellinati, C., & Puppi, L. (1975). Padova Basciliche e Chiese – Parte Prima. *Chiesa di S.Michele-Capella di S.Maria*, 354.
- Bellinati, C. (1969). Padova Da Salvare. *Citta di Padova*, 32-38.
- Bellinati, C. (1971). San Michele da salvare. In B. Parrocchiale, *La Famiglia del Torresino* (pp. 4-11). Padova: Bollettino Parrocchiale.
- Bellinati, C., & Puppi, L. (1975). Padova Basciliche e Chiese-Parte Seconda.
- Beltrame, D. G. (2000). *Appunti di Storia Padovana*. Padua: Messaggero.
- Beltrame, G. (Anno XXV Feb). *Padova, e la sua provincia*.
- Blauer-Bohm, C., & Jagers, E. (1997). Analysis and recognition of dolomitic lime mortars. In *Roman Wall Painting: Materials, Techniques, Analysis and Conservation* (pp. 223-235). Fribourg .
- Brogiolo, G. P. (2017). The Cathedral and Saint Justina Between King Theodoric and Bishop Olderic. In E. o. Arnau, *Research on the Centre Episcopal of Padua , Excavations 2011-2012* (pp. 373-382). Fondazione Cassa di Risparmio di Padova e Rovigo.
- Catalogo collettivo fino al 1968*. Catalogo collettivo delle biblioteche di Padova, Padova.
- Chavarría Arnau, A. (2017). The Christianization of Padua and the Origins of the episcopal complex. In E. b. Arnau, *Research on the Centre Episcopal of Padua, Excavations 2011-2012* (pp. 367-373). Fondazione Cassa di Risparmio di Padova e Rovigo.
- Chuck Eastman, P. T. (2011). *BIM Handbook: A Guide to Building Information Modeling for Owners, Managers, Designers, Engineers and Contractors*.
- Colecchia, A. (2017, August 18). Retrieved from care.huma-num.fr:[https://care.huma-num.fr/it/index.php?title=PADOVA,\\_S.\\_Michele](https://care.huma-num.fr/it/index.php?title=PADOVA,_S._Michele).

- Cossio, A. (2014, 01 27). *St. Paulinus II, Patriarch of Aquileia*. Retrieved from Nobility of Analogous Traditional Elites: <https://nobility.org/2014/01/paulinus-ii-of-aquileia/>.
- DUÒ, C. (2011, 02). Padova-e-il-suo-territorio\_149. *rivista di storia arte cultura* , pp. 17-22.
- Farias, J. C. (2020, 11 13). *Who was Chuck M. Eastman?* Retrieved from SPBIM: <https://spbim.com.br/quem-foi-chuck-m-eastman/>.
- Gasparotto, C. (1969). *La chiesa di San Michele in Vanzo*. Padova: Societa Coporative Topografica.
- Hughes, J., Leslie, A., & Callebaut, K. (2001). The petrography of lime inclusions in historic lime-based mortars. *Euroseminar on Microscopy Applied to Building Materials*, (pp. 359-364).
- Katayama, T. (2009). The so-called alkali-carbonate reaction (ACR) — Its mineralogical and geochemical. *ELSEVIER, Cement and Concrete Research*, 643–675.
- Macmillen, N. (2009). *A history of the Fuller's Earth mining industry around Bath*. Lydney: Lightmoor Press. p. 9. ISBN 978-1-899889-32-7.
- Maurice Murphy, E. M. (2009). Historic building information modelling (HBIM). 311-327.
- Montobbio, L. (1955). *PADOVA, Rassegna mensile A Cura Della "PRO PADOVA"* . Padova: Sede della Academia .
- Nicolaus, S. (1671). *The prodromus of Nicolaus Steno's dissertation concerning a solid body enclosed by process of nature within a solid; an English version with an introduction and explanatory notes*. New York: The Macmillan company; London, Macmillan and company, limited.
- Pecchioni, E., Fratini, F., & Cantisani, E. (2014). *Atlas of the Ancient Mortars in Thin Section under the Optical Microscope*. Florence: Kermes quaderni, Nardini Editore.
- Rocha, G., Luis Mateus, O., Fernandez, J., & Ferreira, V. (2020). A Scan-to-BIM Methodology Applied to Heritage Buildings. *Heritage*, (pp. 3(1), 47-67).
- Ruiz-Agudo, E. &.-N. (2009). *Kinetics of carbonation of calcium hydroxide. Materials Science and Engineering*:. 64(1-2), 1-12. <https://doi.org/10.1016/j.mser.2008.12.001>.
- Talami, E. (2024). *Oratorio di San Michele, Padua* . Padua: IUAV.
- Tobias, E. (2013). *Padua Regia Civitas Identität un Gedächtnis um 1400 im Oratorio di San Michele Arcangelo Eine Fallstudie zum frühen Porträt*. Weimar Verlag und Datenbank für Geisteswissenschaften 2013 .
- Toffanin, G. (1988). *Cento Chiese Padovane Scomparse*. Padova.